Feasibility study of an alternative load path through floor elements for timber column and beam structures in accidental column removal scenarios

van Warmerdam, Teun

Award date:
2024

EINDHOVEN UNIVERSITY OF TECHNOLOGY

Department of Structural Engineering and Design
Innovative Structural Design Research Group

Feasibility study of an alternative load path through floor elements for timber column and beam structures in accidental column removal scenarios

Master's Thesis

Teun van Warmerdam

Supervisors:
dr. ir. S.P.G. Moonen
ir. A.P.H.W. Habraken
ir. T.S.K. Lambrechts

1.0

Eindhoven, May 2024

Abstract

With the emergence of engineered timber as a structural material and, as a result, timber structures increasing in size and height, the robustness of timber buildings becomes of interest. Existing Eurocode recommendations and literature on robustness are written mostly with steel and reinforced concrete structures in mind. Moreover, Eurocode recommendations on robust structures can lead to unsafe design due to a lack of guidance on dynamic amplification in accidental load cases and shortcomings in the tension tie recommendations.

This thesis explores the technical feasibility of continuous and staggered timber floor elements to provide a secondary load path in accidental column loss scenarios for timber column and beam structures. The typology of the analyzed timber structure is a six-story CC2b office structure, analyzed for spans ranging from 3 to 9 meters. Two timber floor element types are assessed: CLT plate elements and Lignatur box floor elements. First, the required cross-sectional height of the floor elements is determined for the standard design situation (*SLS* and *ULS*). Then, the required cross-sectional height in the accidental design state is determined by assessing the demanded capacities in notional corner, edge, and middle column removal scenarios. In the column removal scenarios, a Dynamic Load Factor of 2.0 accounts for the amplification of loads at sudden column loss. The comparison between required cross-sectional heights in standard design situations and accidental scenarios indicates the technical feasibility and possible additional material costs of a secondary load path through timber floor elements. Other elements in the analyzed structure, such as beams, columns, and connections, are checked for required dimensions and capacity in the standard design situation and column loss scenarios as well to see if they need strengthening. The structural analysis, derivation of load distributions, dimensioning of elements, and analysis of elements are all performed by manual calculation methods and validated using several SCIA Engineer models.

The results show that robustness by secondary load paths through timber floor elements is possible for timber column and beam structures. The corner column loss scenario is the most demanding column loss scenario, being most often normative for the cross-sectional height of the floor elements and restricting the floor span to a certain maximum. The CLT floor elements can provide robustness for longer spans than the Lignatur floor elements and at less significant element height increase. The secondary load path through CLT elements does not require additional material for spans between 7.0 and 8.5 meters for the continuous floor element layout. The staggered floor layout performs significantly worse than the continuous layout, with smaller spans possible and a need for a larger cross-sectional height increase. Several column and connection locations along the edge of the building parallel to the floor span require additional strengthening or design for tensile loads in accidental scenarios.

Preface

This research project about the robustness of timber structures concludes my studies at the Faculty of the Built Environment at the TU/e. I want to thank my primary supervisor, ir. Arjan Habraken, for his persistent enthusiasm and guidance on the project and for sharing his knowledge and experience with me and my fellow students at the RESED graduation research group. I want to thank dr. ir. Faas Moonen for his feedback and for chairing my Graduation Committee. Lastly, I would like to thank ir. Thijs Lambrechts for his role as third supervisor.

To my friends, fellow students at KOers, and former roommates: I always had a great time in Eindhoven, thanks to all of you. Special thanks go to my family and girlfriend for their unconditional love and support.

Contents

List of Figures

List of Tables

List of symbols and abbreviations

ALP	alternative load path
CLT	cross laminated timber
DLF	dynamic load factor
E_d	design value of a load in the standard design situation
$E_{d,acc}$	design value of a load in the accidental design situation
$F_{fac,side}$	point load representing the *side* facade load
$F_{t,max}$	maximum tensile force between floor elements and beams
h_{req}	required beam height in the corresponding design situation
I_{ef}	effective moment of inertia CLT for SLS calculations
n	number of floor elements (equals the floor span)
q_{acc}	combined dead and live load of floors in accidental design situation
$R_{AV,F}$	portion of facade load F taken by the remaining column
$R_{AV,qL}$	portion of the distributed facade load q taken by the remaining column
$R_{n,F}$	portion of facade load F taken by outermost floor element
$R_{n,qL}$	portion of distributed facade load q taken by outermost floor element
RC	reinforced concrete
u_{fin}	final deflection of a timber element, considering creep behavior
W_{net}	net section modulus CLT for ULS calculations
CCx	consequence class x
GluLam	glued laminated timber
MDOF	multi degrees of freedom
SLS	serviceability limit state
ULS	ultimate limit state

Chapter 1

Introduction

The construction sector has an enormous environmental footprint. It is responsible for about 50% of globally extracted raw materials and for almost 40% of energy and process-related emissions [18]. While becoming aware of its impact, the construction industry's traditional materials are critically assessed. Cement production for concrete, for example, is responsible for 5-6% of the global CO_2 emissions generated by mankind [19]. Countless efforts are made to lower the environmental impact of traditional construction materials.

In the meantime, the environmental challenges have led to an increased interest in replacing the carbon-intensive traditional construction materials with low-carbon alternatives [20]. Engineered timber products are an example of low-carbon construction materials. They consist of multiple layers of wood glued together to create structural elements like columns, beams, or plates. Using engineered timber products, CO_2 captured during wood growth can be stored in structures.

The design possibilities for building with wood have significantly increased with the emergence of engineered timber products. Timber buildings are becoming larger and taller in size, with the *Mjøstårnet* shown in Figure 1.1 as a thriving example with a record height of 85.4 meters [1].

Figure 1.1: Tall timber building *Mjøstårnet* in Brumunddal, Norway [1].

With the rise of larger and taller timber structures, consequences increase when incidents occur. Over the past centuries, vehicles have crashed into buildings, explosions have occurred in and around buildings, and construction materials have behaved differently than expected, sometimes with catastrophic consequences [21]. Incidents leading to (partial) collapse have triggered research to prevent global consequences for a structure after local damage occurs. The research, however, has mainly focused on traditional construction materials and methods using steel and reinforced concrete.

The research conducted in this thesis will evaluate the current state of guidelines and literature on robustness in general and on the robustness of timber structures specifically. The literature research findings are used to analyze a possible robustness approach for a timber column and beam structure via a secondary load path through continuous floor elements. The results of this analysis will show whether the proposed robustness method for timber structures is technically possible and, if so, at what material costs it comes. The main research question is reformulated after using input from the answers to the sub-questions (e.g., on which robustness strategy is applied) and reads:

How can timber floor elements provide an alternative load path for full-timber column and beam structures in accidental column loss scenarios?

The main research question will be answered using the following sub-questions:

- *What type of full-timber structure is emerging that demands a robustness strategy in its design, considering consequences in case of failure and the number of structures constructed?*
- *What can be learned from designing robust structures with (precast) concrete and steel structures for robustness in timber structures?*
- *What robustness strategies are applicable for full-timber structures?*
- *What of the robustness strategies for full-timber structures can best provide robustness for the determined full-timber structure typology?*
- *How and at what additional material cost can the chosen robustness strategy prevent progressive collapse in the determined full-timber structure typology?*

Chapter 2 provides background information on timber as a structural material. Chapter 3 introduces robustness in general, whereafter the existing guidelines and literature on robustness in general and for steel, reinforced concrete, and timber structures are evaluated. In Chapter 4, the methodology of the structural analysis performed in this thesis is presented, after which the structural analysis itself is elaborated in Chapter 5. The results and discussion of the alternative load path analysis are presented in Chapter 6. Followed by the limitations of the research (Chapter 7), the conclusions (Chapter 8), and the recommendations (Chapter 9).

Chapter 2

Timber as structural material

While the potential of (engineered) timber opens up new possibilities for timber construction, certain particularities in the structural behavior of timber have to be considered carefully to achieve safe design. For his Ph.D. thesis at ETH Zürich, Voulpiotis sharply points out the deal with the robustness of tall timber buildings: "The real concern about tall timber buildings is not due to fire or structural weakness. It is due to the non-negligible possibility for serious errors given timber's complexity as a building material and the potential of unexpected risks emerging when we scale up to new heights" [21]. Examples of such complex, potentially risk-introducing properties and behavior of timber are described by Voulpiotis [21] and summarized as follows:

- **Moisture sensitivity**: Shrinking and swelling in environments with varying moisture content can cause problems. In the worst case, a fungi attack dramatically reduces the structural strength.
- **Orthotropy**: Timber has strong longitudinal strength but weaker tangential and even weaker radial strength, increasing the complexity of designing with timber and increasing risks of failure by stress perpendicular to the grain.
- **Low stiffness**: Since the stiffness of structural timber is relatively low compared to reinforced concrete and steel (three and twenty times less stiff, respectively), the deflections, second-order effects, and comfort of buildings are more complex to satisfy.
- **Brittleness**: The brittle failure modes of timber under tension, bending, and shear make the need for careful design of ductility in steel connections essential to activate new load paths in case of an incident. The typical stress-strain relation of timber is given in Figure 2.1.
- **Creep**: Deflections in timber structures increase slowly over time, even without load increments. This effect has to be accounted for and is particularly complex in hybrid structures where settlements differ per material.

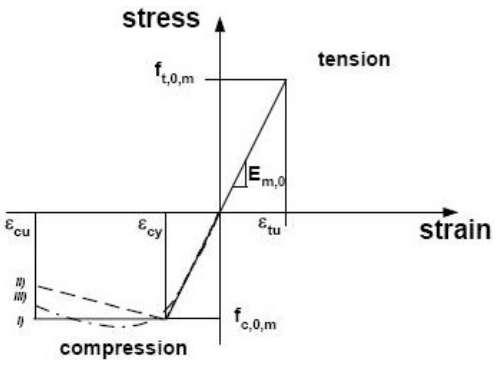

Figure 2.1: Typical stress-strain diagram of timber [2]

Chapter 3

Robustness in literature

3.1 Structural robustness

As described in Chapter 1, incidents with buildings and other structures have been inevitable. A collapse with significant consequences that initiated the research into the resilience of structures is the partial collapse of the Ronan Point tower in London in 1968, as depicted in figure 3.1. After a gas explosion on the 18th floor of the 22-storey Ronan Point tower, all 22 corner floors came down [21].

Figure 3.1: The partial collapse of Ronan Point [3]

While strategies exist to limit the risk of incidents occurring, preventing any damage from all threats in and around buildings is virtually impossible. When an incident damages a specific part of a building (local damage), it should not result in the failure of adjacent sections, resulting in catastrophic consequences (global failure). The phenomenon of local damage resulting in global failure is described as *progressive collapse* [22] and should always be prevented.

Ellingwood and Dusenberry have described the probability of progressive collapse [23][24] in Equation (1).

$$P(C) = P(E) \cdot P(D|E) \cdot P(C|D) \tag{1}$$

Where:

$P(C)$	=	Probability of collapse
$P(E)$	=	Exposure (risk of unexpected events)
$P(D\|E)$	=	Vulnerability (consequences of the event to structure on a local level)
$P(C\|D)$	=	Robustness (consequences for the global structure after local failure)

$P(E)$ and $P(D|E)$ can not be anticipated due to their unpredictable nature. The event is unknown, and thereby the consequences for the structure are hard to control. It is, therefore, preferable for the designer of a structure to focus on the behavior of the structure after the loss of certain elements (e.g., a wall or column), thus omitting the attempt to predict an uncertain incident and the corresponding local damage. *Robustness* [$P(C|D)$] is the term in Equation (1) that covers the vulnerability of the global structure to damage at local levels, for example by activating an alternative load path (ALP) after the loss of a certain element. By omitting the need to predict the type of unexpected event, robustness is an effective and reliable measure to limit the risk of progressive collapse.

Various mechanisms can lead to the progressive collapse of structures. These mechanisms have different causes and counter-mechanisms, which is why it is useful to distinguish them separately. *Starossek* has described six types of progressive collapse types, which are listed and explained below [25]:

1. Pancake collapse
    - After the failure of a load-bearing element, part of the structure falls, releasing potential energy into kinetic energy. The impact of dropping elements on the remaining structure causes more elements to fail and come down, resulting in vertical, stack-of-pancake-like, *progressive* collapse, like the partial collapse of the Ronan Point tower from Figure 3.1.

2. Zipper-type collapse
    - After the failure of a structural element or node, the forces are suddenly redistributed to other elements in the structure. The sudden redistribution of loads causes a dynamic amplification of the redistributed loads, causing overloading and failure of elements similar and adjacent to the initially failed element. The progressive failure of elements and, thereby, collapse progresses to other similar elements or nodes in a direction transverse to the initial load direction. For example, cable-stayed bridges where the failure of one cable leads to the failure of all cables consecutively.

3. Domino-type collapse
    - Like a series of domino blocks, the overturning of one element causes a horizontal impact on an adjacent element (either direct or via intermediate elements like beams or cables), overturning and hitting another element, causing a progressive collapse in the overturning direction.

4. Section-type collapse
    - If an element is cut or damaged partially, the stresses concentrate on the remaining part of the cross-section of the element. The increase in stress in the remaining part of the cross-section can lead to the rupture of more parts in the cross-section, progressing into complete failure of the cross-section. While section-type collapse has similarities to zipper-type collapse, it is distinguished as a separate collapse

type since it is about the progression of failure within one element instead of a failure within a system of elements.

5. Instability type collapse
    - The failure of elements that stabilize load-carrying elements can lead to instability of these load-carrying elements if they are loaded in compression. When destabilized, small perturbations can lead to the collapse of load-carrying elements, leading to the progression of more failures.
6. Mixed-type collapse
    - While the previously described types of collapse are conveniently categorized, real-life collapses have showcased a combination of the described collapse types, where one of the collapse types might trigger another collapse type to occur simultaneously or subsequently.

On the other hand, strategies to prevent progressive collapse have been researched and described. Fascetti et al. found that continuous and redundant frames can generally absorb local damage. However, their ability to resist progressive collapse depends on many factors that have yet to be identified in a methodical and reliable manner [6].

Other acquainted methods to redistribute loads in case of an incident are the arching action of walls as (cantilevering) deep beams, suspension action with truss structures, Vierendeel action, catenary action, and membrane action in floors [5], as visualized in Figures 3.2 to 3.6.

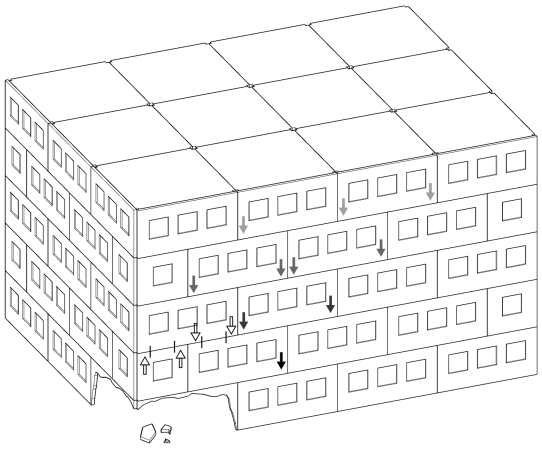

Figure 3.2: Staggered walls bridging the gap of a lost wall element on the ground floor level, adapted from [4].

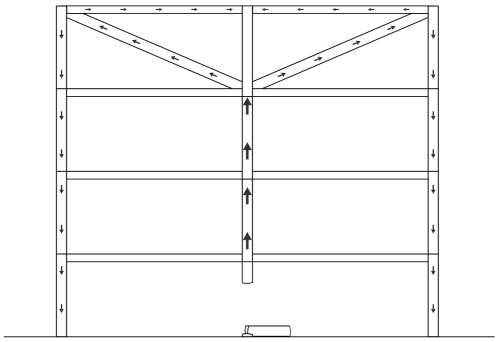

Figure 3.3: Suspension action in a frame after a mid-column is removed, adapted from [5].

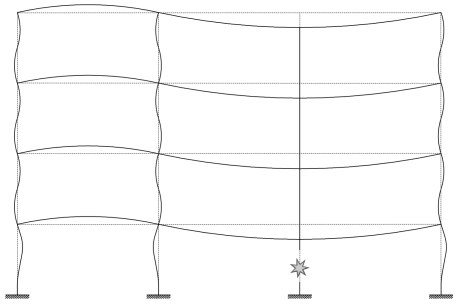

Figure 3.4: Vierendeel action redistributing loads through rigid connections after the loss of a column, adapted from [5].

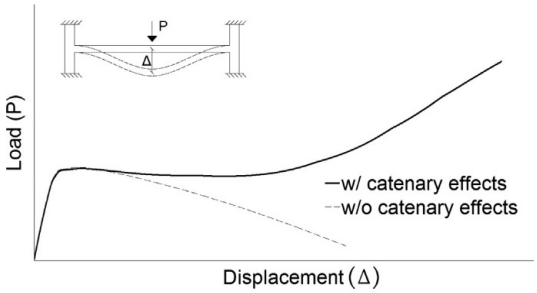

Figure 3.5: Load - displacement graph showing the behavior of catenary effects [6]

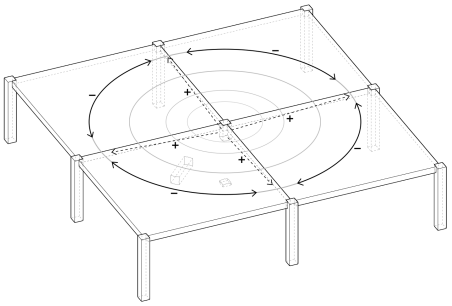

Figure 3.6: Membrane action in a floor after a middle column is lost

3.2 Robustness in the Eurocodes

The robustness of structures is treated in *Eurocode 1: Actions on structures - Part 1-7: General actions - Accidental actions* [7] and for the Netherlands in the corresponding *Dutch Annex* [17]. These documents give guidelines on designing structures to withstand accidental loads such as impact loads and explosions. In *Eurocode 1-1-7*, robustness is defined as *"the ability of a structure to withstand events like fire, explosions, impact or the consequences of human error, without being damaged to an extent disproportionate to the original cause"* [7].

The guideline to design structures in accordance with the risk of accidental loads and to ensure the robustness of a structure is defined as an acceptable boundary for what floor area of a structure may collapse. In paragraph 3.3 of *Eurocode 1-1-7: Accidental actions* [7], requirements are listed to prevent global instability or collapse caused by local failure. The prevention of global instability by local damage is quantified as follows: the maximum allowable floor area to collapse is the smallest value of either 100 m^2 or 15% of the gross floor area of two adjacent floors, caused by the removal of a random supporting column, support or wall, as visualized in Figure 3.7. Notable in the accepted damage described in *Eurocode 1-1-7* is that the consequent (impact) load by debris coming from damaged areas is not regarded [26].

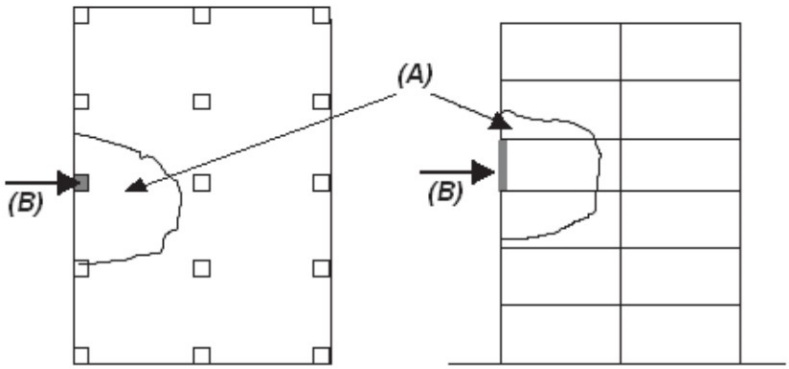

Figure 3.7: By *Eurocode 1-1-7* recommended maximum allowable floor area to collapse [7]

Another listed approach is to design the connections and other details in a structure with sufficient robustness by applying tension ties in three dimensions, designing for sufficient ductility, or similar approaches [7, 17]. Tension ties can be realized in multiple ways, for example, through additional steel reinforcement in cast concrete or by adapting floor beams to act as tension ties in case of damage.

Eurocode 1-1-7 also states that the consequence class of a structure determines what design principles should be regarded in terms of the robustness of a structure. Which structures belong to what consequence class is shown in Table 3.1. The methods recommended by the Eurocodes to provide robustness in the design of buildings for each of the consequence classes are described in Table 3.1.

For designing structures with critical elements (CC2b) mentioned in Table 3.2, an accidental load A_d must be applied in horizontal and vertical directions on the element and connected parts, accounting for their ultimate strength. The recommended value of 34 [kN/m^2] can be a concentrated or a distributed force [7]. The value of 34 [kN/m^2] is disputed. The value originates from an estimated explosion blast pressure level based on observations made at the Ronan Point collapse described in Chapter 3 [27]. E.g., blast loads from vehicle-borne improvised explosive devices (VBIEDs) can exceed the value of 34 [kPa] by over two orders of magnitude [28]. Furthermore, the use of over-designing key elements (critical element method) should be a last resort since the failure of critical elements will result in

Table 3.1: Classification of buildings types to Consequence Classes, adapted from [17].

Consequence Class	Description/example
CC1	Single-family homes with 1,2 or 3 building layers. Agricultural buildings, greenhouses, and industrial buildings with limited people inside.
CC2a (low-risk group)	Single-family homes with 4 or more building layers. Dwellings, hotels, and offices with maximum 4 building layers. Educational buildings with 1 building layer. Public buildings with a floor area below 2000 m^2. Industrial buildings, parking garages or stores with 1 or 2 building layers.
CC2b (high-risk group)	Dwellings, hotels, and offices with 5 or more building layers. Educational buildings with 2 or more building layers. Public buildings with a floor area above 2000 m^2. Hospitals with 1, 2, or 3 building layers. Industrial buildings, parking garages, or stores with 3 or more building layers.
CC3	Buildings above 70 meters tall. Buildings with public functions or with spans over 50 meters that result in danger for over 500 people in case of collapse. Hospitals, nursing homes, and jails with 4 or more building layers. Control towers of international airports. Industrial buildings containing hazardous substances or processes for which an environmental permit is required.

global, brittle failure with disastrous consequences [29].

In *Eurocode 0: Basis of Structural Design*, the standard equation for the combination of loads is given by means of Equation (2), while the accidental load combination is given by Equation (3) [30]:

$$E_d = \sum_{j \geq 1} \gamma_{\mathrm{G},j}\, G_{\mathrm{k},j} + \gamma_{\mathrm{Q},1}\, Q_{\mathrm{k},1} + \sum_{j>1} \gamma_{\mathrm{Q},i}\, \psi_{0,i}\, Q_{\mathrm{k},i} \tag{2}$$

$$E_{d,acc} = \sum_{j \geq 1} G_{\mathrm{k},j} + A_{\mathrm{d}} + (\psi_{1,1}\ or\ \psi_{2,1})\, Q_{\mathrm{k},1} + \sum_{j>1} \psi_{0,i}\, Q_{\mathrm{k},i} \tag{3}$$

Whether A_{d} and $\psi_{1,1}\, Q_{\mathrm{k},1}$ or $\psi_{2,1}\, Q_{\mathrm{k},1}$ should be used, depends on how the accidental load case is assessed. If an actual load describing a shock, fire, or emergency repair is considered, a value for A_{d} is prescribed, and $\psi_{1,1}\, Q_{\mathrm{k},1}$ is used. Alternatively, the condition of the structure after the accidental load can be assessed. A_{d} is then omitted, and the element at issue is considered to be lost entirely. The *Dutch Annex* of *Eurocode 0* also states that $\psi_{1,1}\, Q_{\mathrm{k},1}$ is only to be used when checking the combination of wind and fire. For the assessment of a structure after the loss of a column, $\psi_{2,1} Q_{\mathrm{k},1}$ should be used. As a result, the applied formula for the accidental load combination of equation 3 is adapted into Equation (4) [31]:

$$E_{d,acc} = G_{\mathrm{k}} + \psi_{2,1}\, Q_{\mathrm{k},1} = G_{\mathrm{k}} + 0.3 \cdot Q_{\mathrm{k},1} \tag{4}$$

In the assessment of the loads in the accidental situation, the wind load is not regarded [31], and the load duration can be considered as *very short* [32].

Table 3.2: Recommended analysis method for accidental design situations corresponding to each Consequence Classes [7].

Consequence Class	**Robustness design strategy recommended by *Eurocode 1-1-7***
CC1	If a structure is designed and constructed in line with the governing Eurocode standards, specific accidental load considerations are not needed.
CC2a (low-risk group)	Depending on the specific circumstances of a structure, a simplified calculation using models with equivalent loads may be used, or prescribed design and detailing rules may be used. Effective horizontal tension ties (column structures) or effective anchoring of floors and walls (bearing wall structures) should be applied.
CC2b (high-risk group)	In addition to the recommended strategies of consequence class CC2a, vertical tension ties should be effectively combined with the horizontal tension ties in all load-bearing columns or walls. Or, as an alternative, the structure can be assessed by the imaginary removal of all load-bearing columns (and beams carrying such columns) or random parts of load-bearing walls. During this imaginary removal, the stability of the global structure can not be compromised, and the local damage may not exceed a determined value. If the removal of a column, beam, or wall does lead to global instability or more extensive damage than allowed, this element should be designed as a *critical element*.
CC3	An investigation into the specific circumstances should be performed to assess the required reliability level and depth of the structural calculations. This assessment can lead to the need for a risk analysis using sophisticated methods like dynamic calculations, non-linear models, and the interaction between the load and the structures. Such a systematic risk analysis should be performed concerning foreseen and unforeseen accidental loads.

For structures with columns in consequence class 2, the recommended design strategy for a robust design according to *Eurocode 1-1-7 Accidental Loads* [7] features internal and circumferential tension ties, regardless of the construction material. Virtually all examples and practical applications noted in *Eurocode 1-1-7* refer specifically to concrete and hybrid steel-concrete structures. The design requirements for tension ties are described in Equations (5) and (6).

$$T_i = 0.8 \cdot (g_k + \psi q_k) sL \text{ , with a minimum of } 75\ kN \tag{5}$$

$$T_p = 0.4 \cdot (g_k + \psi q_k) sL \text{ , with a minimum of } 75\ kN \tag{6}$$

Where:

T_i	=	tensile design load for internal tension ties	$[kN]$
T_p	=	tensile design load for circumferential tension ties	$[kN]$
g_1	=	characteristic value of the dead load	$[kN/m^2]$
q_k	=	characteristic value of the variable load	$[kN/m^2]$
ψ	=	factor to combine the value of load effects in the accidental state	[-]
s	=	distance between tension ties	$[m]$
L	=	length of the tension tie	$[m]$

It is unclear what the origin of Equations (5) and (6) is, what the minimum value of $75\ kN$ is based upon and, most importantly, how the tension ties should be implemented. Due to the limited background and implementation instructions, *Bhagwandas* [33] found that for a design case study of a concrete frame building, a progressive collapse would have taken place if the tension ties were to be placed as prescribed by *Eurocode 1-1-7 Annex A*.

Another measure to increase the robustness of a structure that is mentioned in *Eurocode 1-1-7: Accidental loads* is the activation of Alternative Load Paths (ALPs) [7]. The concept behind ALPs is that certain elements are designed to take the loads from other elements in an accidental load situation, thus enabling a secondary load path when needed. However, apart from mentioning ALPs as a possible measure once, no explanatory notes are given in the relevant Eurocodes about what such a secondary load path should fulfill.
In contrast to the Eurocode guidelines for concrete structures, the specific Eurocode guidelines for the design of timber structures and the accompanying Dutch Annex do not mention additional timber-specific measures to ensure the robustness of timber structures or to prevent progressive collapse in case of an incident [34] [32].

3.3 Robustness of non-timber structures

The limited amount of research on the robustness of timber structures will be described in Section 3.4. Since more research has been performed on the robustness of concrete and steel structures, a literature study has been conducted to see what can be learned from the robustness of structures erected from different materials than timber.

Robustness of concrete structures

In-situ-cast concrete structures have a high degree of continuity since the continuously cast concrete connects all elements, and the continuous reinforcement bars run through multiple elements [4]. In case of the loss of a certain structural element, this continuity improves the structural collaboration between different elements, leading to an easier redistribution of loads. However, it should be noted that the performance of cast-in-place concrete structures depends entirely on the reinforcement layout [27].

The structural continuity of cast-in-situ concrete is lost when precast concrete elements are used. Splitting a structure into elements that can be precast in a factory and connecting them on-site requires clever detailing of the connections between the elements to provide (some) continuity. In the early stages of precast concrete construction, the lack of continuity can be illustrated by the collapse of Ronan Point mentioned in Chapter 3, as the partially collapsed tower was an early precast structure [4]. Nowadays, precast elements are often connected through protruding rebars, which are slotted into a recess (*gain*) of another element, after which the gain is filled with a mortar, fixating the protruding rebar from one element in the gain of the other element. To improve the continuity of precast concrete structures, a statically indeterminate structure can be designed to span over damaged building areas. The static indeterminacy can be achieved by moving the connection between the prefab beams from the column location to the zero-moment spot [35].

In the analysis of the measures depicted in *Eurocode 1* against the progressive collapse of precast concrete structures, Van Dijk [4] concluded some important shortcomings when it comes to applying tension ties in the way they are described in the Eurocode. The approach described in *Eurocode 1* does not yield the desired alternative load path for corner columns or walls, nor can the structural elements adjacent to the partial collapse provide enough stability to take the horizontal loads caused by the catenary action of the tension ties. These shortcomings are not accounted for in the Eurocodes, resulting in unsafe design when followed literally. De Boer [36] also showed that tension ties, as described in the Eurocode, do not work when a corner column is lost. De Boer suggests investigating the potential of

diagonals or infill walls to guarantee progressive collapse prevention when a corner column is lost.

Robustness of steel structures

For steel structures, the 75 [kN] tying resistance noted in Equations (5) and (6) can be achieved relatively easily by using a minimum element web thickness of 8 [mm] and a minimum of two M20 grade 8.8 steel bolts with a maximum of 140 [mm] spacing between the centers of the steel bolts in connections that should take the tensile force coming from the tension ties [27]. While this might suggest robustness is straightforward to incorporate into the design of steel structures, the problems with the tying force method described earlier in Section 3.2 also hold for steel structures. Calculations by Byfield et al. [28] show that the tying force method described in design codes only yields a lower bound estimate of the required tying capacity to arrest the downward movement of parts of a structure in an accidental scenario, as the dynamic amplification of the loads in such a scenario are neglected. In addition, Byfield et al. state that industry-standard steel connections do not have the rotational capacities to allow catenary action to develop in steel-framed buildings [28]. However, when properly designed, a flexural response of steel structures is observed first, after which, when the flexural strength and the ductility are high enough, a stiffening phase by catenary action in the steel beams can be achieved [10].

3.4 Robustness of timber structures

The findings in Section 3.3 *Robustness of non-timber structures* are not directly applicable to timber structures due to differences in material properties and subsequent structural application and detailing. C. Lyu et al. summarize the differences for mass timber structures as follows [37]:

- Lack of continuity between prefabricated timber elements.
- Brittle tensile, bending, and shear failure modes of timber.
- Connections between beams and columns in timber frame buildings are not designed to resist bending.
- Lack of ductility in connections.

While the research on the robustness of timber structures specifically is limited, some research has been done in recent years in attempts to take inventory of the challenges described above for the robustness of timber structures and how to overcome the challenges.

Mpidi Bita has performed numerical and experimental research on disproportionate collapse prevention of timber systems. A dynamic non-linear analysis of a twelve-story code-compliant CLT building showed a 32% probability of collapse if the building was not designed with conscious robustness regards. Bita also found that conventional connections between mass-timber floor systems are most often inadequate in generating alternative load paths due to low axial strength and ductility [38]. To overcome the lack of axial strength and ductility, Bita proposed a novel connection design consisting of steel tubes recessed in adjacent timber floor elements, connected by a steel rod. This novel connection design helps to form catenary action, allowing for ductility of up to 15% of the floor span while providing enough axial strength [38]. The novel connection design is visualized in Figure 3.8.

The drawback of such a connection type is the introduction of acoustic leaks between adjacent and superimposed rooms and steel exposure in fire scenarios.

Continuous beams and slabs can help the floor system to cantilever over a removed edge or corner column to prevent disproportionate collapse [39]. Compared to single-span, CLT panels spanning two bays resulted in significantly higher ultimate loads when tested for column removal scenarios in experimental and numerical analyses [37].

The low weight-to-strength ratio of timber can be advantageous in accidental load scenarios. Structural timber is about five times less dense than reinforced concrete and about

(a) Connection element shown above CLT plate (b) Connection element lowered into the CLT plate

Figure 3.8: Novel steel connection designed and tested by Mpidi Bita [8]

fifteen times less dense than steel. A benefit in forming ALPs in timber could be that the self-weight of structural elements, such as floors coming down, is lower than in reference structures, thereby reducing (dynamic) self-weight inertia loading and debris mass [23].

Relevant case studies

J. Huber describes the robustness strategies of several timber buildings constructed around the globe in his PhD thesis [23], as listed below (supplemented by two case studies of other sources):

- Stadthaus, London.
  - CLT panel construction, 29 [m] tall.
  - Designed for loss of one single wall of floor panel and to sustain an impact load pressure of 7.5 [kPa] on a wall panel.
- UBC Brock Commons Building, Vancouver.
  - CLT floors, GluLam elements construction, 53 [m] tall.
  - Designed to lose one column and let the structure above hang from the remaining structure.
- Mjøstårnet, Norway.
  - GluLam column-beam-diagonals structure, 85.4 [m] tall.
  - Columns designed as key elements, designed to afford losing one diagonal and to resist the impact load of one concrete floor coming down to the story below.
- HoHo, Vienna.
  - Concrete core, CLT walls, and GluLam beams and columns, 84 [m] tall.
  - Horizontal and vertical ties cast in concrete in the connections and the ability to afford the loss of one column.
- Treet Building, Bergen (Norway).
  - GluLam trusses, concrete power stories, prefabricated stacked modules, 48 [m] tall.
  - Numerical analysis to check deformation capacity, segmentation per power story, escape route checked for debris load impact [29].
- International House Sydney, Sydney.
  - CLT panels, GluLam beams, and columns, 30 [m] tall.
  - Ground floor: concrete columns to provide protection to vehicle impacts, fire loads, and termite attacks [37, 40].

Three main approaches to incorporate robustness in timber structures can be seen in the reference structures listed above: alternative load path analysis by notional element removal, the design of critical elements, and robustness measures taken in (reinforced) concrete parts of hybrid structures.

3.5 Dynamic effects at column loss

In the case of sudden element loss, static load assumptions of the structure's response might not suffice. Inertia effects of the remaining structure can amplify the resulting redistribution of load, which must be taken into account correctly. The conservative upper limit of the amplification is found by assuming the removal of elements to be instantaneous [27]. In static analysis, this inertia effect is considered using a Dynamic Load Factor (DLF), which converts the displacement of the static analysis to the displacement of a dynamic analysis [27]. The DLF is thus defined as the ratio between dynamic and static displacement.

$$DLF = \frac{w_{dyn}}{w_{stat}} \tag{7}$$

Powell [9] describes that when a column is suddenly removed, the applied load is already present (containing potential energy). The energy in the structure's response builds up as the deformation of the structure occurs. The maximum deformation the structure undergoes is found at the point where the kinetic energies equals zero. At this point, the internally built-up deformation energy equals the (now reduced to zero) potential energy of the load. Figure 3.9 visualizes the load and response energy magnitudes as a function of the displacement for a single-degree-of-freedom system. The maximum deformation, thus the point at which the potential energy of the load and the deformation energy in the structure are equal, is found where the area below the graphs in Figure 3.9 (b) are equal.

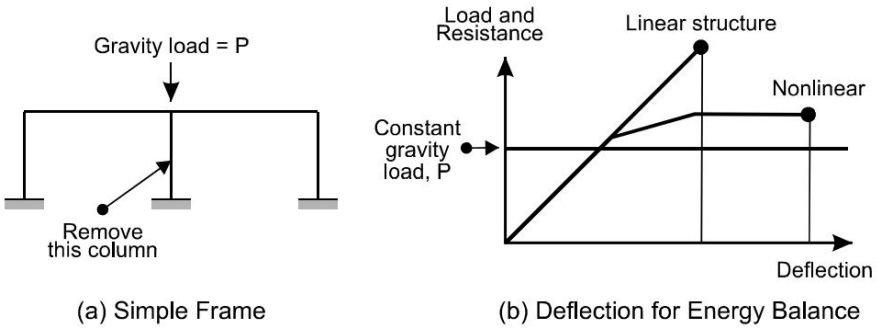

Figure 3.9: Energy response of a linear and a non-linear structure [9].

For illustrative purposes, Figure 3.10 shows the energy response for a linear structure caused by a static load. Figure 3.11 shows the energy response to the same magnitude of load P, but now suddenly applied (analogue to sudden column loss). For a linear elastic structure, the point at which the resulting load R is twice as high as load P, the kinetic energy reaches zero, and the maximum deflection is reached, resulting in a DLF of 2.0. In other words, the triangular area of the internally built-up deformation energy (marked *red* in Figure 3.11) reaches twice the magnitude of load to equal the *blue* area below the rectangular suddenly applied load energy graph.

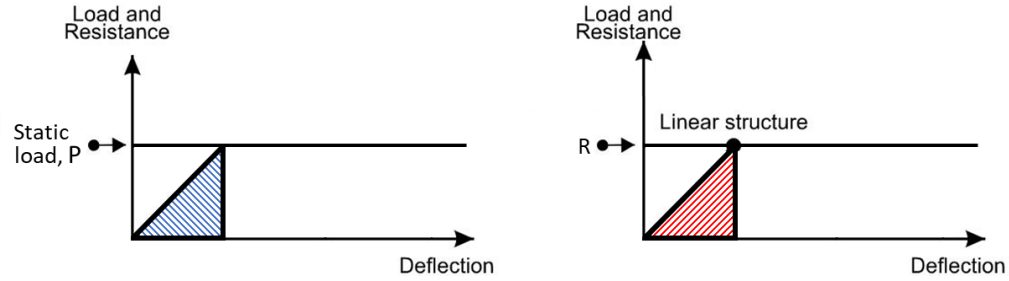

Figure 3.10: Energy response of a linear structure by a static load, adapted from [9].

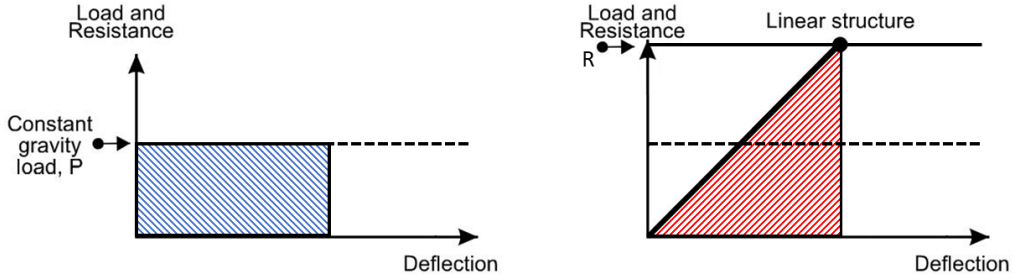

Figure 3.11: Energy response of a linear structure by a suddenly applied load, adapted from [9].

This means that if timber elements take the dynamically amplified loads at the loss of a column, the loads in these elements have to be doubled for static analysis. If the dynamically amplified loads are taken by other parts of a structure consisting of a material with non-linear stress-strain behavior, the maximum deflection and load increment depend on the (non-linear) load-deflection curve [9].

Loads are dynamically amplified only at the location above a lost structural element, as visualized in Figure 3.12. The DLF acts on dead loads G_k (coming from the floor elements, beams, columns, and facade) and on the dominant reduced variable live load $Q_{k,1}$.

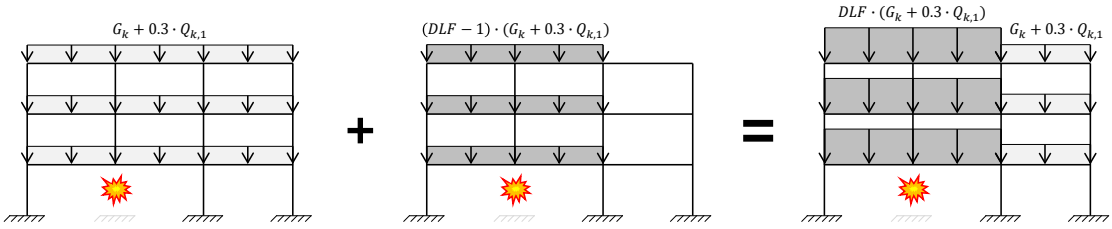

Figure 3.12: Loads amplified with a DLF at the location where a column is lost, adapted from [10].

How (and if) the dynamic amplification of loads is regarded in the accidental load situation described in the Eurocodes for Accidental loads is unclear. In Equations (5) and (6) in Section 3.2, which state the design loads for tension ties, it is not described whether dynamic amplified loads are accounted for. DLFs are mentioned in Annexes of the Eurocode for, e.g., vessel impact loads on civil works, but not for accidental design scenarios in buildings.

3.6 Literature conclusions

The main takeaways of the literature review that will be considered in the further research conducted in this thesis are:

1. The Eurocode recommendations for the accidental design situation do not always result in a safe design for steel, RC, and timber structures (Section 3.2). A lack of (consciously regarded) dynamic load amplifications can be a possible cause. Moreover, tension ties are not activated in corner column loss scenarios (Section 3.3).
2. Ideally, using key elements as a robustness measure should be avoided, as it requires an assumption of the magnitude of the accidental load. If the assumed load is exceeded, catastrophic consequences can occur (Section 3.2). A load-independent robustness approach is preferred, such as ALP analysis (Section 3.1).
3. Continuous and staggered floor elements can (potentially) provide a secondary load path in accidental scenarios (Section 3.4).
4. If sudden accidental loads are absorbed in a linear-elastic (timber) structural element, a DLF of 2.0 should be regarded to consider the dynamically amplified loads (Section 3.5).

Chapter 4

Method

4.1 Analyzed timber structure typology

To assure robustness in full-timber structures, the continuity and staggering of timber floors over more than one floor-bay for alternative load paths are investigated. The idea is that, in case of a sudden column loss, floor elements spanning only one bay lose their structural purpose completely. However, when a floor element spans over two floor bays, thus over three grid lines with beams and columns, two supports always remain in case of sudden column loss. The potential of continuous and staggered timber floor elements is mentioned by Lyu et al. [37] and Bita et al. [39]. In the structural analysis conducted in this thesis, the feasibility of secondary load paths using two-span timber floors in the accidental situation is assessed.

A structure typology has to be decided to see whether continuous and staggered floors can be a feasible robustness strategy. Based on the analysis of the *Eurocode* in relation to robustness in Section 3.2, a timber structure typology belonging to consequence class CC2b will be analyzed for progressive collapse prevention. In lower consequence classes, the consequences are lower in case of an incident, and the prescribed guidelines are less demanding (see Table 3.2). In the higher consequence class (CC3), a greater variety of structure typologies can be found. An example of a CC3 typology is a high-rise structure above 70 meters tall, for which the assessment of robustness methods is of high complexity. At the University of ETH Zürich, K. Voulpiotis has extensively described the complexity of robustness of tall timber structures in his PhD thesis, including possible solutions [21].

A full-timber frame building, constructed using columns and beams, can be a suitable typology for multiple types of CC2b structures (hotels, apartment buildings, and offices between five and fifteen stories tall [7]). To pragmatically assess the robustness of CC2b structures via activation of a secondary load path in the floor elements, an office building consisting of a six-story full-timber structure will be analyzed. An office building type is interesting to investigate due to the demand for an open floor plan layout in office structures. Therefore, the development of an alternative load path can not simply rely on, for instance, the redundancy of walls separating houses in an apartment block.

To analyze the performance of timber floors in column removal scenarios, the structural layout of a timber building is brought back to a simple form. As indicated in Figure 4.1, two building layouts are regarded. The two-bay structure of Figure 4.1a features only two-span floors running over two floor fields. The three-bay structure features single-span and two-span floors in a so-called *staggered* layout, alternating single- and two-span floors behind and next to each other. The staggered layout is assessed because buildings can have features in their floorplan design that make it impossible to use continuous floors only. If three floor-bays are aligned, and no element lengths are available to span the entire structure, the staggered structure, as shown in Figure 4.1b, can still be realized. While the single-span

floors will not be able to form a second load path in case of an accident, there are always continuous floor elements adjacent to the single-span floors that can redistribute the loads. Figure 4.1b highlights a few single-span and double-span floors to visualize the staggered pattern better.

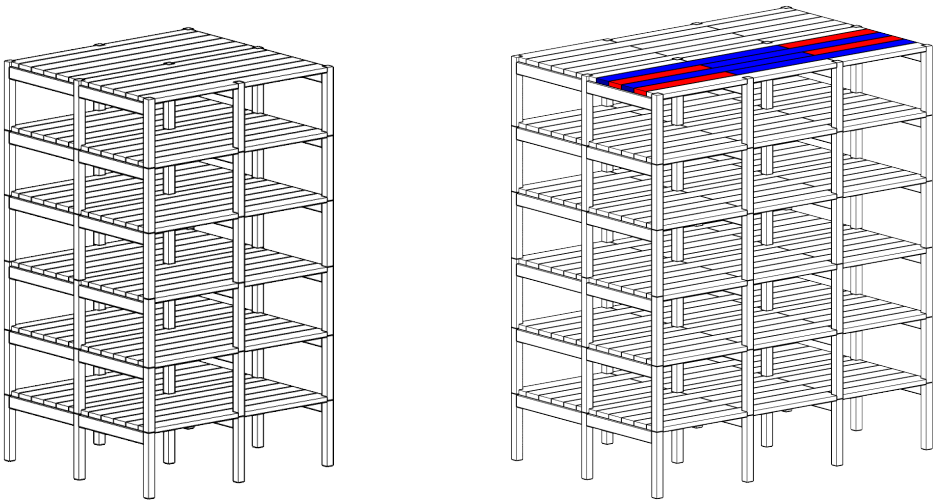

(a) two-bay structure, continuous floors

(b) three-bay structure, staggered floors

Figure 4.1: Simple representation of analyzed structural typologies

Although timber floor elements are connected in practice (e.g., to redistribute horizontal wind loads), they will be regarded as separate elements adjacent to each other for performance in accidental scenarios. It is not likely that the connecting plates (for wind load redistribution) have sufficient capacity to keep the floor elements working together in accidental scenarios.

The calculations are validated by comparing the results with SCIA models in the fundamental and accidental states for multiple spans. The results of this comparison can be found in Appendix E.

4.2 Notional column removal

The approach to analyze the robustness of the chosen typology will be by notional removal of columns. The notional sudden removal of columns does include dynamic load amplification effects while remaining a load-independent analysis strategy [26].

As found by Qian and Li [11], when a column of a multistory frame building is lost, all floors above deform simultaneously and with similar damage at each floor level. This indicates that all floors together redistribute the loads that were up until recently carried by the lost column. Thus, if the type of structural elements, their dimensions, and the loads at each floor level are similar, the performance of the complete structure in column loss scenarios can be assessed by analyzing the performance of one story level, as long as the applicable boundary conditions are correct.

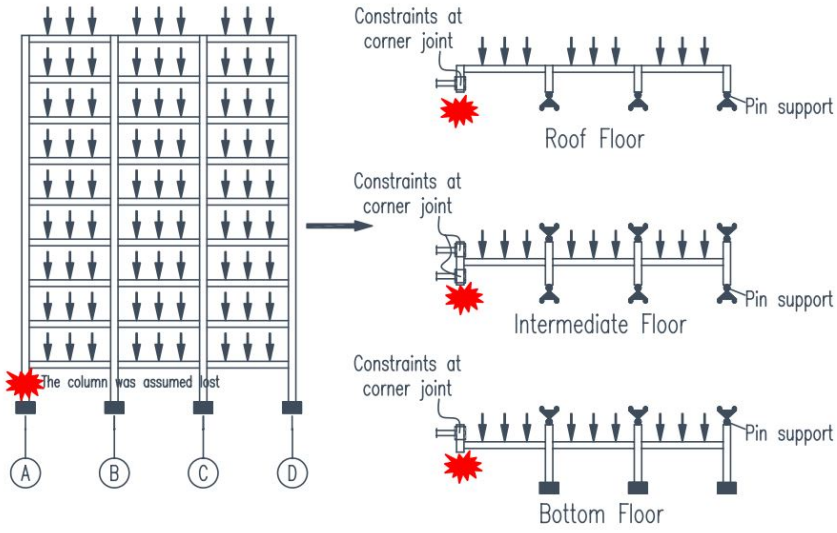

Figure 4.2: Representing a frame building as single story substructures [11]

Since the dynamically amplified load at the loss of a column is taken by full-timber linear elastic floor elements, the DLF is regarded as 2.0 (see Section 3.5).

Since the objective is to see the performance of different types of floors and for several floor spans, a framework is constructed to evaluate the structural elements' performance per design criterion for multiple floor spans and floor types. The criteria for which the timber elements are designed and checked are described in Chapter 5, followed by an elaboration of how the calculations result in an overview that indicates the extent of robustness. An elaborated example of the calculations for one floor span and element size can be found in Appendix B.

Chapter 5

Structural analysis

This chapter presents and elaborates on the structural analysis conducted to assess the feasibility of a secondary load path via two-span timber floor elements in column removal scenarios. The floor elements types regarded in the analysis are described in Section 5.1. The dimensioning of floor elements for standard design criteria is elaborated in Section 5.2. The capacity demands of the floor elements in the accidental scenarios are elaborated in Section 5.3. The required element sizes obtained in Sections 5.2 and 5.3 indicate if the floor elements can provide a secondary load path in accidental column loss scenarios and, if so, at what additional material cost compared to the standard design criteria. The capacity demands of adjacent structural elements (beams, connections, and columns) are compared in the standard and accidental design states in Section 5.4. Figure 5.1 provides a graphical overview of the analysis performed in each section.

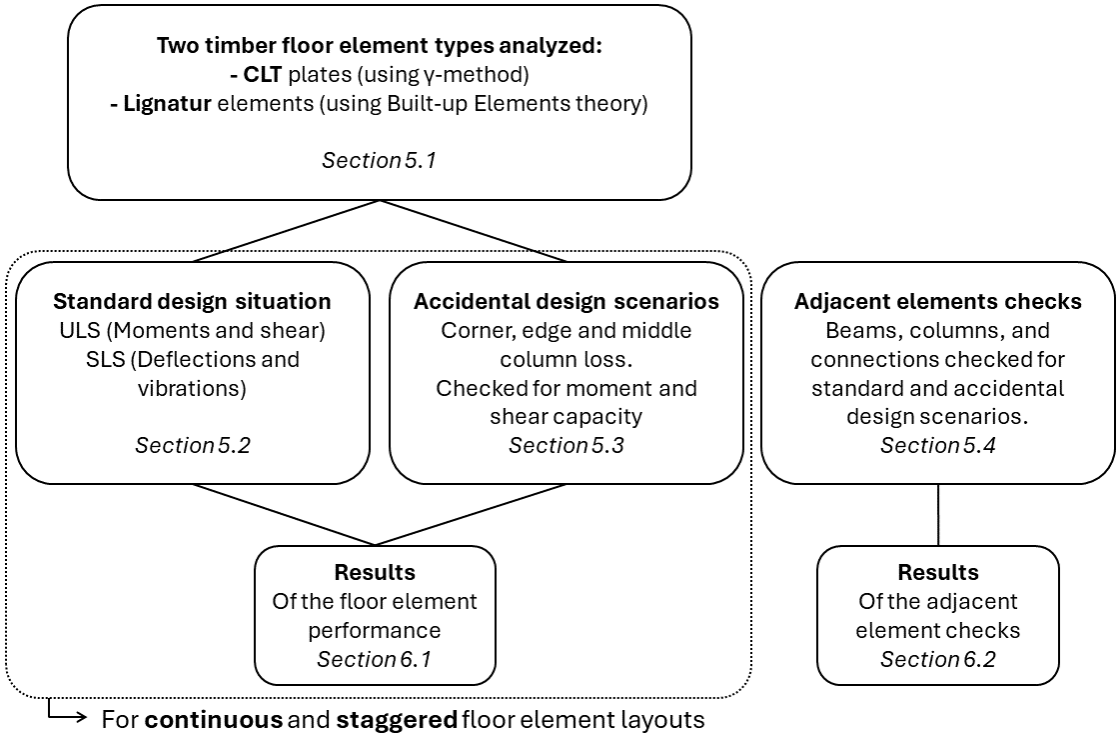

Figure 5.1: Overview of the calculations performed for the structural analysis.

5.1 Floor elements used in analysis

The analyzed timber floor element types are box floor elements (based on elements produced by Lignatur [13]) and CLT plate elements (based on the products of manufacturer Derix [41]), as visualized in Figures 5.2 and 5.3. The additional mass of service and comfort layers for both floor types is considered based on the layers presented in Figures 5.2 and 5.3. Appendix A gives a complete overview of the floor element configurations. Since engineered wood products like CLT and Lignatur elements are manufactured using planks of wood that are glued together in height and length to form structural elements, the dimensions of such elements are well customizable. This allows for long elements to be constructed, which lend themselves well to span multiple floor bays.

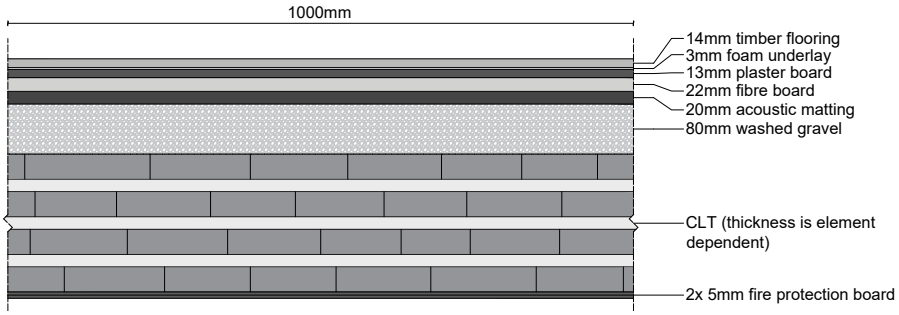

Figure 5.2: Reference configuration used for the CLT elements, adapted from [12]

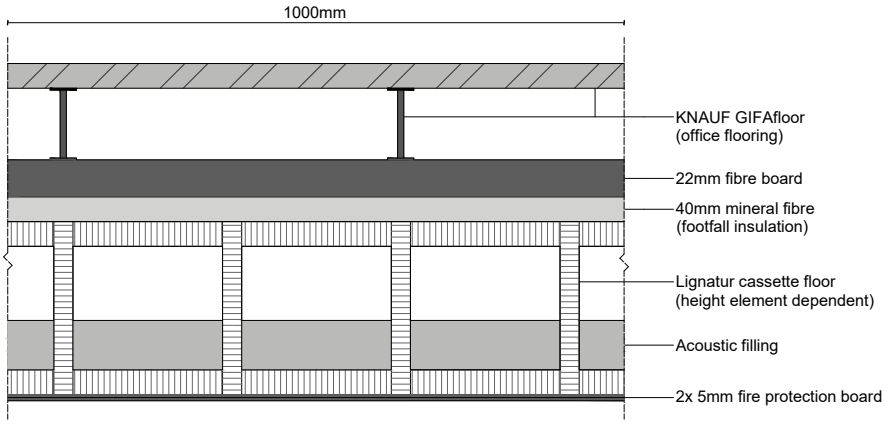

Figure 5.3: Reference Lignatur configuration for the box floor elements, adapted from [13]

5.1.1 Material properties

The timber strength grading class C24 is used for the Lignatur box floor elements and CLT plate elements [13, 12]. The material properties of C24 timber are given in Table 5.1.

Table 5.1: Material properties C24 timber [12] [15]

Characteristic strength values	**[MPa]**
Bending strength $f_{y,k}$	24
Tensile strength along the grain $f_{t,0,k}$	14.5
Tensile strength perpendicular to the grain $f_{t,90,k}$	0.4
Compressive strength along the grain $f_{c,0,k}$	21
Compressive strength perpendicular to the grain $f_{c,90,k}$	2.5
Shear strength $f_{v,k}$	4.0
Rolling shear strength $f_{v,r,k}$	1.1
Stiffness values	**[MPa]**
Mean value of modulus of elasticity, along the grain $E_{m,0,mean}$	11000
Fifth percentile value of modulus of elasticity, along the grain $E_{m,0,05}$	7400
Mean value of modulus of elasticity, perpendicular to the grain $E_{m,90,mean}$	370
Mean value of the shear modulus G_{mean}	690
Density	**[kg/m^3]**
Fifth percentile volume of density ρ_k	350
Mean density ρ_{mean}	420

5.1.2 Moment resistance box floor elements

The moment resistance of the Lignatur box floor elements is considered using the theory of build-up elements, as described by Jorissen [14]. This method evaluates the strains, stresses, and inter-layer relations of each part of a so-called built-up element, a structural element consisting of smaller elements combined using adhesives or fasteners. The cassette floors in this research are assessed as multiple I-shaped profiles combined into cassette-shaped elements of one meter in width, as visualized in Figure 5.4. The (glued) connection between the elements is assumed to be fully connected.

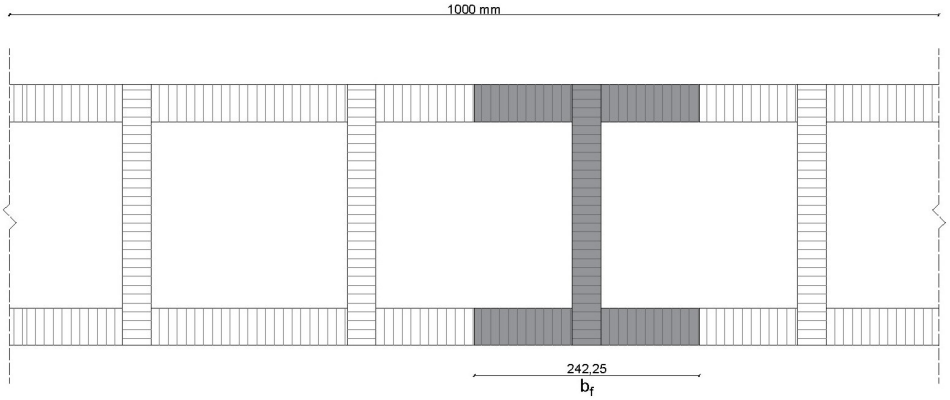

Figure 5.4: Box floor assessed as multiple build-up elements

The width of each of the *fictive* I-profile-shaped build-up elements is $242.25\ [mm]$ [13]. For ease of calculation, the box floor elements are regarded as having a width of $1\ [m]$. Just over four I-profile-shaped elements fit in a box element of $1\ [m]$ width ($1000/242.25 \approx 4.13$).

For a conservative value of the structural performance of the box floors, the structural performance of the I-profile-shaped element is multiplied by 4.0 for the performance per meter width.
Using the theory of build-up elements, the strains indicated in Figure 5.5 are calculated, from which the normal stresses and shear stresses at the critical locations are calculated. By analyzing the structural performance of the elements at the maximum allowable stress levels in the governing element, maximum loads on the Lignatur box floor element are calculated for each configuration. The stresses in the *fictive* I-profile-shaped elements are given by Equations (8).

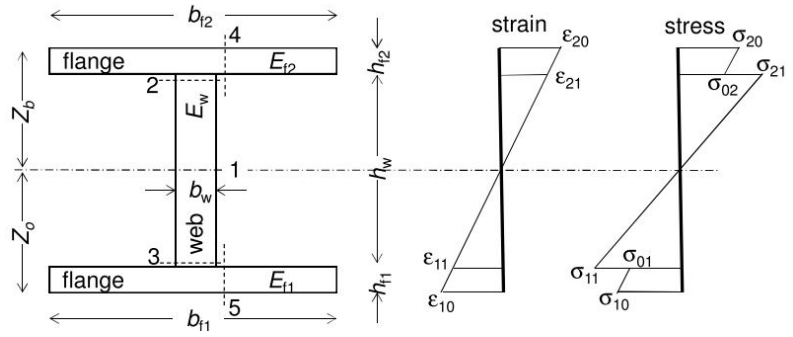

Figure 5.5: Distances and terminology for the assessment of a build-up element [14]

$$
\begin{aligned}
\sigma_{10} &= \frac{E_1 Z_O}{EI} \cdot M \\
\sigma_{11} &= \frac{E_1 (Z_O - h_1)}{EI} \cdot M \\
\sigma_{01} &= \frac{E_0 (Z_O - h_1)}{EI} \cdot M \\
\sigma_{02} &= \frac{E_0 (Z_B - h_2)}{EI} \cdot M \\
\sigma_{21} &= \frac{E_2 (Z_B - h_2)}{EI} \cdot M \\
\sigma_{20} &= \frac{E_2 Z_B}{EI} \cdot M
\end{aligned}
\tag{8}
$$

Where:

σ_{ij}	=	normal stress in element i al location j, see Figure 5.5	$[N/mm^2]$
Z_O	=	distance from bottom of the cross-section to the neutral axis	$[mm]$
Z_B	=	distance from top of the cross-section to the neutral axis	$[mm]$
h_i	=	height of element i	$[mm]$
E_i	=	young's Modulus corresponding to location i	$[N/mm^2]$
I	=	moment of inertia of the cross-section	$[mm^4]$
M	=	bending moment	$[Nmm]$

Since $E = E_0 = E_1 = E_2 = 11000$ [MPa], E_0, E_1 and E_2 are omitted in Equations (8). By computing the applicable tensile or compression design strengths in Equations (8), the maximum bending capacity for each of the regarded Lignatur box elements is calculated. The maximum moment capacities, combined with the load calculations of Section 5.1.6 for the loads, Sections 5.2.1 and 5.3.1 for the load combinations and Section 5.3.2 for the moment distributions, result in required element dimensions for the fundamental and accidental load combinations for all regarded floor spans.

5.1.3 Shear stresses in the box floor elements

The shear stresses in the Lignatur box floor elements are calculated using the build-up elements method, as described by Jorissen [14]. Using the method of build-up elements, the shear stresses in each part of the element and their interfaces can be assessed. In Figure 5.6, the relevant distances, terms, and locations for the calculation of the shear stresses are illustrated.

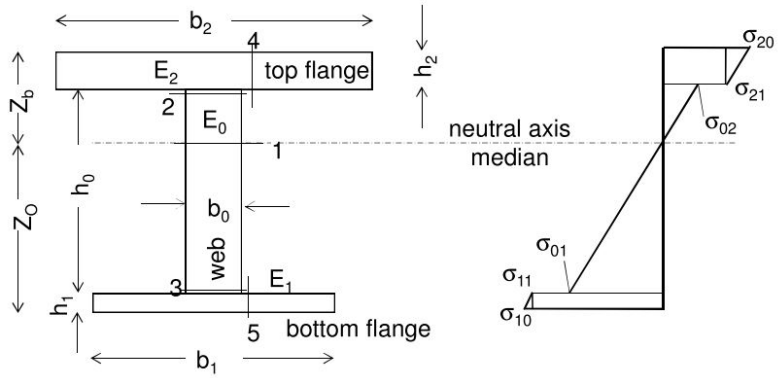

Figure 5.6: Distances and relevant location for shear stress checks [14]

To calculate the shear stresses at the critical intersections and locations 1-5 indicated in Figure 5.6, Equations (9) are used [14].

$$
\begin{aligned}
\sigma_{v,1} &= \frac{E_2\,(2Z_b - h_2)\,b_2 h_2 + E_0\,(Z_b - h_2)^2\,b_0}{2EI\,b_0} \cdot Q \\
\sigma_{v,2} &= \frac{E_2\,(2Z_B - h_2)\,b_2 h_2}{2EI\,b_0} \cdot Q \\
\sigma_{v,3} &= \frac{E_1\,(2Z_O - h_1)\,b_1 h_1}{2EI\,b_0} \cdot Q \\
\sigma_{v,4} &= \frac{E_2\,(2Z_B - h_2)(b_2 - b_0)}{4EI} \cdot Q \\
\sigma_{v,5} &= \frac{E_1\,(2Z_O - h_1)(b_1 - b_0)}{4EI} \cdot Q
\end{aligned}
\tag{9}
$$

Where:

$\sigma_{\mathrm{v,i}}$	=	shear stress at location i, see Figure 5.6	$[N/mm^2]$
Z_{O}	=	distance from bottom of the cross-section to the neutral axis	$[mm]$
Z_{B}	=	distance from top of the cross-section to the neutral axis	$[mm]$
h_{i}	=	height of element i	$[mm]$
b_{i}	=	width of element i	$[mm]$
E_{i}	=	young's Modulus corresponding to location i	$[N/mm^2]$
I	=	moment of inertia of the cross-section	$[mm^4]$
Q	=	maximum shear force	$[N]$

Since $E_0 = E_1 = E_2 = 11000$ [MPa], E_0, E_1 and E_2 are also omitted in Equations (9). The shear stresses acting in the elements are checked with the shear strength of the used C24 timber, resulting in a Unity Check for the shear forces. If the design shear stresses at each location i are lower than the design shear strength, the unity check is fulfilled, as indicated in Equation (11).

$$\frac{\sigma_{v,i,d}}{f_{v,d}} \leq 1.0 \tag{10}$$

The design shear strength $f_{v,d}$ is calculated using Equation (11):

$$f_{v,d} = k_{mod} \cdot \frac{f_{v,k}}{\gamma_M} \tag{11}$$

Where:

k_{mod}	=	0.8	[-]	(medium term load duration, [34])
k_{mod}	=	1.1	[-]	(very short load duration, [34])
$f_{v,k}$	=	4.0	$[N/mm^2]$	see table 5.1
γ_M	=	1.25	[-]	(standard partial factor, [32])
γ_M	=	1.0	[-]	(accidental combination partial factor, [32])

Design shear strength $f_{v,d}$ for the fundamental load combination:

$$f_{v,d} = 1.92 \quad [N/mm^2] \tag{12}$$

Design shear strength $f_{v,d,acc}$ for the accidental load combination:

$$f_{v,d,acc} = 4.4 \quad [N/mm^2] \tag{13}$$

The unity check for the shear stresses in the box floor elements is performed for all spans and configurations in both the fundamental and accidental load combinations. The calculations are checked using the examples given in the *Timber Structures - Build-up elements* reader by Jorissen [14].

5.1.4 Moment resistance CLT floor elements

Cross-laminated timber is a two-dimensional engineered timber product consisting of multiple layers of timber boards glued together at perpendicular angles to another [15]. The glued boards form plates with increased cross-grain dimensional stability [16] that can be used as walls, roofs, and floors.

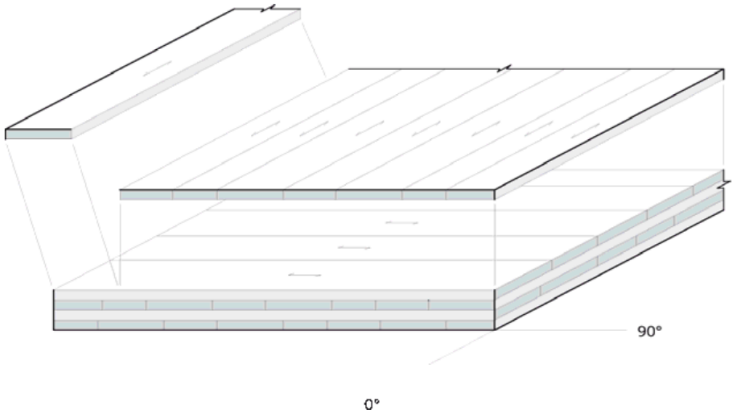

Figure 5.7: CLT element, built-up from glued timber boards [15]

With each layer placed perpendicular to the adjacent layer, not all timber boards are orientated parallel to the span direction. This means that part of the timber is loaded in its weaker (transverse) direction. Since the stiffness in the transverse direction is much lower than the stiffness in the longitudinal direction, the stiffness contribution by layers loaded perpendicular to the grain is assumed to be zero. In Figure 5.8, the stiffness in each layer and the corresponding regarded stresses are visualized.

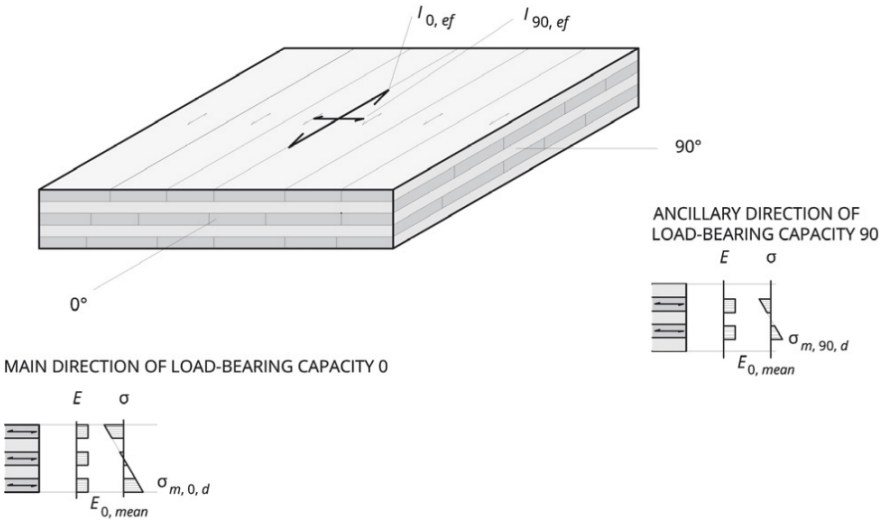

Figure 5.8: Only layers in the span direction of the CLT element contribute structurally [15]

Since only the layers running in parallel with the span should be regarded for the structural performance of a CLT element, a *net* cross-section modulus W_{net} is assessed for the ULS checks, featuring only longitudinally orientated parts of the CLT plate. For enhanced bending moment resistance, multiple layers running in longitudinal orientation can be placed adjacent to each other. To calculate the net moment resistance W_{net} of CLT elements with up to three longitudinally orientated layers, Equation (14) is used [12]. The equation of W_{net} features the total of the sum of the second moment of area of each layer and the sum of the "Steiner" contribution of each layer, meaning the surface area of each layer multiplied by the squared distance of each centroid to the section's neutral axis.

$$W_{\text{net}} = \left(\sum_{i=1}^{n} (I_i) + \sum_{i=1}^{n} \left(A_i e_i^2 \right) \right) / z_s \tag{14}$$

Where:

W_{net}	=	net section modulus of CLT element	$[mm^3]$
I_{i}	=	second moment of area of layer i	$[mm^4]$
A_{i}	=	sectional area of layer i	$[mm^2]$
e_{i}	=	distance from centroid of layer i to neutral axis of the element	$[mm]$
z_{s}	=	distance from center of the element to the edge	$[mm]$

The distance e_{i} is visualized in Figure 5.9.

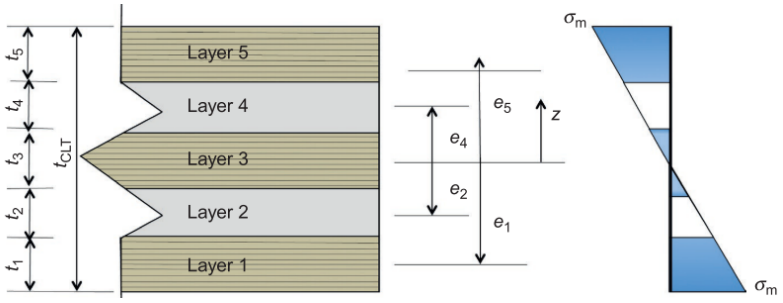

Figure 5.9: Distances and terminology for the assessment of a CLT element [16]

Since the elastic modulus E_i of layers transverse to the span direction is assumed to be zero, only longitudinally orientated timber boards will contribute to the net section modulus W_{net} from equation (14).

In the net section modulus W_{net} given in Equation (14), only the contribution of the longitudinally orientated timber boards is considered. For the deflection calculation, the transverse layers' shear deformation does need to be considered. The extra deformation by shear of the transverse layers is accounted for by applying a reduction factor γ_i to each of the longitudinal layers, which is done using the γ-method. The reduction factor γ_i reduces the "Steiner" part of Equation (14) depending on the span and the properties and the configuration of the transverse layers [12].

$$\gamma_1 = \frac{1}{\left(1 + \frac{\pi^2 \cdot E \cdot A_1}{\ell_{ref}{}^2} \cdot \frac{d_{1,2}}{b \cdot G_{R,12}}\right)} \left[\frac{1}{m}\right] \tag{15}$$

$$\gamma_2 = 1,0 \left[\frac{1}{m}\right] \tag{16}$$

$$\gamma_3 = \frac{1}{\left(1 + \frac{\pi^2 \cdot E \cdot A_3}{\ell_{ref}{}^2} \cdot \frac{d_{2,3}}{b \cdot G_{R,23}}\right)} \left[\frac{1}{m}\right] \tag{17}$$

Where:

γ_i	=	gamma reduction factor for longitudinal layer i	$[\frac{1}{m}]$
l_{ref}	=	reference length of the element	$[m]$
$G_{R,ij}$	=	rolling shear modulus of layer i, j	$[kN/m^2]$
b	=	width of the structural element	$[m]$
$d_{i,j}$	=	thickness of longitudinal layer i	$[m]$

The γ-method yields direct calculation methods for 3-layer and 5-layer CLT but gets more in-depth for CLT elements with 7 layers or more [12]. This more in-depth method is called the extended γ-method [15].

The extended γ-method calculations are based on the method described by Wallner-Novak, Koppelhuber, and Pock in their *Cross-Laminated Timber Structural Design* publication [15]. The calculation becomes more extensive since flexibility in relation to the adjacent layers is now combined with flexible coupling to longitudinal layers further away. For the extended γ-method, the overall center of gravity is calculated first:

$$z_s = \frac{\sum_{i=1}^{n} \frac{E_i}{E_c} \cdot b \cdot d_i \cdot o_i}{\sum_{i=1}^{n} \frac{E_i}{E_c} \cdot b \cdot d_i} \tag{18}$$

Where:

z_s	=	distance between upper edge and overall center of gravity	$[m]$
E_i	=	elastic modulus of layer i	$[kN/m^2]$
E_c	=	reference value for the elastic modulus	$[kN/m^2]$
b	=	width of the structural element	$[m]$
d_i	=	thickness of longitudinal layer i	$[m]$
o_i	=	distance from centroid of longitudinal layer i to the upper edge	$[m]$

The linear equation system to solve is as follows:

$$[V] \cdot \gamma = s \tag{19}$$

$$\begin{bmatrix} v_{1,1} & v_{1,2} & 0 & 0 & 0 \\ v_{2,1} & v_{2,2} & v_{2,3} & 0 & 0 \\ 0 & v_{3,2} & v_{3,3} & v_{3,4} & 0 \\ 0 & 0 & \cdots & \cdots & \cdots \\ 0 & 0 & 0 & v_{m,m-1} & v_{m,m} \end{bmatrix} \cdot \begin{bmatrix} \gamma_1 \\ \gamma_2 \\ \gamma_3 \\ \vdots \\ \gamma_m \end{bmatrix} = \begin{bmatrix} s_1 \\ s_2 \\ s_3 \\ \vdots \\ s_m \end{bmatrix} \tag{20}$$

For the left-hand side of Equation (20) holds:

$$C_{j,k} = \frac{b \cdot G_{R,jk}}{d_{j,k}} \tag{21}$$

$$D_i = \frac{\pi^2 \cdot E_i \cdot b \cdot d_i}{\ell_{ref}^2} \tag{22}$$

$$v_{i,i-1} = -C_{i-1,i} \cdot a_{i-1} \tag{23}$$

$$v_{i,i} = \left(C_{i-1,i} + C_{i,i+1} + D_i\right) \cdot a_i \tag{24}$$

$$v_{i,i+1} = -C_{i,i+1} \cdot a_{i+1} \tag{25}$$

For the right-hand side of equation (20) holds:

$$s_i = -C_{i,j+1} \cdot (a_{i+1} - a_i) + C_{i-1,i} \cdot (a_i - a_{i-1}) \tag{26}$$

As an example, for a seven-layer CLT element (with four longitudinally orientated layers), the linear equation system is given by Equation (27):

$$\begin{bmatrix} v_{1,1} & v_{1,2} & 0 & 0 \\ v_{2,1} & v_{2,2} & v_{2,3} & 0 \\ 0 & v_{3,2} & v_{3,3} & v_{3,4} \\ 0 & 0 & v_{4,3} & v_{4,4} \end{bmatrix} \cdot \begin{bmatrix} y_1 \\ y_2 \\ y_3 \\ y_4 \end{bmatrix} = \begin{bmatrix} s_1 \\ s_2 \\ s_3 \\ s_4 \end{bmatrix} \tag{27}$$

After inserting equations (21) - (26) in to equation (27):

$$\begin{bmatrix} \left(C_{1,2} + D_1\right) \cdot a_1 & -C_{1,2} \cdot a_2 & 0 & 0 \\ -C_{1,2} \cdot a_1 & \left(C_{1,2} + C_{2,3} + D_2\right) \cdot a_2 & -C_{2,3} \cdot a_3 & 0 \\ 0 & -C_{2,3} \cdot a_2 & \left(C_{2,3} + C_{3,4} + D_3\right) \cdot a_3 & -C_{3,4} \cdot a_4 \\ 0 & 0 & -C_{3,4} \cdot a_3 & \left(C_{3,4} + D_4\right) \cdot a_4 \end{bmatrix} \cdot \begin{bmatrix} y_1 \\ y_2 \\ y_3 \\ y_4 \end{bmatrix} =$$

$$\begin{bmatrix} -C_{1,2} \cdot (a_2 - a_1) \\ -C_{2,3} \cdot (a_3 - a_2) + C_{1,2} \cdot (a_2 - a_1) \\ -C_{3,4} \cdot (a_4 - a_3) + C_{2,3} \cdot (a_3 - a_2) \\ C_{3,4} \cdot (a_4 - a_3) \end{bmatrix} \tag{28}$$

The γ-values can be obtained by rewriting the linear equation system of Equation (19) into Equation (29):

$$\gamma = [V]^{-1} \cdot s \tag{29}$$

After obtaining the γ-values, the effective moment of inertia I_{ef} can be calculated using:

$$I_{ef} = \sum_{i=1}^{4} \frac{E_i}{E_c} \cdot \frac{b \cdot d_i^3}{12} + \sum_{i=1}^{4} y_i \cdot \frac{E_i}{E_c} \cdot b \cdot d_i \cdot a_i^2 \tag{30}$$

5.1.5 Rolling shear CLT

The γ-method accounts for the shearing of transverse layers for the deflection of CLT elements. Separate calculations are required to check whether these transverse layers can actually take the applied shear forces. Since these shear forces are applied perpendicularly to the timber grain, failure is caused by a break tangential to the annual rings, as visualized in Figure 5.10. The strength related to this behavior is called *rolling strength* $(f_{R,k})$, and the strength value is typically about one-third of the shear strength parallel to the grain [15].

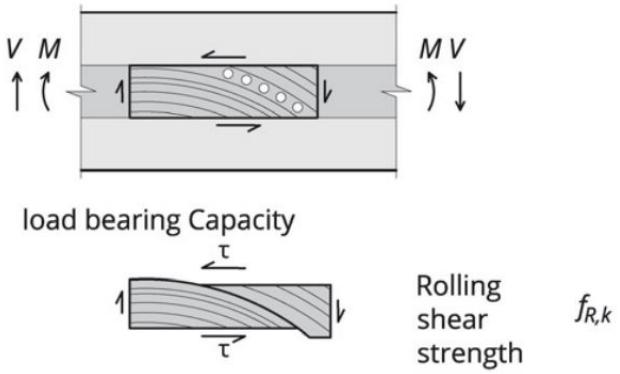

Figure 5.10: Rolling shear in the timber boards [15]

For the CLT element to withstand the applied rolling shear, the structure should meet the following requirement:

$$\tau_{v,R,d} \leq f_{v,R,d} \tag{31}$$

Where:

$\tau_{v,R,d}$	=	rolling shear design stress	$[N/mm^2]$
$f_{v,R,d}$	=	rolling shear design strength	$[N/mm^2]$

The rolling shear design stress $\tau_{v,R,d}$ is calculated using Equation (32) [15]:

$$\tau_{v,R,d} = \frac{V_{0,d} \cdot S_{0,R,net}}{I_{0,net} \cdot b} \tag{32}$$

Where:

$V_{0,d}$	=	design shear force	$[N]$
$S_{0,R,net}$	=	net static moment	$[mm^3]$
$I_{0,net}$	=	net moment of inertia	$[mm^4]$
b	=	width of the element $(= 1000mm)$	$[mm]$

The net static moment $S_{0,R,net}$ is calculated using Equation (33) [12]:

$$S_{0,R,net} = \sum_{i=1}^{m_L} b \cdot t_i \cdot a_i \tag{33}$$

Where:

b	=	width of the element $(= 1000mm)$	$[mm]$
t_i	=	thickness of longitudinal layer i	$[mm]$
a_i	=	distance from centroid of layer i to neutral axis of the element	$[mm]$

On the *resistance* side of Equation (31), the rolling shear design strength $f_{v,R,d}$ is obtained using Equation (34).

$$f_{v,R,d} = k_{mod} \cdot \frac{f_{v,R,k}}{\gamma_M} \tag{34}$$

Where:

k_{mod}	=	modification factor for load duration and moisture content	[-]
$f_{v,R,k}$	=	characteristic rolling shear strength	$[N/mm^2]$
γ_M	=	material factor	[-]

The material factor γ_M is 1.25 for glued laminated timber in the standard load combinations and is lowered to 1.00 in the accidental combination [34, 30]. The values for k_{mod} depend on the load duration: 0.6 for permanent, 0.8 for the combination of permanent and live load, 0.9 for short and 1.1 for very short load duration [34]. The increase of k_{mod} and reduction of γ_M for the very short (dynamic) load peak resulting from the loss of a column result in a momentarily increased rolling shear strength by a factor 2.3 compared to the permanent load situation.

5.1.6 Loads on the structure

The loads regarded in the calculations are:

- Permanent action
  - Dead weight of the structural floor elements.
  - Dead weight of material in the service layers on the floor elements for (acoustic) comfort, fire safety, and usability.
  - Dead weight of the facade.
- Variable action
  - Imposed loads on the structure by usage type.

The variable action is regarded as $q_k = 3.0\ [kN/m^2]$, which corresponds to the variable load governing in office buildings ($2.5\ [kN/m^2]$) and an added $0.5\ [kN/m^2]$ for removable partition walls according to the *Dutch Annex* of *Eurocode 1: Actions on Structures* [42]. Since the value of the load for the variable action in offices is also governing for school buildings, and it is slightly higher than for dwellings [42], using the office variable action value gives a

relatively non-specific indication for the robustness of timber buildings that should hold for various functions.

To take into account the weight of the facade, a load of $1.0\ kN/m^2$ is assumed per meter of story height [39] and the story height is set to 3 $[m]$. What area of the facade is taken by which floor element in case of the loss of a corner column is elaborated in Section 5.3.2. As described in Section 3.5, the regarded Dynamic Load Factor is 2.0 in the column loss scenarios in this research.

As the accidental load at the loss of a structural element is amplified dynamically only briefly, the load will be regarded with a *very short* load duration [32]. The load duration determines the strength value of the used structural material. The situation immediately after the dynamically amplified response of the structure will be regarded as a *short* load duration, listed in the *Eurocode for Design of Timber Structures* as load duration up to one week [34].

5.2 Standard design situation

The standard design situation will provide the required structural element height for the floor elements in the *normal* (non-accidental) load situation. The required dimensions of the floor elements in the standard situation are of interest to compare to the demands in the accidental scenarios calculated in Section 5.3. The required structural height of the floor elements in the standard design situation and the accidental scenarios will be compared in Chapter 6 Results.

5.2.1 Standard load combination

The load combinations described in *Eurocode 0* yield the applicable loads acting on the assessed structure [30]. For the validation of the strength of the elements in the structure, the loads are calculated using the least favorable of equations (6.10a) and (6.10b) from *Eurocode 0* [30]:

$$E_d = \begin{cases} \sum_{j\geq 1} \gamma_{\mathrm{G},j} G_{\mathrm{k},j} + \gamma_{\mathrm{P}} P + \gamma_{\mathrm{Q},1} \psi_{0,1} \mathrm{Q}_{\mathrm{k},1} + \sum_{i>1} \gamma_{\mathrm{Q},i} \psi_{0,i} \mathrm{Q}_{\mathrm{k},i} \\ \sum_{j\geq 1} \xi_j \gamma_{\mathrm{G},j} G_{\mathrm{k},j} + \gamma_{\mathrm{P}} P + \gamma_{\mathrm{Q},1} \mathrm{Q}_{\mathrm{k},1} + \sum_{i>1} \gamma_{\mathrm{Q},i} \psi_{0,i} \mathrm{Q}_{\mathrm{k},i} \end{cases} \tag{35}$$

Where:

$\gamma_{\mathrm{G},j}$	=	partial factor for the permanent load j	[-]
$G_{\mathrm{k},j}$	=	characteristic value of the permanent load j	$[kN/m^2]$
γ_{P}	=	partial factor of the prestress load	[-]
P	=	characteristic value of the prestress load	$[kN]$
$\gamma_{\mathrm{Q},1}$	=	partial factor for the variable load	[-]
$\psi_{0,1}$	=	factor to combine the value of the variable load	[-]
$\mathrm{Q}_{\mathrm{k},1}$	=	characteristic value of the dominant variable load	$[kN/m^2]$
$\gamma_{\mathrm{Q},i}$	=	partial factor for the variable load	[–]
$\mathrm{Q}_{\mathrm{k},i}$	=	characteristic value of variable load i	$[kN/m^2]$
ξ_j	=	reduction factor	[-]

Since no prestress is applied in the assessed structure, and only one variable load is present on the floor elements, Equations (35) reduce to:

The least favorable of:

$$E_d = \begin{cases} \gamma_{\mathrm{G},j} G_{\mathrm{k},j} + \gamma_{\mathrm{Q},1} \psi_{0,1} \mathrm{Q}_{\mathrm{k},1} \\ \xi_j \gamma_{\mathrm{G},j} G_{\mathrm{k},j} + \gamma_{\mathrm{Q},1} \mathrm{Q}_{\mathrm{k},1} \end{cases} \tag{36}$$

The permanent load $G_{k,j}$ depends on the dimensions of the floor elements. To incorporate this into the calculations, the weight of the floor elements is described as a function of their height. All layers that do not depend on the structural height (for instance, acoustic or convenience layers) remain the same for each floor height. The mass of the layers dependent on the dimensions of the elements, such as the ribs in the box floors and the total timber slab thickness for CLT, is described as a function of the structural height to consider accurately by Equation (37). In Figures 5.3 and 5.2, the dimensions of the layers that depend on the height of the structural elements are indicated as *element dependent*. The height-dependent value for the permanent load of the floor elements is given by Equation 37.

$$G_{\mathrm{k,j}} = G_{\mathrm{k,j,nhd}} + h_{\mathrm{str}} \cdot G_{\mathrm{k,j,hd}} \tag{37}$$

Where:

$G_{\mathrm{k,j}}$	=	characteristic value of the permanent load j	$[kN/m^2]$
$G_{\mathrm{k,j,nhd}}$	=	permanent load not depending on structural height	$[kN/m^2]$
h_{str}	=	varying height for elements governing the structural performance	$[m]$
$G_{\mathrm{k,j,hd}}$	=	permanent load depending on structural height	$[kN/m^2/m]$

For an overview of the assessed CLT and box floor elements regarded in the calculations, see Appendix A.

5.2.2 Deflection

To calculate the deflections of the floor elements, formulae for the deflection of continuous beams are used. For convenience of the calculations, the floor elements are regarded as strips with a width of 1 meter. Since the assessed elements are continuous, spanning over three supporting beams, the permanent load is always applied on both floor fields. The variable load has to be regarded for both floor fields, as well as being applied on only one of the floor fields. The difference between applying the variable load on both or on only one floor field can be seen in Figure 5.11.

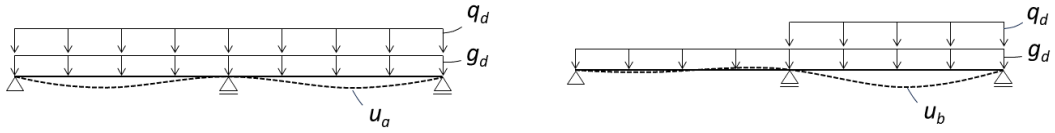

(a) Both loads on both floor areas (b) Live load on a single floor area

Figure 5.11: The two load configurations to assess the deflection of continuous floor elements.

The maximum deflection for a distributed load over two adjacent floor fields is described by Equation (38) [43].

$$u_{\mathrm{a}} = \frac{1}{185} \frac{q l^4}{EI} \tag{38}$$

The maximum deflection for a distributed load on a single floor field for a continuous beam over three supports is given by Equation (39) [44].

$$u_{\mathrm{b}} = 0.00911 \frac{ql^4}{EI} \tag{39}$$

As timber structures experience creep behavior, increasing deflections over time even without increasing the load level, the so-called "final" deflection u_{fin} of timber elements is larger than the instantaneous deflection. To account for this effect, k_{def} factors are applied, which increase the instantaneous deflection for the relevant permanent and variable loads [34]:

$$u_{\mathrm{fin}} = u_{\mathrm{fin,G}} + u_{\mathrm{fin,Q_1}} + \sum u_{\mathrm{fin,Q_i}} \tag{40}$$

The final deflection by the permanent load G:

$$u_{\mathrm{fin,G}} = u_{\mathrm{inst,G}} \left(1 + k_{\mathrm{def}}\right) \tag{41}$$

The final deflection by the governing variable load Q_1:

$$u_{\mathrm{fin,Q,1}} = u_{\mathrm{inst,Q,1}} \left(1 + \varphi_{2,1} k_{\mathrm{def}}\right) \tag{42}$$

Since the deflection in Figure 5.11a is caused by two loads both acting on both floor areas, the final deflection can be found by applying Equation (38) for both the permanent load (g_{d}) and the variable load (q_{d}).

$$u_{\mathrm{fin},1} = \frac{1}{185} \frac{g_{\mathrm{d}} l^4}{EI} \left(1 + k_{\mathrm{def}}\right) + \frac{1}{185} \frac{q_{\mathrm{d}} l^4}{EI} \left(1 + \varphi_{2,1} k_{\mathrm{def}}\right) \tag{43}$$

The deflection of the structure in Figure 5.11b is caused by the permanent load acting on both floor areas, while the variable load only acts on one floor area. The final deflection is then governed by applying Equation (38) for the permanent load (g_{d}), and adding the deflection by the variable load (q_{d}) using Equation (39).

$$u_{\mathrm{fin},2} = \frac{1}{185} \frac{g_{\mathrm{d}} l^4}{EI} \left(1 + k_{\mathrm{def}}\right) + 0.00911 \frac{q_{\mathrm{d}} l^4}{EI} \left(1 + \varphi_{2,1} k_{\mathrm{def}}\right) \tag{44}$$

Since $0.00911 > \frac{1}{185}$ $(0.00911 > 0.00541)$, $u_{\mathrm{fin},2}$ is always larger than $u_{\mathrm{fin},1}$, meaning that $u_{\mathrm{fin},2}$ is the normative deflection. Thus, for the governing load case, the variable load is applied only on one of the two floors.

The maximum allowed deflection of the floor according to the *Dutch Annex* of *Eurocode 0* is [31]:

$$u_{\mathrm{max}} \leq \frac{l}{500} \tag{45}$$

Combining Equations (44) and (45) results into the normative equation for the maximum deflection of the floor elements:

$$\frac{1}{185} \frac{g_{\mathrm{d}} l^4}{EI} \left(1 + k_{\mathrm{def}}\right) + 0.00911 \frac{q_{\mathrm{d}} l^4}{EI} \left(1 + \varphi_{2,1} k_{\mathrm{def}}\right) \leq \frac{l}{500} \tag{46}$$

The total deflection of the floor is the combined deflection of the floor elements themselves and the deflection of the beams that support the floor elements, which should be

checked for the same deflection requirement u_{max} over the distance between two diagonal columns. The diagonal deflection requirement of combined deflection of the floor elements and the beams is given by Equation (47).

$$u_{\text{beam}} + u_{\text{floor}} \leq \frac{\sqrt{2} \cdot l}{500} \tag{47}$$

To check the deflection calculations, the calculated cross-sectional heights are compared to the recommended values in handbooks. The Lignatur box elements are checked using the Lignatur Workbook [13]. The CLT elements are checked using the supplier manual of DERIX [41]. As can be seen in Table 5.2, the demanded cross-section for the deflection requirement of Lignatur elements is slightly higher for the handbook than for the calculations. In the handbook, a deflection limit of $L/600$ is used, while the calculations are based on a deflection limit of $L/500$ is used. In Table 5.3, the calculations are also based upon $L/600$ deflection limit. Table 5.3 shows a good agreement between the calculated and handbook values.

Table 5.2: Comparing the calculated required element height for deflections with the recommended value from a Lignatur handbook

Floor span	3.0	3.5	4.0	4.5	5.0	5.5	6.0	6.5	7.0	7.5	8.0	8.5	9.0
Calculations	120	120	120	120	140	160	180	180	200	220	240	280	280
Handbook	120	120	120	140	160	180	220	240	240	240	280	-[1]	-[1]

Table 5.3: Comparing the calculated required element height for deflections with the recommended value from a Lignatur handbook, both for a $L/600$ deflection limit.

Floor span	3.0	3.5	4.0	4.5	5.0	5.5	6.0	6.5	7.0	7.5	8.0	8.5	9.0
Calculations	120	120	120	140	140	160	180	200	220	240	280	280	320
Handbook	120	120	120	140	160	180	220	240	240	240	280	-[1]	-[1]

[1] = table in handbook does not extent to this span.

Table 5.4: Comparing the calculated required element height for deflections with the recommended value from a CLT handbook.

Floor span	3.0	3.5	4.0	4.5	5.0	5.5	6.0	6.5	7.0	7.5	8.0	8.5	9.0
Calculations	80	120	120	120	150	150	180	180	220	220	220	250	280a
Handbook	80	120[2]	120[2]	120[2]	120	150[2]	180[2]	180[2]	180	-[1]	-[1]	-[1]	-[1]

[2] = table in handbook states element height not selected for calculations, therefore the first higher element size that is used in the calculations is stated in the table.

The required cross-sectional heights stated in the CLT supplier manual of DERIX [41] are comparable to but often lower than the calculated required cross-section. The difference can be explained by the deviating deflection limits assessed in the manual ($w_{inst} \leq L/350, w_{fin} \leq L/150$ and $w_{net,fin} \leq L/250$) and the calculations ($w_{fin} \leq L/500$).

5.2.3 Vibrations

Zhang and Kilpatrick [45] developed an analytical approach to assess the first modal frequency of the two-span floors and check the corresponding requirements for structural vibrations, yielding Equation (48) [45] to be solved for the first modal frequency of the two-span floors.

$$f_1 = \frac{(\beta_1 L)^2}{2\pi L^2}\sqrt{\frac{(EI)_L}{m}} \tag{48}$$

Where:

f_1	=	first modal frequency of the two-span floor	$[Hz]$
$\beta_1 L$	=	frequency parameter for the first mode (depending on BC's)	[-]
L	=	floor span	$[m]$
$(EI)_L$	=	equivalent bending stiffness per meter width	$[Nm^2/m]$
m	=	total self weight floor per square meter	$[kg/m^2]$

Eurocode 5 for the design of timber structures prescribes a minimum first frequency (for dwelling floors) of 8 Hz (Equation (49)), after which two extra checks have to be performed regarding the instantaneous deflection by a static load (Equation (50)) and the vertical velocity by a unit impulse, as seen in Equation (51) [34]. The design requirements for vibrations in the floor elements are:

$$f_1 \geq 8\,[Hz] \tag{49}$$

$$\frac{w}{F} \leq a\,[mm/kN] \tag{50}$$

Where:

w	=	maximum instantaneous deflection by the vertical point load F	$[mm]$
F	=	vertical point load of value 1 [12]	$[kN]$
a	=	value of 1 stated by Dutch Annex [32]	$[mm/kN]$

$$v \leq b^{(f_1\zeta-1)}\,[m/Ns^2] \tag{51}$$

Where:

v	=	vertical velocity response	$[m/Ns^2]$
b	=	value of 120 (Dutch Annex of Eurocode 5, timber structures [32])	[-]
f_1	=	first modal frequency of two-span floor	$[Hz]$
ζ	=	relative damping factor of value 0.01 [34]	[-]

Similar to the deflection calculation of Section 5.2.2, the vibration calculation results are compared to handbook values in Tables 5.5 and 5.6. While the CLT calculation results and manual recommendations correspond well for all spans, the Lignatur results correspond well for middle spans but deviate more towards the shorter and longer spans.

Table 5.5: Comparing the calculated required element height for vibrations with the recommended value from a Lignatur handbook

Floor span	3.0	3.5	4.0	4.5	5.0	5.5	6.0	6.5	7.0	7.5	8.0	8.5	9.0
Calculations	120	120	120	140	160	180	220	240	280	320	360	400	440
Handbook	-[1]	-[1]	-[1]	180	200	200	220	240	280	320	360	360	360

[1] = table in handbook does not extent to this span.

Table 5.6: Comparing the calculated required element height for vibrations with the recommended value from a CLT handbook

Floor span	3.0	3.5	4.0	4.5	5.0	5.5	6.0	6.5	7.0	7.5	8.0	8.5	9.0
Calculations	80	120	120	150	180	180	220	250	$280b$	$280b$	$360b$	400	-[3]
Handbook	80	120[2]	120[2]	120[2]	150[2]	180[2]	220[2]	250[2]	-[2]	-[2]	-[2]	-[2]	-[2]

[2] Table in handbook states element height not selected for calculations, therefore the first higher element size that is used in the calculations is stated in Table 5.6.

[3] No cross-section available that can satisfy the requirement.

5.2.4 Fire design

The predictable rate at which timber burns (0.63 [mm] per minute for spruce) introduces the fire design concept for timber structures where the charcoal layer on the outside of mass-timber elements insulates and protects the inner timber [46]. Since this fire concept can result in timber elements with larger dimensions (e.g. a bigger bottom plate for Lignatur elements), the additional strength can increase the performance in column loss scenarios as well. However, for the fire design, only the timber thickness of the bottom plates is increased for Lignatur elements. When a corner column is lost, the bending moment in the floor elements in the corner of a building flips from positive to negative. This leads to (normative) tensile stresses on the top side of the floor element, where no increase in thickness for the fire situation is applied. Hence, the increased dimensions for fire design are not beneficial in the most important locations, which is why fire design is committed as a design criterion in this calculation framework. For CLT elements, added thickness for fire safety could be beneficial in an accidental situation. However, the performance of CLT in fire scenarios is a novel research field on its own (due to risks of delamination of layers, depending on the glue used). Therefore, the fire design of CLT is left out of the calculation framework as well.

5.3 Accidental (column loss) design scenarios

This section presents how the loads in the accidental scenario are determined. The obtained loads determine which cross-section of the Lignatur or CLT elements is required for each regarded span and scenario combination, based upon the element strength calculations described in Section 5.1.2 for the Lignatur box floor elements and in Section 5.1.4 for CLT. In Section 6.1, the required cross-sections in the accidental scenarios are compared to the demands in the standard situation of Section 5.2. The comparison shows whether a secondary load path through the floor elements is possible, and at what additional cross-sectional demands.

5.3.1 Accidental load combination

To assess the accidental situation when, in the case for this research, a column is lost, the load combination prescribed in *Eurocode 0* alters to Equation (52) [30]:

$$E_d = \sum_{j \geq 1} G_{\mathrm{k},j} + A_{\mathrm{d}} + \left(\psi_{1,1} \text{ or } \psi_{2,1}\right) Q_{\mathrm{k},1} + \sum_{i>1} \psi_{2,i} Q_{\mathrm{k},i} \tag{52}$$

Where:

$G_{\mathrm{k},j}$	=	characteristic value of the permanent load j	$[kN/m^2]$
A_d	=	design value of the accidental load j	$[kN/m^2]$
$\psi_{1,1}$	=	factor for the frequent value of the dominant variable load	[-]
$\psi_{2,1}$	=	factor for the quasi-permanent value of the dominant variable load	[-]
$\mathrm{Q}_{\mathrm{k},1}$	=	characteristic value of the dominant variable load	$[kN/m^2]$
$\psi_{2,i}$	=	factor for quasi-permanent value of non-dominant variable loads	[-]
$\mathrm{Q}_{\mathrm{k},i}$	=	characteristic value of the non-dominant variable load i	$[kN/m^2]$

Only one (thus dominant) variable load is applied on the assessed structure, and only one permanent load is present on the floor elements. The factor for the dominant variable load for office buildings is prescribed by the *National Dutch Annex* of *Eurocode 0* as $\psi_{2,1} = 0.3$ [31]. And since the situation after the incidental occurrence is assessed (meaning $A_d = 0$ [30], Equation (52) reduces to:

$$E_{d,acc} = G_{\mathrm{k}} + 0.3 \cdot Q_{\mathrm{k}} \tag{53}$$

5.3.2 Derivation of loads in column loss scenarios

The loads introduced on the floors can be regarded as distributed and point loads. In each load combination and column-loss scenario, different load contributions are added together, and the resistance of the floor elements to the resulting forces is checked. An overview of the used structural schemes with corresponding shear and bending moment diagrams can be found in Appendix F. By means of superposition, the resulting bending moments corresponding to each combination of loads and column-loss scenario are found. The width of the floor elements is assumed to be 1 meter for ease of calculation and comparison. As mentioned in Section 4.2, the performance of the timber floors in the accidental situation can be assessed by regarding only one story level. How the (outer two) floor elements are considered for a corner column loss situation is visualized in Figures 5.12-5.14.

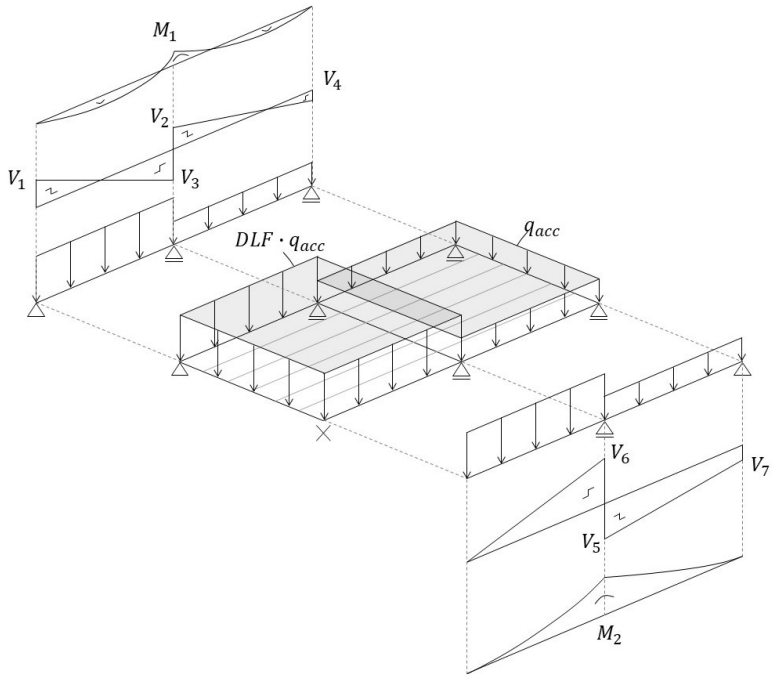

Figure 5.12: Redistribution of the accidental loads in a corner column removal scenario

Where, resulting from the schemes Appendix F, the shear force V and bending moment M in the two outermost floor elements indicated in the exploded views are given by:

Left side		*Right side*	
$M_1 = -\frac{3}{16} \cdot q_{acc} \cdot l^2$	$[kNm]$	$M_2 = -q_{acc} \cdot l^2$	$[kNm]$
$V_1 = \frac{13}{16} \cdot q_{acc} \cdot l$	$[kN]$	$V_5 = -\frac{3}{2} \cdot q_{acc} \cdot l$	$[kN]$
$V_2 = \frac{11}{16} \cdot q_{acc} \cdot l$	$[kN]$	$V_6 = 2 \cdot q_{acc} \cdot l$	$[kN]$
$V_3 = -\frac{19}{16} \cdot q_{acc} \cdot l$	$[kN]$	$V_7 = -\frac{1}{2} \cdot q_{acc} \cdot l$	$[kN]$
$V_4 = \frac{5}{16} \cdot q_{acc} \cdot l$	$[kN]$		

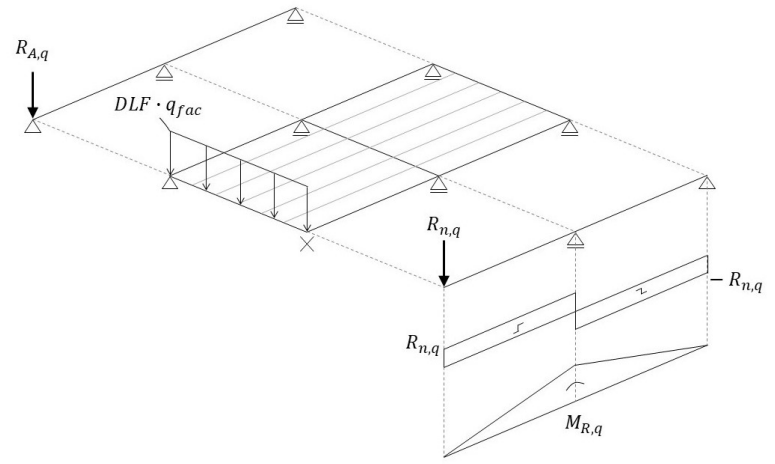

Figure 5.13: Redistribution of the *front* facade load in a corner column removal scenario

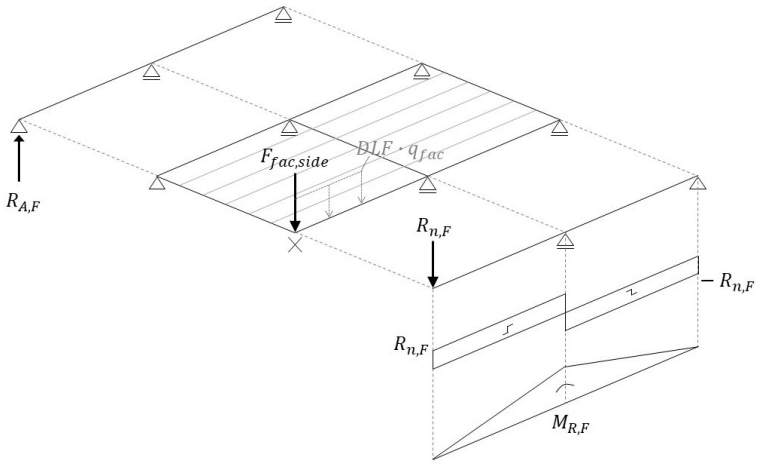

Figure 5.14: Redistribution of the *side* facade load in a corner column removal scenario

Where $F_{fac,side}$ represents the facade load of half the floor span l:

$$F_{fac,side} = \frac{l}{2} \cdot l \cdot q_{fac} \quad [kN]$$

As one can observe by comparing the moment distributions in each of the floor elements in Figures 5.12 - 5.14, the floor element closest to the location of the lost column is subject to the highest loads. Now that the corner column is lost, the loads take a different path, resulting in the beam at the end of the floor elements connecting the ends of the floor elements. In the *normal* situation, the floor beams are resting on the front beam. The schemes indicating the structural behavior of the floor elements and the front beam in the accidental (corner column loss) scenario are given in Figure 5.15.

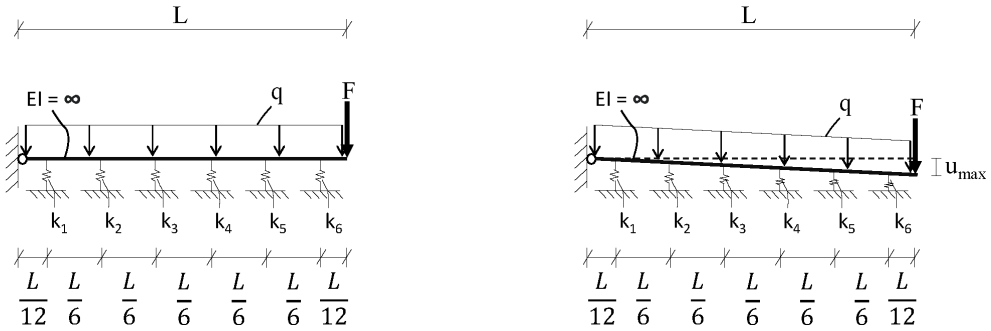

(a) Front beam after a column is lost

(b) Front beam after a column is lost, deflected

Figure 5.15: Structural schematization of the front beam after column removal

Of interest are the loads dissipated to the connection and column on the left R_{AV} and to the heaviest loaded floor element on the right, at the location of $k_6\, R_n$, as indicated in Figure 5.16.

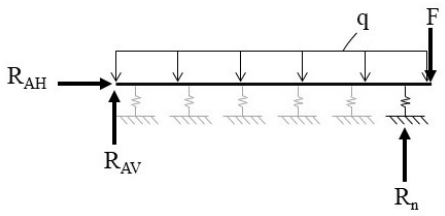

Figure 5.16: Locations of reaction forces of interest R_{AV} and R_n for number of floor elements $n = 6$.

In Figure 5.15, the spring supports represent each floor element, in this case, six elements adjacent to each other, corresponding to a six-meter span. As the beam element is significantly stiff compared to the floor elements (that also span 6 meters), the beam element is regarded as infinitely stiff. As the spring stiffness k_i equals $(EI)_{beam}$ for all values of i, $k_1 = k_2 = k_i$. As the front beam is regarded as infinitely stiff and thus remains straight under loading, the ratios of deflections u_i at each of the spring support locations i as functions of u_{max} are known as well. Applying the known value of stiffness k_i and the relative displacement u_i with Hooke's law $F = k \cdot u$ yields the contribution of each spring i to the total carried loads q and F. Computing the contribution of the spring closest to the location of the lost column for multiple spans (and thus for multiple amounts of springs) yields a relation between the number of springs and the structural contribution of this outer spring support. This relation describes which portion of the load is carried by the floor element closest to the location of the lost column. The relations are given by Equations (54) and (55) for point load F and distributed load q, respectively. Point load F represents the load of the facade at the side of the building for half the floor span L.

$$R_{n,F} = \frac{6}{2n+1} \cdot F \tag{54}$$

$$R_{n,qL} = \frac{3}{2n+1} \cdot qL \tag{55}$$

Where:

$R_{n,F}$	=	portion of point load F taken by spring support n	$[kN]$
$R_{n,qL}$	=	portion of distributed load q taken by spring support n	$[kN]$

By applying the relations described in Equations (54) and (55) together with the loads described in Section 5.3.1 and the standard beam equations listed in Appendix F, the resistance of the governing floor element is checked for the loading situation in the column loss scenarios.

In a similar approach, the vertically dissipated load R_{AV} by the hinge on the left in Figure 5.15 is acquired. The vertically dissipated load at the location of the hinge gives the forces loads q and F dissipate to the connection and the column, which is used for the check of the adjacent elements in Section 5.4. For $R_{AV,qL}$ and $R_{AV,F}$, elegant relations (like for $R_{n,F}$ and $R_{n,qL}$ in Equations (54) and (55)) are not found. Instead, a relation for $R_{AV,qL}$ and $R_{AV,F}$ is found by analyzing the graphical representations of the values for $R_{AV,qL}$ and $R_{AV,F}$ for the assessed spans, indicated in Figure 5.17. The *number of spring supports* on the horizontal axis of the graphs are analogous to the span in meters since floor elements of one-meter width are assessed, and the springs represent the floor elements. The graphs for $R_{AV,qL}$ and $R_{AV,F}$ in Figure 5.17 both show an asymptote, to which the values for all assessed spans are relatively close. For the *front* facade load F, an asymptotic value of 0.5 is obtained from Figure 5.17a. Since

F causes an upward reaction force at the opposing side of the beam (and is thus advantageous), the value of 0.5 is conservative. For the *front* facade load, the asymptotic value of 0.25 is obtained from Figure 5.17b. Consequently, the vertically dissipated loads at the connection are obtained using Equations (56) and (57) for the side facade load F and the front facade load q, respectively.

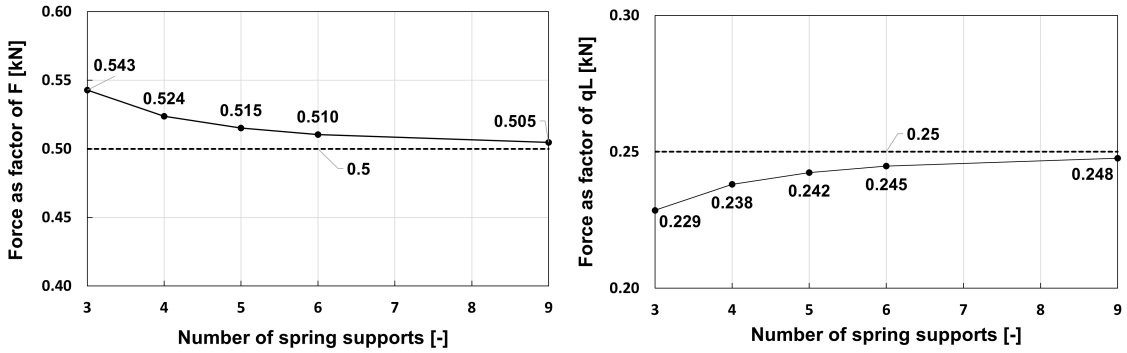

(a) $R_{AV,F}$ (b) $R_{AV,qL}$

Figure 5.17: Vertical load dissipated to the remaining column per number of spring supports

$$R_{AV,F} = 0.5 \cdot F \quad [kN] \tag{56}$$

$$R_{AV,qL} = 0.25 \cdot qL \quad [kN] \tag{57}$$

The acquired relations and loads are compared to the results of SCIA models. The relations found for $R_{AV,F}$, $R_{AV,qL}$, $R_{n,F}$, and $R_{n,qL}$ are validated by the simple beam on springs model presented in Figure 5.18, with the hand- and SCIA-calculated values compared in Table 5.7.

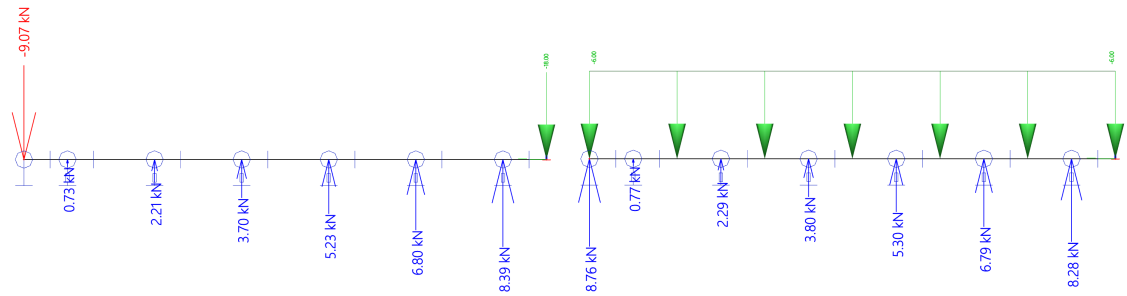

(a) Reaction forces by the side facade pointload (b) Reaction forces by the front facade load

Figure 5.18: SCIA results of a beam on spring supports that represent floor elements.

Table 5.7: Comparison of reaction forces of facade loads obtained using derived Equations (54)-(57) and the simple SCIA model (Figure 5.18) for a span of 6 meters.

Method	$R_{AV,F}$ $[kN]$	$R_{AV,qL}$ $[kN]$	$R_{n,F}$ $[kN]$	$R_{n,qL}$ $[kN]$
Hand	-9.0	9.0	8.3	8.3
SCIA	-9.1	8.8	8.4	8.3

By means of an example, the resulting accidental floor and facade loads from the hand calculations and SCIA models for the connection at the front in the corner column loss scenario are presented in Tables 5.8 and 5.9. Figure 5.19 shows the SCIA model support reaction caused by the accidental floor load q_{acc}.

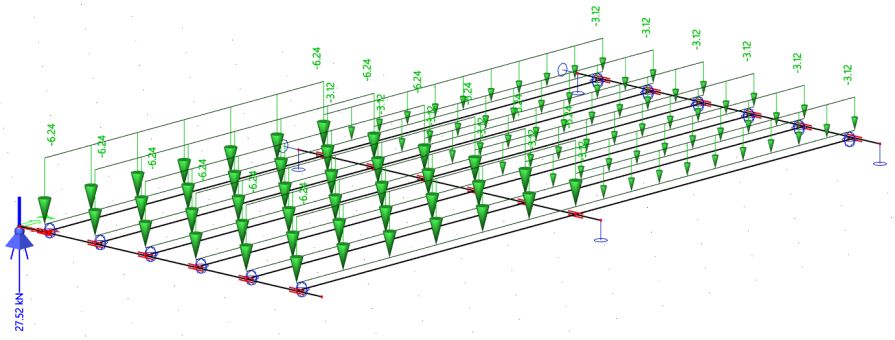

Figure 5.19: SCIA model showing support reaction force $R_{AV,q,acc}$ remaining column by the accidental floor load

Table 5.8: Comparison of found loads by hand calculations and the SCIA model for the beam-column connection at the front in a corner column loss scenario, for a span of 6 meters.

Method	$R_{AV,q,acc}$ $[kN]$	$R_{AV,qL}$ $[kN]$	$R_{AV,F}$ $[kN]$	Combined $[kN]$
Hand	28.1	9.0	-9.0	28.1
SCIA	27.5	10.9	-7.7	28.9
				2.8 %

Table 5.9: Comparison of found loads by hand calculations and the SCIA model for the beam-column connection at the front in a corner column loss scenario, for a span of 9 meters.

Method	$R_{AV,q,acc}$ $[kN]$	$R_{AV,qL}$ $[kN]$	$R_{AV,F}$ $[kN]$	Combined $[kN]$
Hand	63.2	13.5	-13.5	63.2
SCIA	62.5	15	-11.6	65.9
				4.2 %

In the hand calculations, the assumption is made that the beams below the floor elements remain straight. To validate the assumption, two versions of a SCIA model are compared. In the first model (Figure 5.20a), the beams are deflecting elements. In the second model (Figure 5.20b), the deflection of the middle and back beams is prevented by vertical supports.

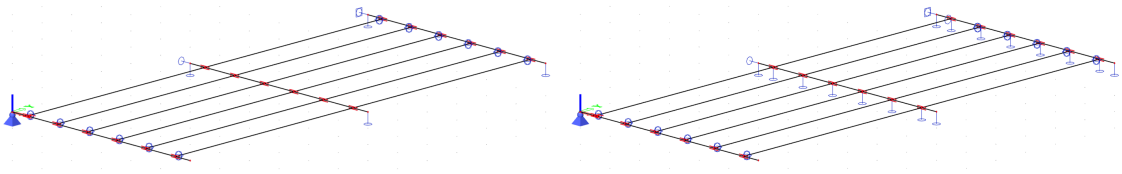

(a) Beams below floor elements can deflect. (b) Deflection of beams is prevented.

Figure 5.20: Two SCIA models to see influence of deflection of the middle and back beams.

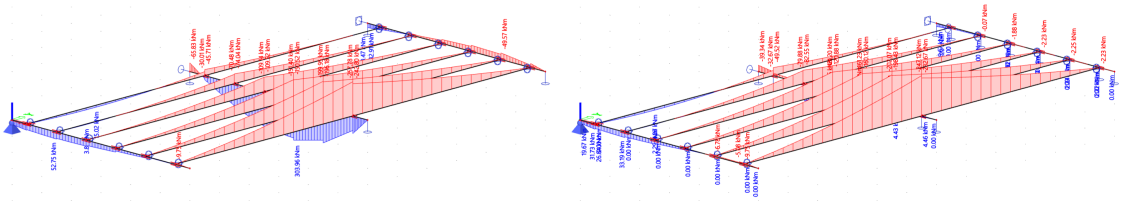

(a) Beams below floor elements can deflect. (b) Deflection of beams is prevented.

Figure 5.21: Bending moment diagrams for the SCIA models of Figure 5.21.

The bending moment distributions in the floor elements of the structures shown in Figures 5.21a and 5.21b are very similar. The maximum bending moment in the most loaded floor element is -257.8 $[kNm]$ for the structure with deflecting beams (Figure 5.21a) and -247.1 $[kNm]$ (-4.3 %) for the structure with a prevented deflection of the beams (Figure 5.21b). Both structures are loaded with the corner column loss combination scenario described in Section 5.3.2. The deflections of the *middle* and *back* beams are small compared to the deflection of the *front* beam (that has lost its end support due to the lost column). The significant difference in deflections explains why the deflections of the *middle* and *back* beams have a relatively small influence on the redistribution of forces compared to the deflection of the *front* beam (and thus the floor elements). The *Location along the beam [x/L]* on the horizontal axis represents the location along each beam from left to right. The data points in the graph represent the locations of the middle of each of the $1\ [m]$ wide floor elements. A complete overview of the comparison between SCIA results and manual calculations can be found in Appendix E.

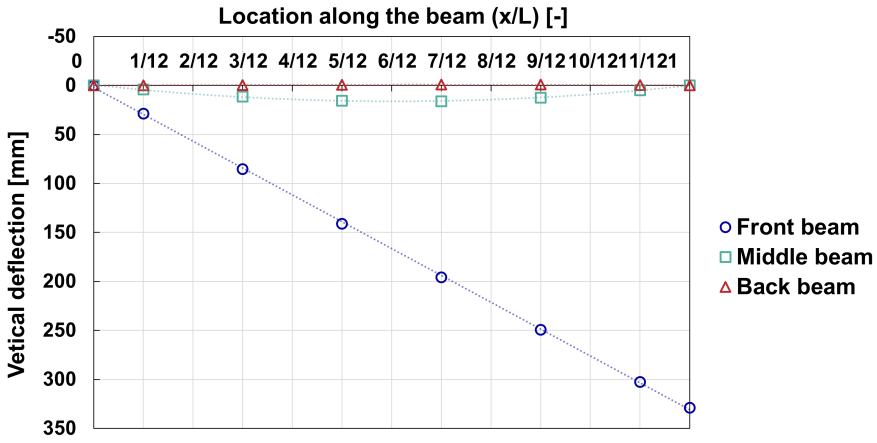

Figure 5.22: Deflections in SCIA model of the beams supporting the floor elements plotted for the corner column loss scenario.

5.4 Checks of adjacent structural elements

In addition to checking and calculating dimensions for the floor elements, the structural elements adjacent to the floor elements are assessed to see if they can withstand the loads in accidental scenarios or if they need to be strengthened. The loads on each adjacent element are assessed using the approach elaborated in Section 5.3.2. For each of the column removal scenarios, the distribution of forces is assessed per loading type (q_{acc} and facade loads), interpolating between the schematizations on each side of the floor field to obtain the distributed force on the beam and the vertically transferred loads for the connections and columns. The equations are set up to work for any span L, meaning all regarded spans can be assessed for all scenarios and load combinations after setting up the equations. For each column loss scenario and accidental loading type, the resulting structure loads on the adjacent elements are acquired in accordance with the upcoming sections. Ofcourse, standard loads like dead weight of elements and accidental live loads on parts of the structure that are not directly linked to a lost column location are regarded as well.

Corner column loss scenario: accidental live load

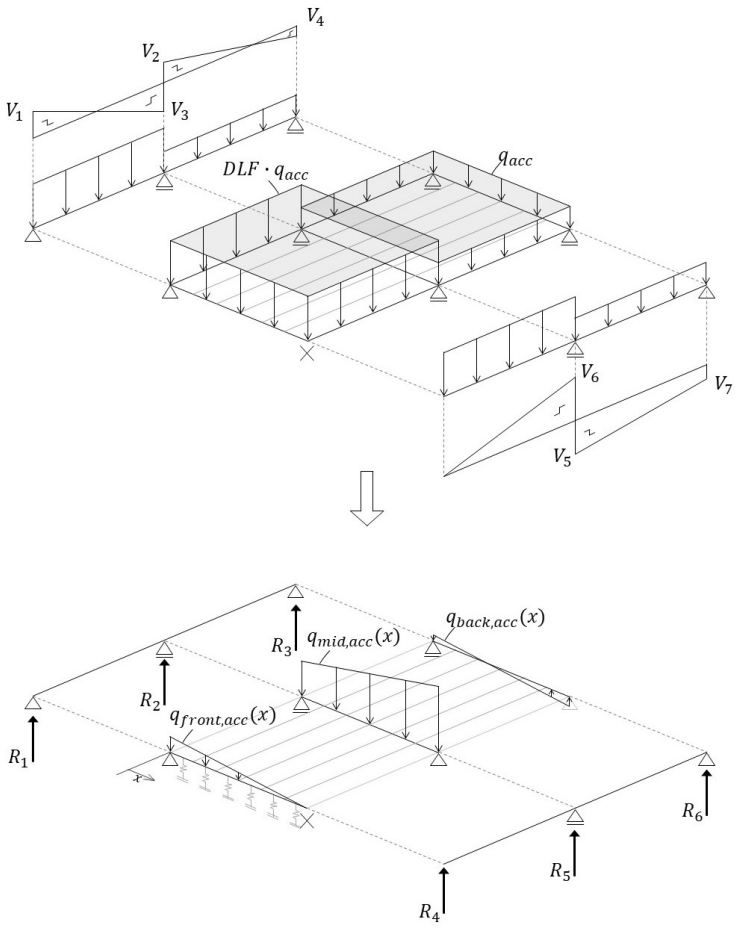

Figure 5.23: Schematization of how the accidental live loads are regarded in the corner column removal scenario

Where, resulting from the schemes Appendix F, the dissipated loads by the two outermost floor elements indicated in the exploded views are given by:

Left side		*Right side*	
$R_1 = \frac{13}{16} \cdot q_{acc} \cdot l$	$[kN]$	$R_4 = 0$	[lost column location]
$R_2 = \frac{5}{4} \cdot q_{acc} \cdot l$	$[kN]$	$R_5 = \frac{7}{2} \cdot q_{acc} \cdot l$	$[kN]$
$R_3 = \frac{5}{16} \cdot q_{acc} \cdot l$	$[kN]$	$R_6 = -\frac{1}{2} \cdot q_{acc} \cdot l$	$[kN]$

Equations (58)-(66) describe the distributed load on each of the beams supporting the floor elements are obtained by interpolating between the values obtained for the two outermost floor elements.

$$q_{front,acc}(x) = R_1 \cdot \left(1 - \frac{x-1}{L-1}\right) \tag{58}$$

$$q_{mid,acc}(x) = R_2 + \frac{x-1}{L-1} \cdot \left(R_4 - R_2\right) \tag{59}$$

$$q_{back,acc}(x) = R_3 + \frac{x-1}{L-1} \cdot (R_6 - R_3) \tag{60}$$

Where:

x	=	location along the beam	$[m]$
L	=	span of the beam	$[m]$

The distributed loads of Equations (58)-(66) are used to calculate the bending moments in the beams and to calculate what forces are dissipated to the connections and columns in the corner column loss scenario, for the accidental live load. The same goes for the equations described in the upcoming sections for the corresponding load type and column loss scenario.

Corner column loss scenario: front facade load

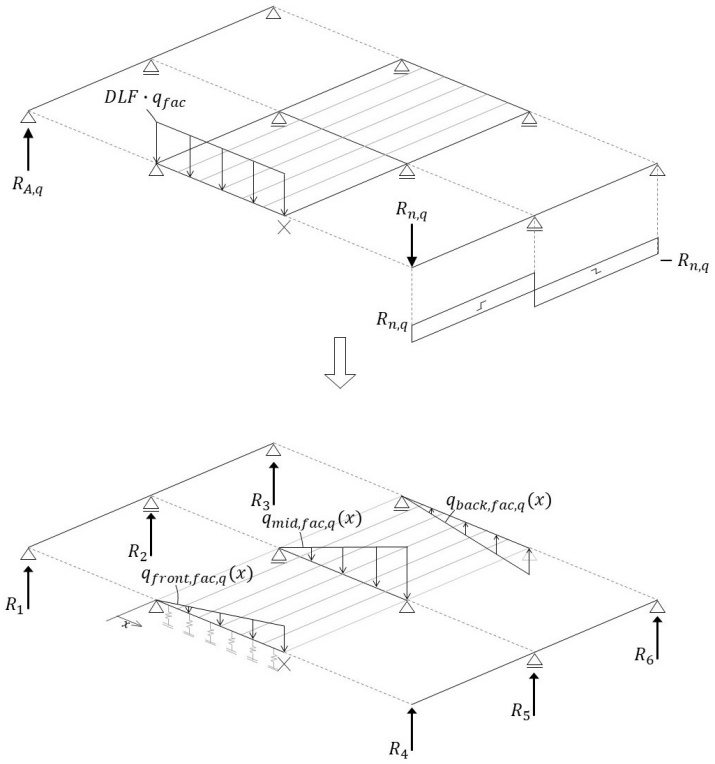

Figure 5.24: Schematization of how the front facade load is regarded in the corner column removal scenario

Where, resulting from the schemes Appendix F, the dissipated loads by the two outermost floor elements indicated in the exploded views are given by:

Left side		*Right side*	
$R_1 = R_{AV,qL} = 0.25 \cdot q_{fac} \cdot l$	$[kN]$	$R_4 = 0$	[lost column location]
$R_2 = 0$	[–]	$R_5 = 2 \cdot R_{n,qL}$	$[kN]$
$R_3 = 0$	[–]	$R_6 = -R_{n,qL}$	$[kN]$

The equations describing the distributed load on each of the beams supporting the floor elements are obtained by interpolating between the values obtained for the two outermost floor elements:

$$q_{mid,fac,qL}(x) = 2 \cdot R_{n,qL} \cdot \frac{x}{L} \tag{61}$$

$$q_{end,fac,qL}(x) = -R_{n,qL} \cdot \frac{x}{L} \tag{62}$$

Applying the relation found for $R_{n,qL}$ described by Equation (55) yields:

$$q_{mid,fac,qL}(x) = 2 \cdot \frac{3}{2n+1} \cdot q_{fac} \cdot l \cdot \frac{x}{L} \tag{63}$$

$$q_{back,fac,qL}(x) = -\frac{3}{2n+1} \cdot q_{fac} \cdot l \cdot \frac{x}{L} \tag{64}$$

Corner column loss scenario: side facade load

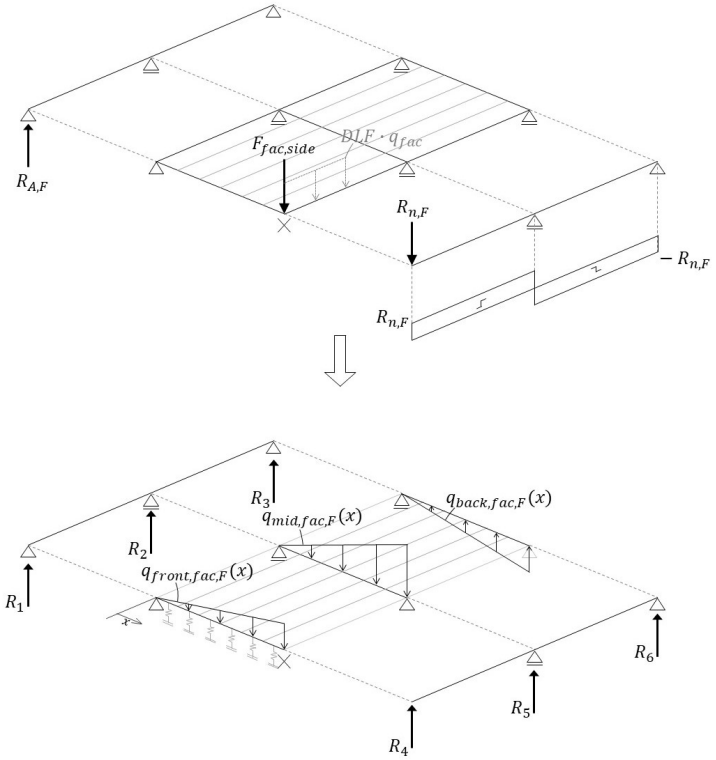

Figure 5.25: Schematization of how the side facade load is regarded in the corner column removal scenario

Where, resulting from the schemes Appendix F, the dissipated loads by the two outermost floor elements indicated in the exploded views are given by:

Left side		*Right side*	
$R_1 = R_{AV,F} = -0.5 \cdot F_{fac,side}$	$[kN]$	$R_4 = 0$	[lost column location]
$R_2 = 0$	[–]	$R_5 = 2 \cdot R_{n,F}$	$[kN]$
$R_3 = 0$	[–]	$R_6 = -R_{n,F}$	$[kN]$

The equations describing the distributed load on each of the beams supporting the floor elements are obtained by interpolating between the values obtained for the two outermost floor elements:

$$q_{mid,fac,F}(x) = 2 \cdot R_{n,F} \cdot \frac{x}{L} \tag{65}$$

$$q_{back,fac,F}(x) = -R_{n,F} \cdot \frac{x}{L} \tag{66}$$

Applying the relation found for $R_{n,F}$ described by Eq. (54) yields:

$$q_{mid,fac,F}(x) = 2 \cdot \frac{6}{2n+1} \cdot q_{fac} \cdot \frac{l}{2} \cdot \frac{x}{L} \tag{67}$$

$$q_{back,fac,F}(x) = -\frac{6}{2n+1} \cdot q_{fac} \cdot \frac{l}{2} \cdot \frac{x}{L} \tag{68}$$

Edge column loss scenario: accidental live load

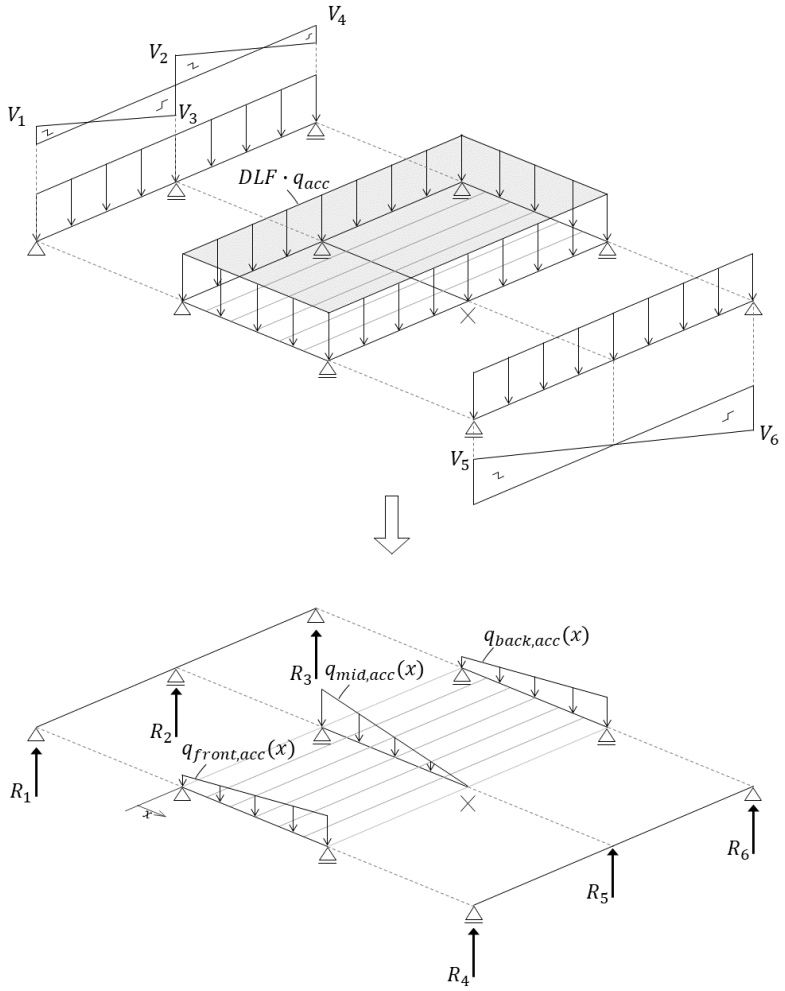

Figure 5.26: Schematization of how the accidental live loads are regarded in the edge column removal scenario

Where:

Left side		*Right side*	
$R_1 = \frac{3}{8} \cdot q_{acc} \cdot l$	$[kN]$	$R_4 = q_{acc} \cdot l$	$[kN]$
$R_2 = \frac{10}{8} \cdot q_{acc} \cdot l$	$[kN]$	$R_5 = 0$	[lost column location]
$R_3 = \frac{3}{8} \cdot q_{acc} \cdot l$	$[kN]$	$R_6 = q_{acc} \cdot l$	$[kN]$

Resulting in the following (equal) equations for the q-loads on the beams:

$$q_{front,acc}(x) = R_1 + \frac{x-1}{L-1} \cdot \left(R_4 - R_1\right) \tag{69}$$

$$q_{mid,acc}(x) = R_2 - \frac{x-1}{L-1} \cdot (R_2) \tag{70}$$

$$q_{back,acc}(x) = R_3 + \frac{x-1}{L-1} \cdot (R_6 - R_3) \tag{71}$$

Edge column loss scenario: side facade load

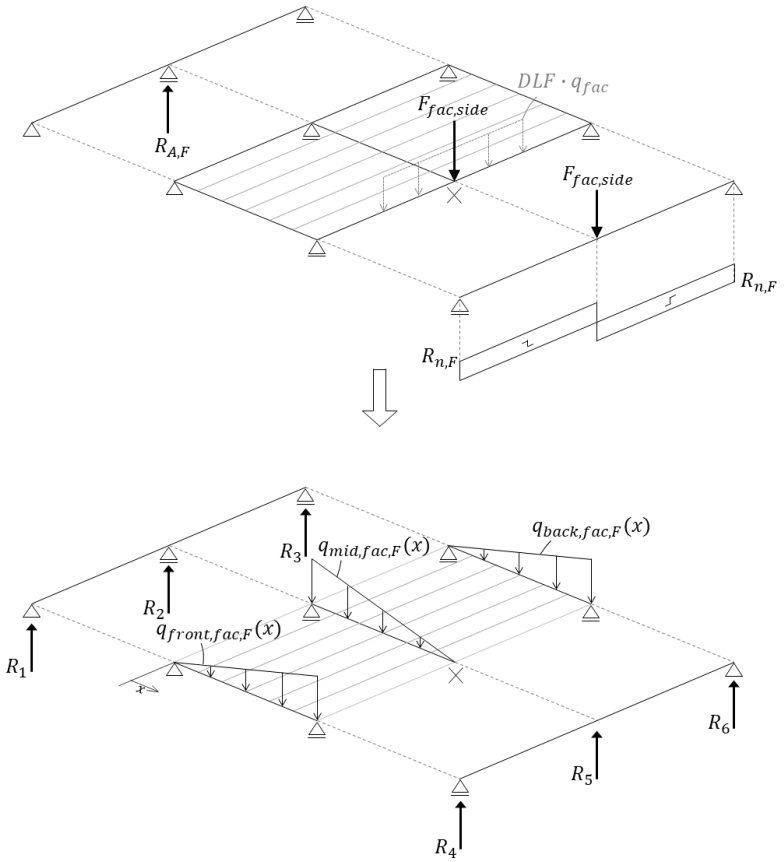

Figure 5.27: Schematization of how the side facade load is regarded in the edge column removal scenario.

Where:

Left side		*Right side*	
$R_1 = 0$	$[kN]$	$R_{n,F}$	$[kN]$
$R_{AV,F} = -\frac{1}{2} \cdot F$	$[kN]$	$R_5 = 0$	[lost column location]
$R_3 = 0$	$[kN]$	$R_{n,F}$	$[kN]$

Resulting in the following equations for the q-loads on the beams:

$$q_{front,fac,F}(x) = \frac{1}{2} \cdot \frac{6}{2n+1} \cdot \frac{x}{L} \cdot q_{fac} \cdot L \tag{72}$$

$$q_{mid,fac,F}(x) = -\frac{1}{2} \cdot q_{fac} \cdot L \cdot \left(1 - \frac{x}{L}\right) \tag{73}$$

$$q_{back,fac,F}(x) = \frac{1}{2} \cdot \frac{6}{2n+1} \cdot \frac{x}{L} \cdot q_{fac} \cdot L \tag{74}$$

Middle column loss scenario: accidental live load

The middle column loss scenario can be regarded as two edge column loss scenarios facing each other. It is, therefore, highly similar to the edge column loss scenario but without the facade loads.

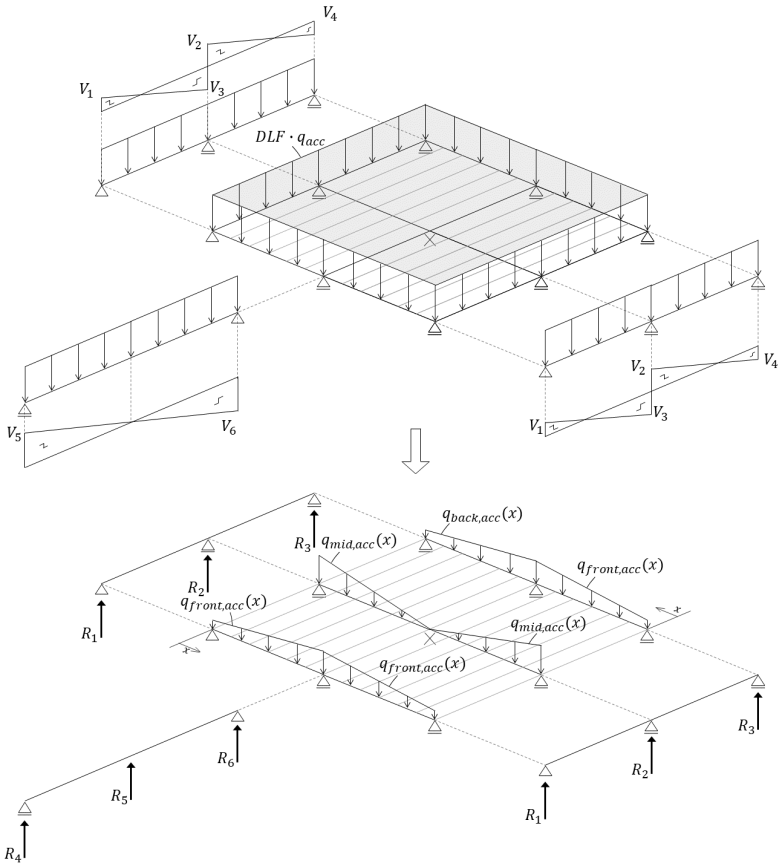

Figure 5.28: Schematization of how the accidental live loads are regarded in the middle column removal scenario

Where:

Left and right sides		*Middle*	
$R_1 = \frac{3}{8} \cdot q_{acc} \cdot l$	$[kN]$	$R_4 = q_{acc} \cdot l$	$[kN]$
$R_2 = \frac{10}{8} \cdot q_{acc} \cdot l$	$[kN]$	$R_5 = 0$	[lost column location]
$R_3 = \frac{3}{8} \cdot q_{acc} \cdot l$	$[kN]$	$R_6 = q_{acc} \cdot l$	$[kN]$

Resulting in the following equations for the q-loads on the beams:

$$q_{front,acc}(x) = R_1 + \frac{x-1}{L-1} \cdot \left(R_4 - R_1\right) \tag{75}$$

$$q_{mid,acc}(x) = R_2 - \frac{x-1}{L-1} \cdot (R_2) \tag{76}$$

$$q_{back,acc}(x) = R_3 + \frac{x-1}{L-1} \cdot (R_6 - R_3) \tag{77}$$

5.4.1 Check of the beams

The beams supporting the floor elements are checked in both the fundamental and the accidental states. In the fundamental state, the ULS and SLS criteria are assessed. In the accidental state, the beam is checked for the changing load paths in the column loss scenarios. Since the goal is to see if and, if so, to what extent the beams should be strengthened, the required beam height h_{req} is calculated for the fundamental and accidental load situations. The beam width is kept constant at 250 $[mm]$. Shear force checks of the beams are performed as well but not presented as they are easily satisfied.

The design bending moment in the fundamental combination is calculated using Equation (78).

$$M_d = \frac{1}{8} \cdot q_d \cdot l^2 \tag{78}$$

Where:

q_d	=	floor element self-weight, live load, and facade load (where applicable)	$[kN/m]$
l	=	beam length	$[m]$

The bending stress $\sigma_{y,d}$ by the design bending moment is calculated using Equation (79).

$$\sigma_{y,d} = \frac{M_d}{W} \tag{79}$$

Where:

$$W \quad = \quad \tfrac{1}{6} \cdot b \cdot h^2 \quad [mm^3]$$

Using the value for $b = 250$ $[mm]$ and the design bending strength $f_{y,d}$ for C24 timber, the required beam height $h_{req,fund}$ for the fundamental ULS can be obtained using Equation (80), by rewriting Equation (79) for h.

$$h_{req,fund} = \sqrt{\frac{6 \cdot M_d}{b \cdot f_{y,d}}} \tag{80}$$

$$h_{req,fund} = \sqrt{\frac{6 \cdot M_d}{250 \cdot 15.4}} \tag{81}$$

The beams are dimensioned for both individual deflection and combined deflection of the floor beams and the floor elements, and for the situation where both floor fields are loaded by the live loaded and where only one floor field is loaded by the live load.

The individual beam deflection is checked using Equation (82).

$$\frac{5}{384} \frac{g_d l^4}{EI} (1 + k_{\text{def}}) + \frac{5}{384} \frac{q_d l^4}{EI} \left(1 + \varphi_{2,1} k_{\text{def}}\right) \leq \frac{l}{500} \tag{82}$$

Where:

$$I \quad = \quad \tfrac{1}{12} \cdot b \cdot h^3 \quad [mm^4]$$

Rewriting I and consequently Equation (82) for h results in the required beam height for the deflection requirement $h_{req,SLS}$.

For the required beam heights in the accidental situations, the governing bending moments are assessed in the momentarily dynamically amplified situation and the static situation after the dynamic response, with the corresponding C24 timber bending strength values.

$$h_{req,acc,dyn} = \sqrt{\frac{6 \cdot M_{d,acc,dyn}}{250 \cdot 26.4}} \tag{83}$$

$$h_{req,acc,static} = \sqrt{\frac{6 \cdot M_{d,acc}}{250 \cdot 21.6}} \tag{84}$$

5.4.2 Check of the connections

To assess the connections between the beams and the columns, the vertically transferred load is calculated at each connection location for all spans in the fundamental and accidental column loss scenarios. By comparing the vertically transferred loads, an indication is created that shows the possible need to strengthen the connections in structures designed for secondary load paths through floor elements. By no means, the simplification of schematizing connection calculations as simple vertical loads should be regarded as fulfilling connection analysis.

Since the load duration factor and material factor differ for the fundamental, dynamic, and post-dynamic load scenarios, the loads can temporarily exceed the fundamental design strength. To account for this, load values in the accidental situations will be presented both as actual values and as the values divided by the factor that the material strength properties (momentarily) increase. The accidental loads are assessed both for the *very short* dynamic response and the *short* static situation afterward, of which the normative load is used to compare with the fundamental connection load.

$$F_{d,acc} = \max\left[F_{d,acc,dyn}, F_{d,acc}\right] \tag{85}$$

Where:

$F_{d,acc,dyn}$	=	dynamic accidental load assessed as *very short* load duration	$[kN]$
$F_{d,acc}$	=	post-dynamic static accidental load assessed as *short* load duration	$[kN]$

5.4.3 Checking the columns

The columns are dimensioned for both the fundamental and accidental load situations to check whether they need additional strengthening to withstand the loads in the accidental column loss scenarios. The structural analysis of the columns loaded by combined compression and bending is based upon the approach given in *Eurocode 5: Design of timber structures* [34] and is explained below.

$$\lambda_{rel,y} = \frac{\lambda_y}{\pi}\sqrt{\frac{f_{c,0,k}}{E_{0.05}}} \tag{86}$$

$$\lambda_{rel,z} = \frac{\lambda_z}{\pi}\sqrt{\frac{f_{c,0,k}}{E_{0.05}}} \tag{87}$$

Where:

λ_y	=	relative slenderness for bending around y-axis	[–]
λ_z	=	relative slenderness for bending around z-axis	[–]
$f_{c,0,k}$	=	characteristic compressive strength of the timber used	$[MPa]$
$E_{0.05}$	=	5-percentile value of the Young's Modulus	$[MPa]$

If both Equations (86) and (87) values ≤ 0.3, Equations (88) and (89) can be used to check the columns. Otherwise, Equations (90) and (91) should be used.

$$\left(\frac{\sigma_{c,0,d}}{f_{c,0,d}}\right)^2 + \frac{\sigma_{m,y,d}}{f_{m,y,d}} + k_m \frac{\sigma_{m,z,d}}{f_{m,z,d}} \leq 1 \tag{88}$$

$$\left(\frac{\sigma_{c,0,d}}{f_{c,0,d}}\right)^2 + k_m \frac{\sigma_{m,y,d}}{f_{m,y,d}} + \frac{\sigma_{m,z,d}}{f_{m,z,d}} \leq 1 \tag{89}$$

$$\frac{\sigma_{c,0,d}}{k_{c,y} \cdot f_{c,0,d}} + \frac{\sigma_{m,y,d}}{f_{m,y,d}} + k_m \frac{\sigma_{m,z,d}}{f_{m,z,d}} \leq 1 \tag{90}$$

$$\frac{\sigma_{c,0,d}}{k_{c,z} \cdot f_{c,0,d}} + k_m \frac{\sigma_{m,y,d}}{f_{m,y,d}} + \frac{\sigma_{m,z,d}}{f_{m,z,d}} \leq 1 \tag{91}$$

Where:

$\sigma_{c,0,d}$	=	design value of the compressive stress	$[MPa]$
$f_{c,0,d}$	=	design value of the compressive strength	$[MPa]$
$\sigma_{m,y,d}$	=	design value of the bending stress (around y-axis)	$[MPa]$
$f_{m,y,d}$	=	design value of the bending strength (around y-axis)	$[MPa]$
$\sigma_{m,z,d}$	=	design value of the bending stress (around z-axis)	$[MPa]$
$f_{m,z,d}$	=	design value of the bending strength (around z-axis)	$[MPa]$
k_m	=	factor that considers redistribution of stress and heterogeneity timber	[–]
$k_{c,y}$	=	instability factor (around y-axis)	[–]
$k_{c,z}$	=	instability factor (around z-axis)	[–]

The combination of the vertical load and the moments introduced by connection eccentricity and imperfectly centered vertical load application causes an additional moment, which is included by the factor described in Equation (92) [47].

$$\frac{n}{n-1}\,[\text{-}] \tag{92}$$

Where:

$$n = \frac{F_{cr}}{F}\,[\text{-}] \tag{93}$$

$$F_{cr} = \frac{\pi^2 EI}{L_{eff}^2}\,[kN] \tag{94}$$

The equations used to obtain the eccentricities for the connections e_y, e_z, element imperfections e_0, and imperfectly centered vertical load application e_i are given by Equations (95)-(98) respectively.

$$e_y = 150 + \frac{b_y}{2} \tag{95}$$

$$e_z = 150 + \frac{b_z}{2} \tag{96}$$

Where:

150	=	assumed distance between column-beam connection to the column	$[mm]$
b_y	=	width of column in y-direction	$[mm]$
b_z	=	width of column in z-direction	$[mm]$

Imperfections in the columns are incorporated using e_0. Imperfectly centered vertical load application is considered by e_i.

$$e_0 = \frac{L}{500} \qquad [34] \tag{97}$$

$$e_i = \frac{1}{400} \cdot L_{eff} \qquad [48] \tag{98}$$

An elaborated calculation example of a column in the standard and accidental situations can be found in Appendix C.1.

5.4.4 Connection between floor element and beams

In the standard loading scenario, the floor elements dissipate their loads to the beams that support them, after which the beams distribute the loads to columns at each of the beam's ends. This load path changes significantly in the accidental loading scenarios. In the accidental scenario, a beam that was connected to a now-lost column acts as an element that keeps the floor elements working together. Loads are only dissipated to one side of the beam, as the column on the other side is lost. The beams that experience this change in load configuration in the corner and edge column loss scenarios are indicated in Figure 5.29.

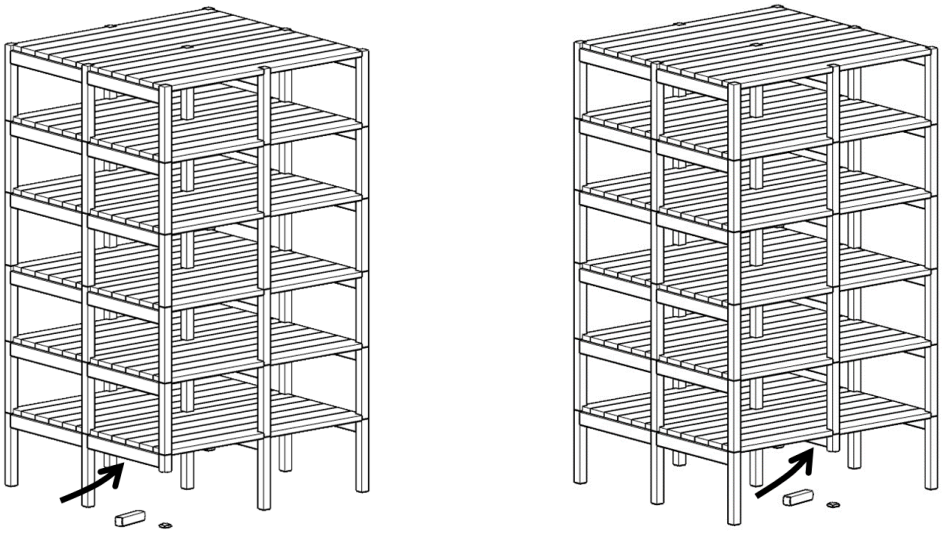

(a) Corner column loss scenario (b) Edge column loss scenario

Figure 5.29: Locations of beams indicated that were connected to a now-lost column for two column loss scenarios.

The changing loading scheme introduces tensile forces in the connections between the floor elements and the beams. These connections should thus be designed to withstand tensile forces in accidental scenarios. The magnitudes of the tensile forces are taken from the SCIA models that describe the structural behavior of the analyzed structure in the accidental scenarios. By means of example, the middle beam is visualized in Figures 5.30 and 5.31 with shear and bending moment diagrams in the standard and edge column loss scenarios.

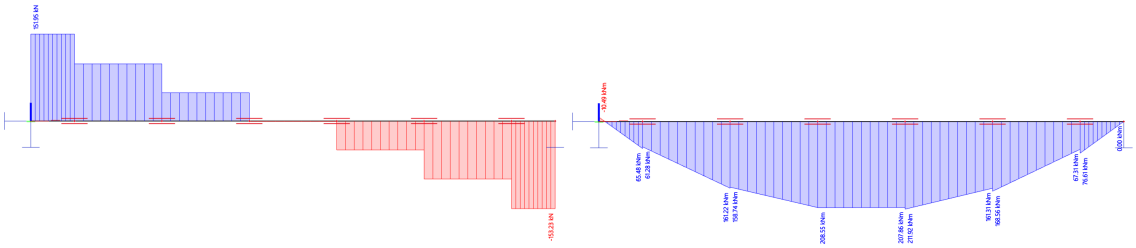

(a) Shear diagram with $V_{max} = 153\ kN$ (b) Moment diagram with $M_{max} = 212\ kNm$

Figure 5.30: SCIA model - middle beam isolated in the standard load scenario ($L = 6\ m$).

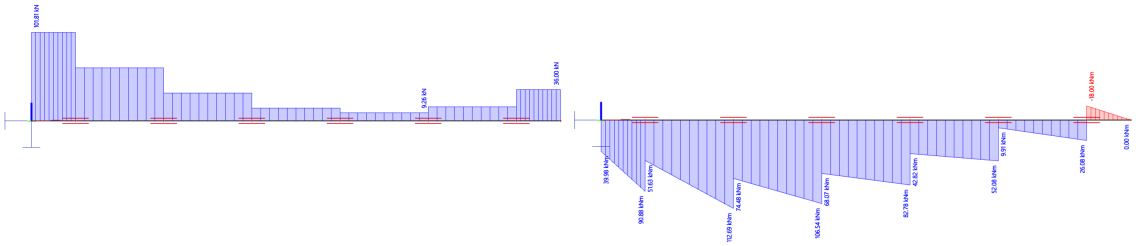

(a) Shear diagram with $V_{max} = 102\ kN$ (b) Moment diagram with $M_{max} = 113\ kNm$

Figure 5.31: SCIA model - middle beam isolated in the edge column loss scenario ($L = 6\ m$).

The maximum (tensile) force $F_{t,max}$ that should be transferred between the timber floor elements and the beams occurs in the corner column loss scenario in the connection between the outermost floor element and the beam. From a $9x9$ meters floor span SCIA model, $F_{t,max}$ is found in the most extreme scenario, given by Equation (99).

$$F_{t,max} = 61.7 \quad [kN] \tag{99}$$

CLT floor elements can be connected to beams using long screws that go through the plate elements into the beams, as visualized in Figure 5.32a for the corner column loss scenario and Figure 5.32b for the edge (and middle) column scenario. With capacities above 10 $[kN]$ [49], the tensile forces can be taken by ≈ 6 screws in a floor element of 1 $[m]$ wide in the most demanding situation described by Equation (99).

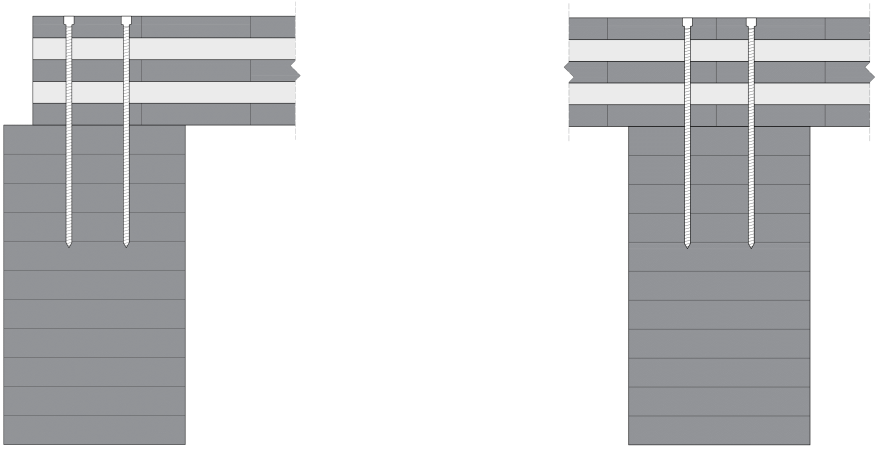

(a) Connection CLT floor elements to end beam. (b) Connection CLT floor elements to middle beam.

Figure 5.32: Screws connecting the CLT floor elements to beams supporting them.

Connecting the Lignatur box floor elements to the beams is more challenging. The approach using screws for the CLT elements does not work with the geometry of the Lignatur elements. To properly connect the Lignatur elements to the beams, the ribs of the box floor elements have to be fastened to the beams using anchors or metal profiles. A proposal of what such a connection could look like can be seen in Figure 5.33. Using anchors, capacities similar to the screws in CLT can be achieved. Capacities above 10 [kN] can be achieved [50], resulting in ≈ 6 anchors per meter floor width in the most demanding (9 [m]) span corner column loss scenario.

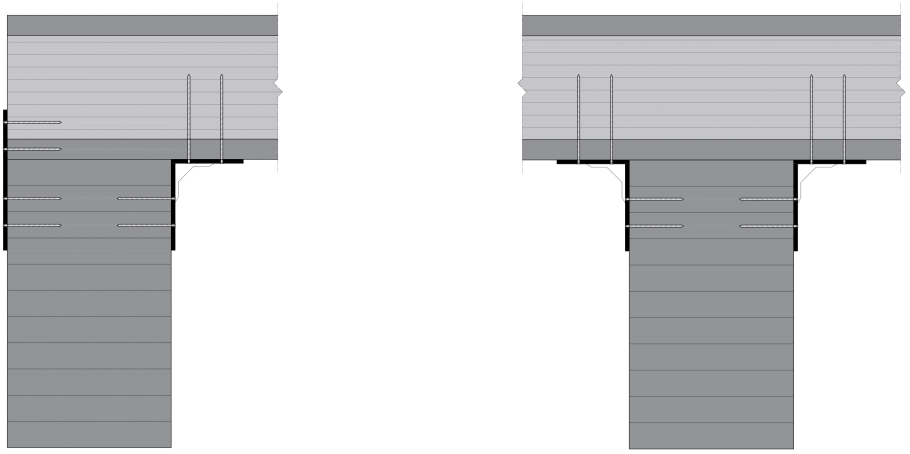

(a) Connection Lignatur elements to end beam. (b) Connection Lignatur elements to middle beam.

Figure 5.33: Screws and anchors connecting the Lignatur floor element ribs to beams supporting them.

Chapter 6

Results and discussion

6.1 Alternative load path analysis: floor elements

The results of the analysis of the floor elements in the standard and accidental design scenarios are presented in Sections 6.1.1-6.1.3. Per floor element type and span, the required cross-sectional element height is presented for each assessed design criteria. Figures 6.1-6.7 indicate the extent to which a secondary load path through floor elements is technically possible and, if possible, at what (additional) material cost. The discussion of the results is presented with each result graph.

Appendix D provides the full tables that present the required element height per design criterion, column loss scenario, floor element type, and floor element layout.

6.1.1 CLT floor elements

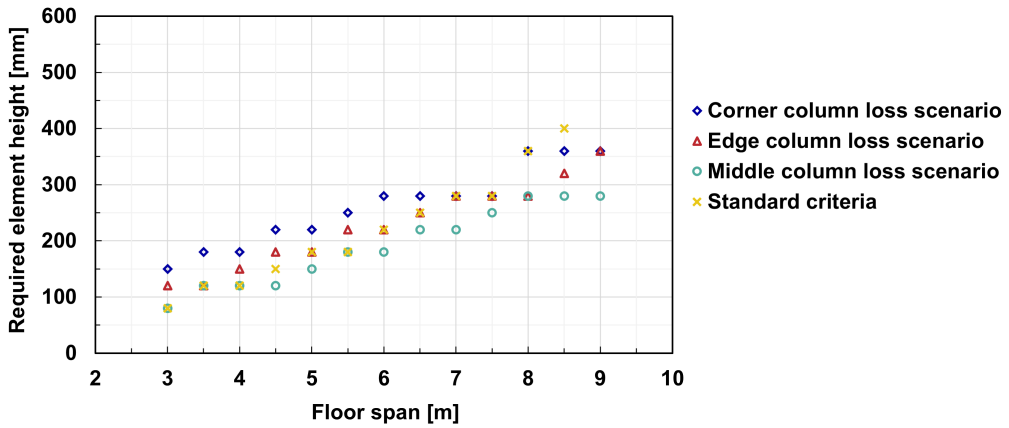

Figure 6.1: Required CLT element height per design scenario for continuous floor elements.

The results presented in Figure 6.1 indicate the performance of continuous CLT floor elements in column loss scenarios:

- Robustness through CLT floor elements can be achieved for all assessed floor spans.
- Robustness requirements govern the element size up to a span of 6.5 meters. For longer spans, vibration requirements are equally or more demanding.
- Up to 6.5 meters, robustness through floor elements requires a one- or two-step larger floor element cross-section.

- For most spans, the element height does not need to be increased to take the accidental loads in the edge and middle column loss scenarios.

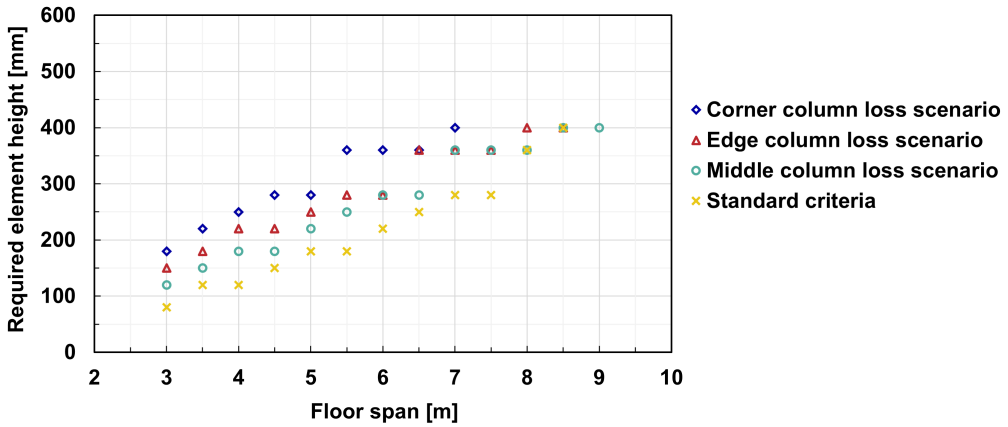

Figure 6.2: Required CLT element height per design scenario for staggered floor elements.

The results presented in Figure 6.2 indicate the performance of staggered CLT floor elements in column loss scenarios:

- A secondary load path through CLT floor elements in a corner column loss scenario can be achieved for spans up to 7 meters and up to 8.5 meters for edge and middle column loss scenarios.
- Robustness through CLT floor elements for staggered layout does require a significant increase in the CLT plate thickness.

6.1.2 Lignatur box floor elements

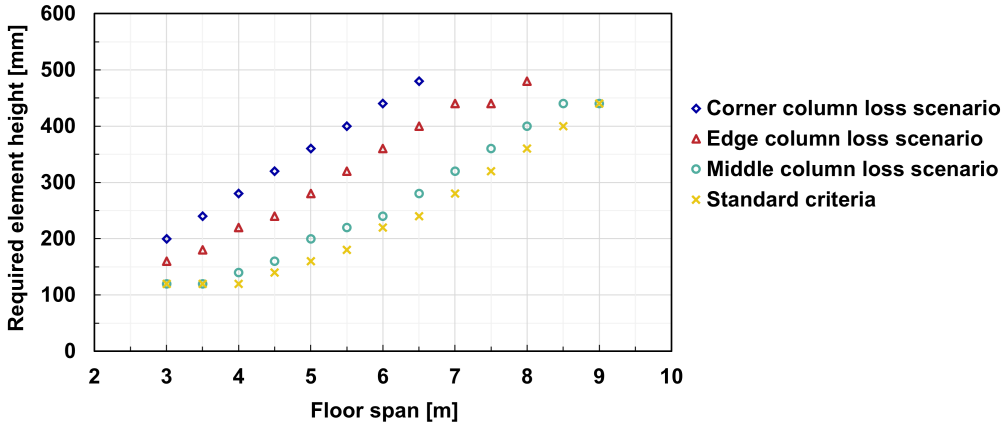

Figure 6.3: Required Lignatur element height per design scenario for continuous floor elements.

The results presented in Figure 6.3 indicate the performance of continuous Lignatur floor elements in column loss scenarios:

- Robustness through floor elements can be achieved for spans up to 6.5 meters for the corner column removal scenario, up to 8 meters in the edge column removal scenario, and up to 9 meters in the middle column removal scenario.

- The robustness through floor elements comes at a significant material cost, with the structural floor height required in the corner column loss scenario being about double the height needed for other design criteria. For example, double the structural height at a span of six meters results in an element height increase from 220 [mm] to 440 [mm].

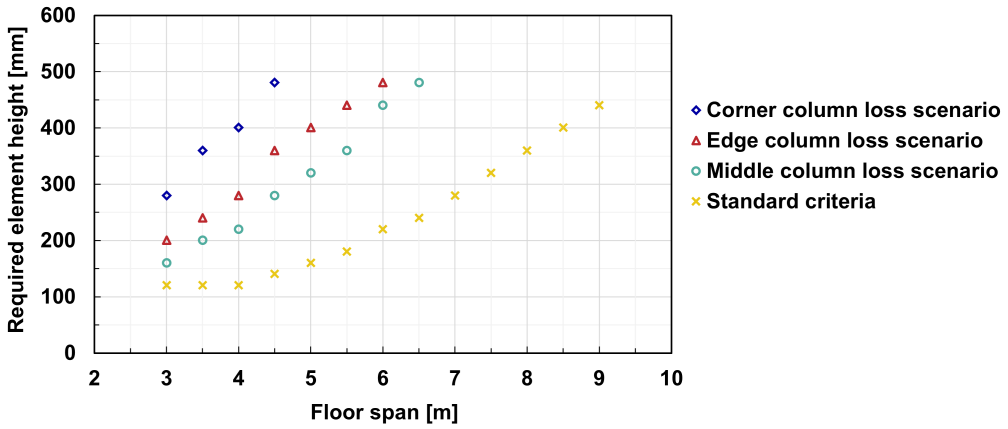

Figure 6.4: Required Lignatur element height per design scenario for staggered floor elements.

The results presented in Figure 6.4 indicate the performance of staggered Lignatur floor elements in column loss scenarios:

- Robustness through floor elements can be achieved for spans up to only 4.5 meters for the corner column removal scenario, up to 6 meters in the edge column removal scenario, and up to 6.5 meters in the middle column removal scenario.
- The robustness through floor elements comes at a great additional material cost.

6.1.3 Lignatur box floor elements with double plate thicknesses

To improve the performance of the Lignatur elements in the accidental scenarios, the same calculation procedure described in Chapter 5 is performed for Lignatur elements with double the standard top and bottom plate thickness. Both plate thicknesses are raised from the standard *31* [mm] to *62* [mm]. The performance in the accidental scenarios is presented in Figures 6.6 and 6.7.

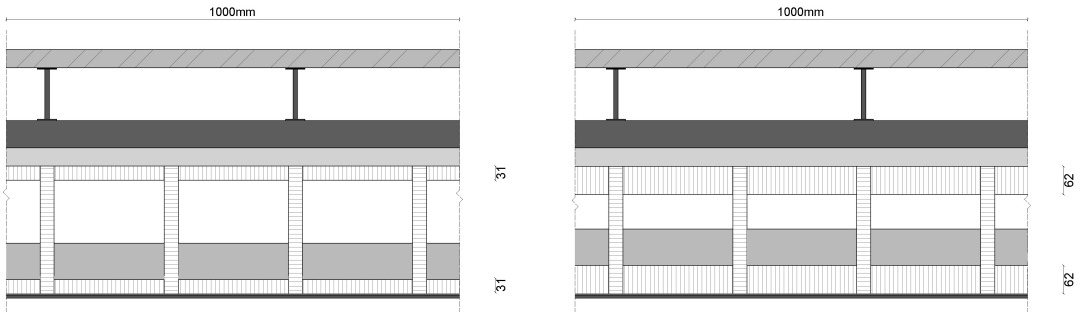

(a) standard 31 [mm] top and bottom plate (b) doubled 62 [mm] top and bottom plate

Figure 6.5: Standard and adapted Lignatur box floor elements.

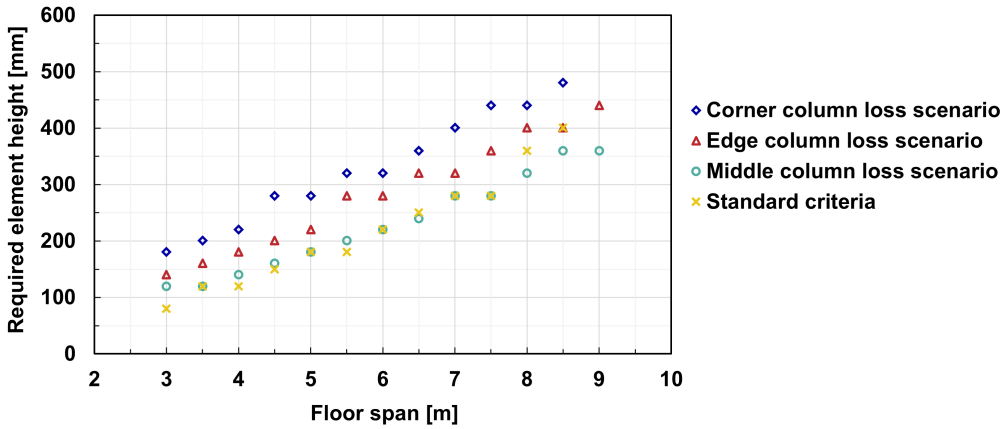

Figure 6.6: Required Lignatur element height per design scenario for continuous floor elements (double plate thickness).

The results presented in Figure 6.6 indicate the performance of continuous Lignatur floor elements with double top and bottom plate thicknesses in column loss scenarios:

- An increased performance compared to the elements with standard plate thicknesses can be seen, with secondary load paths possible for larger spans.
- The differences in required structural height for each design criterion are smaller than for the elements with a standard plate thickness.

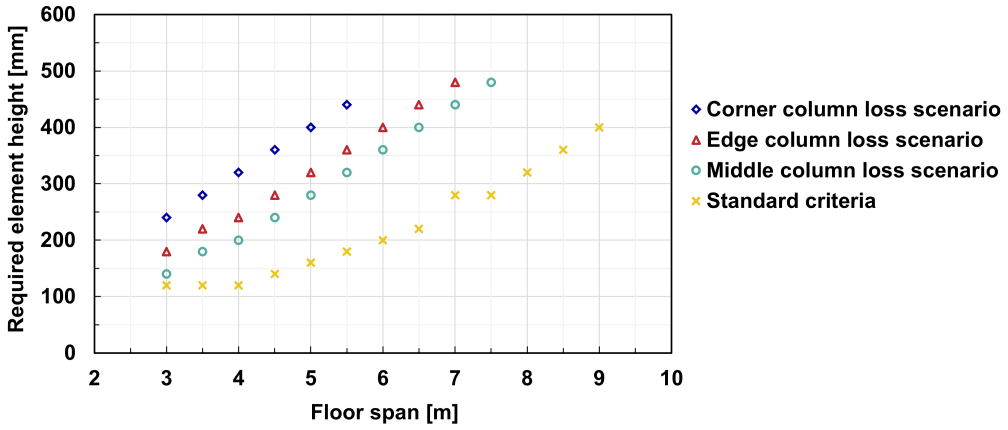

Figure 6.7: Required Lignatur element height per design scenario for staggered floor elements (double plate thickness).

The results presented in Figure 6.7 indicate the performance of staggered Lignatur floor elements with double top and bottom plate thicknesses in column loss scenarios:

- An increased performance compared to the elements with standard plate thicknesses can be seen, with secondary load paths possible for larger spans.
- The differences in required structural height for each design criterion are smaller than for the elements with a standard plate thickness.

6.2 Adjacent element checks

6.2.1 Beams

Tables 6.1 - 6.3 present the results of the assessment of the beams supporting the floor elements. The beams are dimensioned for the standard and accidental situations, as described in Section 5.4.1. The normative beam height and, thus, criterion are indicated by bold numbers in the tables. If the ULS or SLS in the standard situation is normative, no additional capacity is required for the accidental scenarios. The location of the elements is visualized in Figure 6.8.

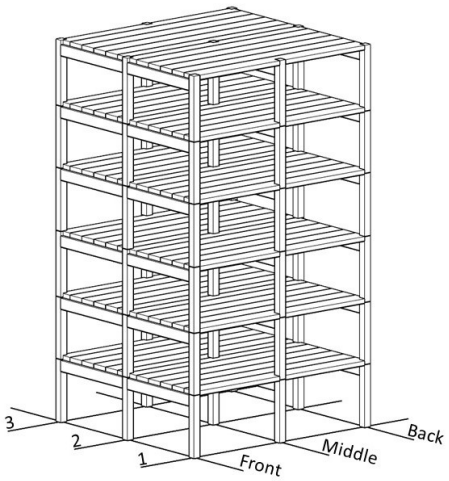

Figure 6.8: Locations of assessed adjacent elements

Table 6.1: Results check adjacent elements: front beam

	Design criteria, req. structural height [mm]:				
	Standard situation:		Accidental situation, loss of:		
Span [m]	ULS	SLS	Corner column	Edge column	Middle column
3	187	**210**	-	143	143
3.5	218	**250**	-	176	176
4	249	**300**	-	211	211
4.5	281	**360**	-	248	248
5	312	**410**	-	287	287
5.5	343	**470**	-	327	327
6	374	**540**	-	369	369
6.5	405	**590**	-	413	413
7	436	**730**	-	458	458
7.5	468	**870**	-	505	505
8	499	**820**	-	553	553
8.5	530	**880**	-	603	603
9	561	**980**	-	654	654

The SLS (deflection) requirement is always normative for the front beam. The required cross-sectional height in the corner column loss scenario is left out of the table since the loading pattern and demand in this scenario are significantly reduced. The beam only connects the floor elements, resulting in low bending moments.

Table 6.2: Results check adjacent elements: middle beam

	Design criteria, req. structural height [mm]:				
	Standard situation:		Accidental situation, loss of:		
Span [m]	ULS	SLS	Corner column	Edge column	Middle column
3	**305**	290	205	-	-
3.5	356	**360**	252	-	-
4	406	**430**	302	-	-
4.5	457	**510**	355	-	-
5	508	**590**	410	-	-
5.5	559	**670**	467	-	-
6	610	**760**	527	-	-
6.5	660	**850**	588	-	-
7	711	**930**	652	-	-
7.5	762	**1090**	718	-	-
8	813	**1140**	786	-	-
8.5	864	**1240**	856	-	-
9	914	**1340**	928	-	-

The SLS (deflection) requirement is also normative for (virtually) all spans for the middle beam.

Table 6.3: Results check adjacent elements: end beam

	Design criteria, req. structural height [mm]:				
	Standard situation:		Accidental situation, loss of:		
Span [m]	ULS	SLS	Corner column	Edge column	Middle column
3	187	**210**	96	143	143
3.5	218	**250**	114	176	176
4	249	**300**	132	211	211
4.5	281	**360**	151	248	248
5	312	**410**	170	287	287
5.5	343	**470**	189	327	327
6	374	**540**	208	369	369
6.5	405	**590**	228	413	413
7	436	**730**	248	458	458
7.5	468	**870**	269	505	505
8	499	**820**	289	553	553
8.5	530	**880**	310	603	603
9	561	**980**	331	654	654

The SLS (deflection) requirement is also always normative for the end beam, meaning that none of the beam locations have to be strengthened.

6.2.2 Connections between beams and columns

Tables 6.4 - 6.9 present the results of the assessment of the connections between the beams and columns. The required capacity for vertical load dissipation is calculated for the standard and accidental situations, as described in Section 5.4.2. The normative capacity and, thus, criterion are indicated by bold numbers in the tables. If the ULS in the standard situation is normative, no additional capacity is required for the accidental scenarios. The demanded capacity is normalized for (momentarily) increased material properties and is presented between brackets, as described in Section 5.4.2.

Table 6.4: Results check adjacent elements: Front connection 1

	Required connection capacity [kN]:			
	Standard situation:	Accidental situation, loss of:		
Span [m]	ULS	Corner column	Edge column	Middle column
3	18	-	**34 (20)**	20 (12)
3.5	23	-	**45 (26)**	27 (16)
4	29	-	**56 (33)**	34 (20)
4.5	36	-	**69 (40)**	43 (25)
5	43	-	**83 (48)**	52 (30)
5.5	51	-	**98 (57)**	63 (36)
6	60	-	**115 (67)**	74 (43)
6.5	69	-	**132 (77)**	86 (50)
7	79	-	**151 (88)**	99 (58)
7.5	90	-	**171 (100)**	113 (66)
8	101	-	**193 (112)**	128 (74)
8.5	113	-	**215 (125)**	144 (84)
9	125	-	**239 (139)**	160 (93)

The Edge column loss scenario increases the capacity demand for Connection Front 1 by $\approx 11\%$.

Table 6.5: Results check adjacent elements: Front connection 2

	Required connection capacity [kN]:			
	Standard situation:	Accidental situation, loss of:		
Span [m]	ULS	Corner column	Edge column	Middle column
3	**18**	7	25 (14)	21 (12)
3.5	**23**	10	32 (19)	28 (16)
4	**29**	12	40 (24)	35 (20)
4.5	**36**	16	50 (29)	44 (25)
5	**43**	20	60 (35)	53 (31)
5.5	**51**	24	71 (41)	63 (37)
6	**60**	28	83 (48)	75 (43)
6.5	**69**	33	96 (56)	87 (50)
7	**79**	38	109 (64)	100 (58)
7.5	**90**	44	124 (72)	114 (66)
8	**101**	50	140 (81)	128 (75)
8.5	**113**	56	156 (91)	144 (84)
9	**125**	63	174 (101)	161 (94)

The momentarily increased material properties in the accidental scenario mean that Connection Front 2 does not have to be strengthened.

Table 6.6: Results check adjacent elements: Middle connection 1

	Required connection capacity [kN]:			
	Standard situation:	Accidental situation, loss of:		
Span [m]	ULS	Corner column	Edge column	Middle column
3	40	**81 (47)**	-	14 (8)
3.5	54	**107 (62)**	-	21 (12)
4	70	**135 (79)**	-	30 (17)
4.5	89	**167 (97)**	-	39 (23)
5	110	**202 (117)**	-	50 (29)
5.5	133	**240 (139)**	-	62 (36)
6	159	**280 (163)**	-	76 (44)
6.5	186	**324 (189)**	-	90 (53)
7	216	**371 (216)**	-	106 (62)
7.5	**248**	421 (245)	-	124 (72)
8	**282**	474 (276)	-	142 (83)
8.5	**318**	530 (309)	-	162 (94)
9	**357**	589 (343)	-	184 (107)

The corner column loss scenario increases the capacity demand for Connection Middle 1 for spans up to 7 meters. For spans above 7.5 meters, the standard loading combination is normative, meaning no strengthening of the connection is required.

Table 6.7: Results check adjacent elements: Middle connection 2

	Required connection capacity [kN]:			
	Standard situation:	Accidental situation, loss of:		
Span [m]	ULS	Corner column	Edge column	Middle column
3	**40**	47 (28)	14 (8)	-
3.5	**54**	62 (36)	21 (12)	-
4	**70**	78 (46)	30 (17)	-
4.5	**89**	96 (56)	39 (23)	-
5	**110**	116 (68)	50 (29)	-
5.5	**133**	138 (80)	62 (36)	-
6	**159**	161 (94)	76 (44)	-
6.5	**186**	187 (109)	90 (53)	-
7	**216**	214 (124)	106 (62)	-
7.5	**248**	242 (141)	124 (72)	-
8	**282**	273 (159)	142 (83)	-
8.5	**318**	305 (178)	162 (94)	-
9	**357**	339 (197)	184 (107)	-

Although the loads in the accidental scenarios exceed those in the standard combinations for spans up to 6.5 meters, the momentarily increased material properties in the accidental scenario mean that Connection Front 2 does not have to be strengthened for any of the spans.

Table 6.8: Results check adjacent elements: End connection 1

	Required connection capacity [kN]:			
	Standard situation:	Accidental situation, loss of:		
Span [m]	ULS	Corner column	Edge column	Middle column
3	18	-6 (-4)	**34 (20)**	20 (12)
3.5	23	-7 (-5)	**45 (26)**	27 (16)
4	29	-8 (-5)	**56 (33)**	34 (20)
4.5	36	-8 (-6)	**69 (40)**	43 (25)
5	43	-9 (-6)	**83 (48)**	52 (30)
5.5	51	-9 (-7)	**98 (57)**	63 (36)
6	60	-10 (-7)	**115 (67)**	74 (43)
6.5	69	-10 (-7)	**132 (77)**	86 (50)
7	79	-10 (-7)	**151 (88)**	99 (58)
7.5	90	-10 (-7)	**171 (100)**	113 (66)
8	101	-10 (-7)	**193 (112)**	128 (74)
8.5	113	-10 (-7)	**215 (125)**	144 (84)
9	125	-10 (-7)	**239 (139)**	160 (93)

The edge column loss scenario increases the capacity demand for Connection Back 1 by $\approx 11\%$. In the corner column loss scenario, the load direction switches, meaning an upwards force is acting from the beam on the connection with the column.

Table 6.9: Results check adjacent elements: End connection 2

	Required connection capacity [kN]:			
	Standard situation:	Accidental situation, loss of:		
Span [m]	ULS	Corner column	Edge column	Middle column
3	**18**	0 (0)	25 (18)	21 (12)
3.5	**23**	0 (0)	32 (23)	28 (16)
4	**29**	1 (1)	40 (29)	35 (20)
4.5	**36**	2 (1)	50 (35)	44 (25)
5	**43**	3 (2)	60 (43)	53 (31)
5.5	**51**	4 (3)	71 (50)	63 (37)
6	**60**	6 (4)	83 (59)	75 (43)
6.5	**69**	7 (5)	96 (68)	87 (50)
7	**79**	9 (7)	109 (78)	100 (58)
7.5	**90**	11 (8)	124 (88)	114 (66)
8	**101**	14 (10)	140 (99)	128 (75)
8.5	**113**	16 (11)	156 (111)	144 (84)
9	**125**	19 (13)	174 (124)	161 (94)

Although the loads in the accidental scenarios exceed the loads in the standard combinations, the momentarily increased material properties in the accidental scenario make that Connection Back 2 does not have to be strengthened.

6.2.3 Columns

The columns at two locations require attention for design in the accidental scenarios, compared to the demand for fundamental load combinations. The second column (*Middle 1* in Figure 6.8) needs to be strengthened to be able to take the additional loads in the corner column loss scenario. The required dimensions of the second column for the fundamental and the (normative) corner column loss scenario are presented in Table 6.10. The required cross-sections for the accidental loads in the corner column loss scenario are $\approx 20\%$ larger than the fundamental combination. The third column (*Back 1* in Figure 6.8) needs to be designed for tensile forces occurring in the same corner column loss scenario. The tensile loads the third column needs to be able to take in the accidental corner column loss scenario is presented in Table 6.11.

Table 6.10: Required dimensions ($b \times h$) column *Middle-1* in fundamental and corner column loss scenario [mm^2].

Span [m]	Fundamental combination	Corner columns loss scenario
3	220×220	$\mathbf{240 \times 240}$
3.5	240×240	$\mathbf{270 \times 270}$
4	270×270	$\mathbf{290 \times 290}$
4.5	290×290	$\mathbf{320 \times 320}$
5	310×310	$\mathbf{340 \times 340}$
5.5	330×330	$\mathbf{370 \times 370}$
6	360×360	$\mathbf{390 \times 390}$
6.5	380×380	$\mathbf{420 \times 420}$
7	400×400	$\mathbf{440 \times 440}$
7.5	420×420	$\mathbf{460 \times 460}$
8	450×450	$\mathbf{490 \times 490}$
8.5	470×470	$\mathbf{510 \times 510}$
9	490×490	$\mathbf{540 \times 540}$

Table 6.11: Tensile loads in column *Back-1* in the corner column loss scenario.

Span [m]	Tensile load [kN]
3	47.7
3.5	62.4
4	78.3
4.5	95.2
5	113.3
5.5	132.5
6	152.8
6.5	174.2
7	196.7
7.5	220.2
8	244.9
8.5	270.6
9	297.3

Chapter 7

Limitations

Dynamic Load Factor
The DLF is assumed to be 2.0 for the entirety of the accidental floor load and facade load at the bay(s) connected to a lost column because the linear-elastic timber elements take the dynamically amplified accidental loads. In practice, a more favorable dissipation of the loads might occur closer to the remaining columns or due to energy dissipation in the deformation of the facade system, which is not regarded in this thesis.

Notional column removal
Only one column is removed at the time in the ALP analysis. The risk remains that more columns fail simultaneously in an accidental scenario, for which the structures in this research are not checked.

In the column loss scenarios, the assumption is made that the lost column *disappears* without, e.g., damaging the structural node above or dragging down connected elements.

This research does not assess the stability of the structures in either the fundamental or accidental scenarios. Of course, the stability in both fundamental and accidental states should be carefully evaluated to design an actual structure.

Connections
The performance and capacity of the connections between the columns and the beams are immensely simplified for ease of calculating all assessed spans and structural variations. More in-depth analysis is required to design specific structures in standard and accidental scenarios.

CLT plate elements
The CLT plate elements analyzed in this thesis have an assumed width of 1.0 meters and thus behave as beam elements. In practice, wider CLT plate elements with widths up to 3.5 meters are common, significantly influencing the structural behavior as they behave more plate-like.

Chapter 8

Conclusions

Extending timber floor elements over more than one floor span can provide an alternative load path in CC2b timber column and beam structures in corner, edge, and middle column removal scenarios. The extent to which timber floor elements can provide robustness in column removal scenarios depends on the type of timber floors used, the floor span, the location of the lost column, and the pattern in which the timber floor elements are placed:

CLT floor elements
With CLT floor elements, secondary load paths in accidental scenarios are possible for virtually all scenarios and spans. Only for a staggered floor layout, a maximum floor span of 7 meters in the corner column loss scenario and 8.5 meters in the edge column loss scenario is restrictive. In the continuous floor element layout, robustness through the CLT floor elements requires minor to no increase in cross-sectional height, meaning robustness is already built-in or simple to achieve. In the staggered layout, robustness through CLT floor elements does require an increase in the height of the elements.

Lignatur box floor elements
Providing a secondary load path in column loss scenarios using the Lignatur box floor elements in accidental column loss scenarios is technically possible for some spans and accidental loading scenarios but comes at significant additional material cost. For continuous element layouts, the element height needs to be doubled to take the accidental loads in the corner column loss scenario; in the staggered floor layout, an even more significant increase in element size is needed. The attempt to increase the performance of Lignatur box floor elements by doubling the top and bottom plate thicknesses showed smaller differences in the required element size for the standard and accidental design scenarios.

Staggered floor layout
For both the CLT and Lignatur floor elements, the staggered floor element layout led to a significant increase in element capacity demands for the accidental loads. The staggered layout is, therefore, less feasible than the continuous floor layout, and the focus should be on maintaining a continuous floor element layout in structures to effectively activate a secondary load path through the floor elements in accidental load scenarios at limited additional material costs.

Capacity adjacent elements
For the beams that support the floor elements, the cross-sectional demands for the deflection requirements are always normative, meaning the beams do not have to be strengthened to sustain the loads in the accidental scenarios.

The connections on the corners and edges of the structure, parallel to the floor span direction, do have to be strengthened to take the increased loads in the accidental scenarios.

The second column location, parallel to the floor span, requires strengthening to sustain the loads in the corner column loss scenario. The third column location, parallel to the floor span, should be designed to take the tensile loads in the corner column loss scenario.

Chapter 9

Recommendations

The following recommendations for further research are formulated based on the findings in this thesis:

- **Dynamic Load Factor**: Look into the assessment of the DLF for 3D MDOF structures in sudden column loss scenarios. While the DLF of 2.0 does make sense when instantaneously applied loads are taken by a linear-elastic timber structure, the load itself can undergo a lower dynamic amplification (e.g., energy absorbed in a deforming facade system or floor loads located in the proximity of remaining columns resulting in limited amplification).
- **More detailed structural analysis of the timber structure**: The research described in this thesis is a study on whether a second load path via timber floor elements would be feasible, and thereby remains general in some aspects and the level of detail (e.g., in how connections are regarded). It would be interesting to apply the continuous floor elements in a more detailed structural design with a higher level of connections, fire design, and stability analysis.
- **Lignatur elements connection to beam**: The connection between the Lignatur elements and the beams, which should take significant tensile loads, should be further developed before actual application.
- **Eurocode recommendations:** Investigate the (need for) dynamic amplifications in the Eurocode recommendations on robustness.

Bibliography

[1] "Moelven Mjøstårnet." https://www.moelven.com/mjostarnet/. ix, 1

[2] P. H. Kirkegaard, J. D. Sørensen, D. Cizmar, and V. Rajčić, "Robustness analysis of a wide-span timber structure with ductile behaviour," *Civil-Comp Proceedings*, vol. 93, no. December 2014, 2010. ix, 3

[3] "Ronan Point." https://www.skyscrapercenter.com/building/id/32910, 2016. ix, 5

[4] Menno van Dijk, "Afstudeerverslag Voortschrijdende Instorting bij Prefab Betonconstructies," Master's thesis, Eindhoven University of Technology, 2011. ix, 7, 12

[5] M. Smith, "Progressive Collapse Assessment: Non-linear behaviour of concrete structures in damaged state," Master's thesis, TU Delft, 2007. ix, 7, 8

[6] A. Fascetti, S. K. Kunnath, and N. Nisticò, "Robustness evaluation of RC frame buildings to progressive collapse," *Engineering Structures*, vol. 86, pp. 242–249, 2015. ix, 7, 8

[7] N. N. Instituut, "Nen-en 1991-1-7+c1+a1:2015," 2015. ix, xiii, 9, 11, 12, 19

[8] H. M. Bita, "Disproportionate Collapse Prevention Analyses for Mid-Rise Cross-Laminated Timber Platform-Type Buildings," no. May, 2019. ix, 14

[9] G. Powell, "Progressive Collapse: Case Studies Using Nonlinear Analysis," no. 1, pp. 1–14, 2004. ix, 15, 16

[10] M. Ferraioli, "A modal pushdown procedure for progressive collapse analysis of steel frame structures," *Journal of Constructional Steel Research*, vol. 156, pp. 227–241, 2019. ix, 13, 16

[11] K. Qian and B. Li, "Analytical Evaluation of the Vulnerability of RC Frames for Progressive Collapse Caused by the Loss of a Corner Column," *Journal of Performance of Constructed Facilities*, vol. 29, no. 1, pp. 1–14, 2015. ix, 21

[12] Swedish Wood, "The CLT Handbook," 2019. ix, xiii, 24, 25, 29, 30, 33, 38, 90, 92

[13] Lignatur, "Lignatur workbook," ix, 24, 25, 37

[14] A. Jorissen, "Timber Structures - Build up elements," *Lecture notes, TU/e*, pp. 1–32, 2013. ix, 25, 26, 27, 28

[15] M. Wallner-Novak, J. Koppelhuber, and K. Pock, *Cross-Laminated Timber Structural Design*. 2014. ix, xiii, 25, 28, 29, 30, 32

[16] R. Harris, *Cross laminated timber*. Elsevier Ltd., 2015. ix, 28, 30

[17] N. N. Instituut, "Nen-en 1991-1-7+c1/nb (dutch annex)," 2011. xiii, 9, 10

[18] M. Norouzi, M. Chàfer, L. F. Cabeza, L. Jiménez, and D. Boer, "Circular economy in the building and construction sector: A scientific evolution analysis," *Journal of Building Engineering*, vol. 44, no. April, 2021. 1

[19] M. Ö. Arıoğlu Akan, D. G. Dhavale, and J. Sarkis, "Greenhouse gas emissions in the construction industry: An analysis and evaluation of a concrete supply chain," *Journal of Cleaner Production*, vol. 167, no. 2017, pp. 1195–1207, 2017. 1

[20] B. D'Amico, F. Pomponi, and J. Hart, "Global potential for material substitution in building construction: The case of cross laminated timber," *Journal of Cleaner Production*, vol. 279, p. 123487, 2021. 1

[21] K. Voulpiotis, J. Köhler, R. Jockwer, and A. Frangi, "A holistic framework for designing for structural robustness in tall timber buildings," *Engineering Structures*, vol. 227, 2021. 2, 3, 5, 19

[22] S. P. G. Moonen, "Capita Selecta - Safety, reliability and loadings - 7KT1M0," 2020. 5

[23] J. A. J. Huber, *Numerical Modelling of Timber Building Components to Prevent Disproportionate Collapse*. PhD thesis, Luleå University of Technology, Skellefteå, Sweden, 2021. 6, 14

[24] B. R. Ellingwood and D. O. Dusenberry, "Building design for abnormal loads and progressive collapse," *Computer-Aided Civil and Infrastructure Engineering*, vol. 20, no. 3, pp. 194–205, 2005. 6

[25] U. Starossek, "Typology of progressive collapse," *Engineering Structures*, vol. 29, no. 9, pp. 2302–2307, 2007. 6

[26] B. A. Izzuddin, A. G. Vlassis, A. Y. Elghazouli, and D. A. Nethercot, "Progressive collapse of multi-storey buildings due to sudden column loss - Part I: Simplified assessment framework," *Engineering Structures*, vol. 30, no. 5, pp. 1308–1318, 2008. 9, 21

[27] CPNI (Arup), "Review of International Research on Structural Robustness and Disproportionate Collapse," 2011. 9, 12, 13, 15

[28] M. Byfield, W. Mudalige, C. Morison, and E. Stoddart, "A review of Progressive Collapse research and regulations," *Proceedings of the Institution of Civil Engineers: Structures and Buildings*, vol. 167, no. 8, pp. 447–456, 2014. 9, 13

[29] H. Mpidi Bita, J. A. J. Huber, P. Palma, and T. Tannert, "Prevention of Disproportionate Collapse for Multistory Mass Timber Buildings: Review of Current Practices and Recent Research," *Journal of Structural Engineering*, vol. 148, no. 7, pp. 1–15, 2022. 10, 14

[30] N. N. Instituut, "Eurocode 0: Grondslagen van het constructief ontwerp," 2013. 10, 33, 34, 40

[31] N. N. Instituut, "Eurocode 0: Grondslagen van het constructief ontwerp Nationale Bijlage," 2017. 10, 36, 40

[32] N. Annex, "Eurocode 5: Ontwerp en berekening van houtconstructies Nationale Bijlage," 2012. 10, 12, 28, 34, 38, 90

[33] A. Bhagwandas, "Constructieve samenhang van prefab gebouwconstructies na een gasexplosie," Master's thesis, TU Delft, 2007. 12

[34] H. Utrecht, "Eurocode 5: Ontwerp en berekening van houtconstructies," vol. 2005, no. november 2011, 2016. 12, 28, 33, 34, 36, 38, 55, 57, 90, 91, 97, 99

[35] M. Kars, "Tweede draagweg volgens de norm: Voorstel voor wijzigingen in de regelgeving met betrekking tot het rekenen met een tweede draagweg," Master's thesis, Hogeschool van Amsterdam, 2018. 12

[36] J. de Boer, "Tweede draagweg van een hoekveld in prefab beton," Master's thesis, Eindhoven University of Technology, 2012. 12

[37] C. H. Lyu, B. P. Gilbert, H. Guan, I. D. Underhill, S. Gunalan, and H. Karampour, "Experimental study on the quasi-static progressive collapse response of post-and-beam mass timber buildings under corner column removal scenarios," *Engineering Structures*, vol. 242, no. May, p. 112497, 2021. 13, 14, 19

[38] H. Mpidi Bita and T. Tannert, "Experimental Study of Disproportionate Collapse Prevention Mechanisms for Mass-Timber Floor Systems," *Journal of Structural Engineering*, vol. 146, no. 2, pp. 1–14, 2020. 13

[39] H. Mpidi Bita and T. Tannert, "Disproportionate collapse prevention analysis for post and beam mass timber building," *Journal of Building Engineering*, vol. 56, no. June, p. 104744, 2022. 13, 19, 34

[40] J. Evans, "The Future of Office Buildings," 2018. 14

[41] Derix, "DERIX Kruislaaghouten bouwelementen." 24, 37

[42] N. Annex, "Eurocode 1: Belastingen op constructies – Deel 1-1: Algemene belastingen Nationale Bijlage," no. december 2011, 2011. 33

[43] StructX, "Continuous Beams – Two Equal Spans with UDL." https://structx.com/Beam_Formulas_041.html. 35

[44] L. Dominik, "13 Beam deflection formulas." https://www.structuralbasics.com/beam-deflection-formulas/#2span-continuous-beam-uniformly-distributed-line-load-on-1-span. 35

[45] B. Zhang and T. Kilpatrick, "Vibrational modal frequencies and shapes of two-span continuous timber flooring systems," *Shock and Vibration*, vol. 2019, 2019. 37, 89

[46] L. Muszyński, R. Gupta, S. hyun Hong, N. Osborn, and B. Pickett, "Fire resistance of unprotected cross-laminated timber (CLT) floor assemblies produced in the USA," *Fire Safety Journal*, vol. 107, no. April 2017, pp. 126–136, 2019. 39

[47] A. Jorissen, "7KP7M0 – Stability of Structures - Material aspects of structural stability - Timber Lecture notes ," 2020. 56

[48] N. Normalisatie-instituut, "NEN-EN 1992-1-1 + C2, Eurocode 2: Design of concrete structures – Part 1-1: General rules and rules for buildings," 2017. 57

[49] Rothoblaas, "VGZ EVO: Fully threaded screw with cylindrical head." 58

[50] S. Rezvani, L. Zhou, and C. Ni, "Experimental evaluation of angle bracket connections in CLT structures under in- and out-of-plane lateral loading," *Engineering Structures*, vol. 244, no. June, p. 112787, 2021. 59

[51] StructX, "Continuous Beam - Two Span with Central Point Load Over One Span." https://structx.com/Beam_Formulas_030.html. 90

Appendix A

Floor element configurations

A.1 Lignatur box floor elements

The Lignatur box floor elements used in this research are all highly similar to the Lignatur element illustrated in Figure 5.3. Only the *ribs* change in height per element size, resulting in the element height and corresponding bending stiffness presented in Table A.1.

For the calculation of the characteristic permanent load G_k, j described by (37), the following values are used for the Lignatur elements:

$G_{\mathrm{k,j,nhd}}$	=	1.25	$[kN/m^2]$
h_{str}	=	element height *minus* top and bottom plate thicknesses	$[m]$
$G_{\mathrm{k,j,hd}}$	=	0.87	$[kN/m^2/m]$

Table A.1: Lignatur box floor elements used in analysis

element height $[mm]$	perm. load $G_{\mathrm{k,j}}$ $[kN/m^2]$	EI per meter width $[Nmm^2]$
120	1.55	$1.38 \cdot 10^{12}$
140	1.56	$2.07 \cdot 10^{12}$
160	1.57	$2.91 \cdot 10^{12}$
180	1.59	$3.91 \cdot 10^{12}$
200	1.60	$5.07 \cdot 10^{12}$
220	1.61	$6.40 \cdot 10^{12}$
240	1.63	$7.91 \cdot 10^{12}$
280	1.65	$1.15 \cdot 10^{13}$
320	1.68	$1.58 \cdot 10^{13}$
360	1.70	$2.09 \cdot 10^{13}$
400	1.73	$2.69 \cdot 10^{13}$
440	1.76	$3.38 \cdot 10^{13}$
480	1.78	$4.17 \cdot 10^{13}$

A.2 CLT floor element layups

For the calculation of the characteristic permanent load G_k, j $[kN/m^2]$ described by (37), the following values are used for the CLT elements:

$G_{\mathrm{k,j,nhd}}$	=	1.1	$[kN/m^2]$
h_{str}	=	element height	$[m]$
$G_{\mathrm{k,j,hd}}$	=	4	$[kN/m^2/m]$

Table A.2: Properties of the CLT elements used in the analysis

height $[mm]$	Layers	Configuration	$G_{\mathrm{k,j}}$	EI_{net} $[Nmm^2]$	$S_{R,x,net}$ $[mm^3]$	W_{net} $[mm^3]$
60	3	20-20-20	1.34	$1.91 \cdot 10^{11}$	400000	$5.78 \cdot 10^5$
80	3	30-20-30	1.42	$4.62 \cdot 10^{11}$	750000	$1.05 \cdot 10^6$
120	3	40-40-40	1.58	$1.53 \cdot 10^{12}$	1600000	$2.31 \cdot 10^6$
150	5	30-30-30-30-30	1.7	$2.45 \cdot 10^{12}$	1800000	$2.97 \cdot 10^6$
180	5	40-30-40-30-40	1.82	$4.49 \cdot 10^{12}$	2800000	$4.53 \cdot 10^6$
220	7	40-20-40-20-40-20-40	1.98	$7.88 \cdot 10^{12}$	4800000	$6.51 \cdot 10^6$
250	7	40-30-40-30-40-30-40	2.1	$1.05 \cdot 10^{13}$	5600000	$7.60 \cdot 10^6$
280a	7	40-40-40-40-40-40-40	2.22	$1.34 \cdot 10^{13}$	6400000	$8.68 \cdot 10^6$
280b	7	40-40-40-40-40-40-40	2.22	$1.86 \cdot 10^{13}$	8000000	$1.21 \cdot 10^7$
320	9	40-30-40-30-40-30-40-30-40	2.38	$2.19 \cdot 10^{13}$	8400000	$1.24 \cdot 10^7$
360a	9	40-40-40-40-40-40-40-40-40	2.54	$2.85 \cdot 10^{13}$	9600000	$1.44 \cdot 10^7$
360b	9	40-40-40-40-40-40-40-40-40	2.54	$3.70 \cdot 10^{13}$	12800000	$1.87 \cdot 10^7$
400	11	40-40-30-40-30-40-30-40-30-40-40	2.7	$5.05 \cdot 10^{13}$	15600000	$2.29 \cdot 10^7$

Table A.3: Effective flexural rigidity $(EI)_{ef}$ $[\cdot 10^{11}\ Nmm^2]$ CLT elements, dependent on span L.

	Span L $[m]$												
height $[mm]$	3.0	3.5	4.0	4.5	5.0	5.5	6.0	6.5	7.0	7.5	8.0	8.5	9.0
60	1.83	1.85	1.86	1.87	1.88	1.89	1.89	1.89	1.89	1.89	1.89	1.90	1.90
80	4.36	4.42	4.46	4.50	4.52	4.53	4.55	4.56	4.57	4.57	4.58	4.58	4.59
120	13.3	13.7	14.0	14.2	14.4	14.5	14.6	14.7	14.8	14.8	14.9	14.9	15.0
150	20.3	21.2	21.9	22.4	22.8	23.1	23.3	23.5	23.6	23.7	23.8	23.9	23.9
180	35.2	37.3	38.8	40.0	40.8	41.5	42.0	42.4	42.7	43.0	43.2	43.4	43.5
220	62.0	66.2	69.2	71.5	73.2	74.5	75.5	76.4	77.0	77.6	78.1	78.4	78.8
250	74.6	81.5	86.8	90.8	93.9	96.4	98.3	99.9	101	102	103	104	105
280a	87.4	97.4	105	111	116	120	123	126	128	130	131	133	134
280b	109	122	133	141	148	153	157	161	164	167	169	171	172
320	126	142	155	165	173	180	185	188	192	195	197	201	202
360a	144	165	183	198	210	220	228	236	242	246	249	253	255
360b	172	200	224	244	259	273	285	295	303	311	317	323	327
400	224	264	295	323	350	367	383	396	409	420	429	436	442

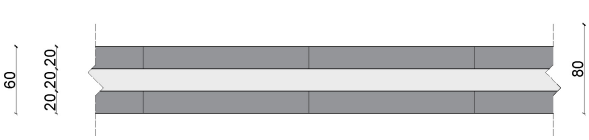

(a) CLT 60mm

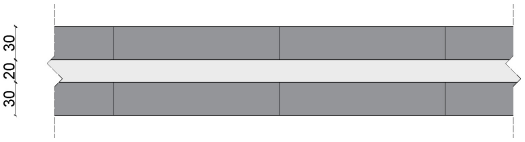

(b) CLT 80mm

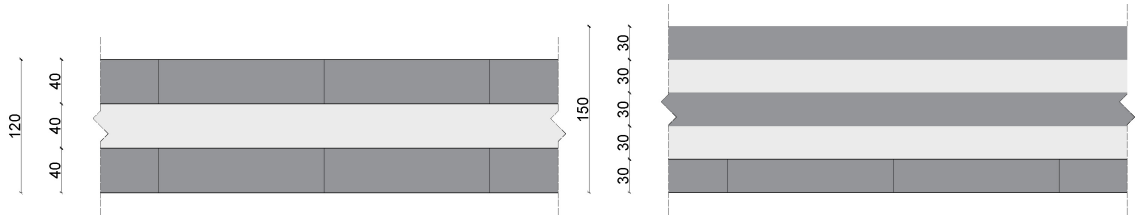

(a) CLT 120mm (b) CLT 150mm

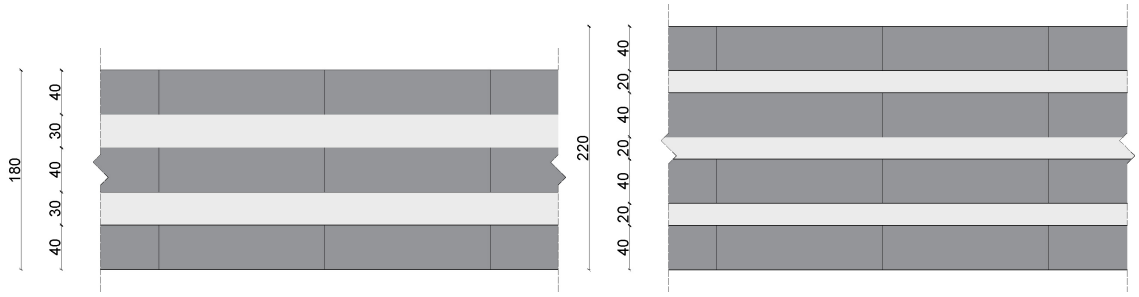

(a) CLT 180mm (b) CLT 220mm

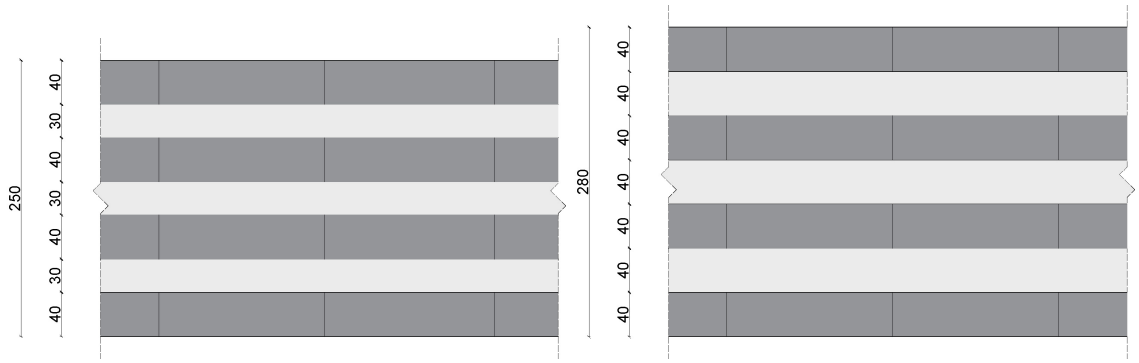

(a) CLT 250mm (b) CLT 280mm (a)

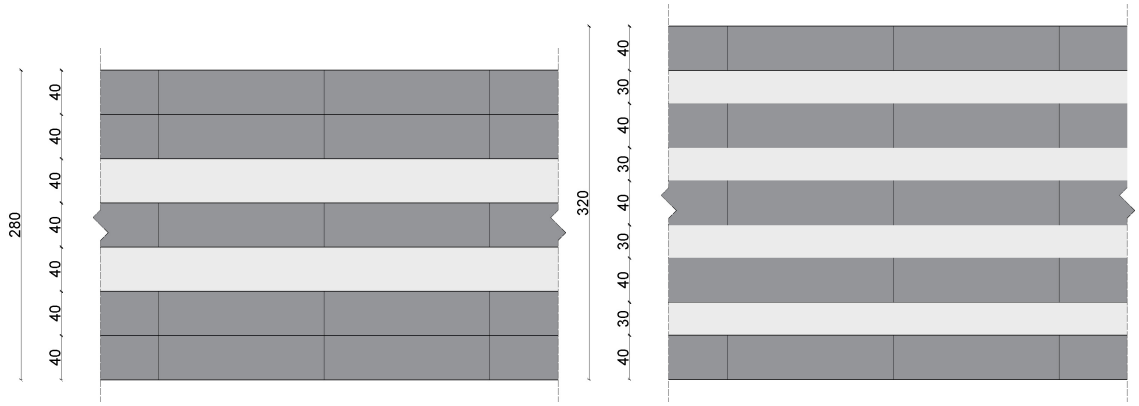

(a) CLT 280mm (280b) (b) CLT 320mm

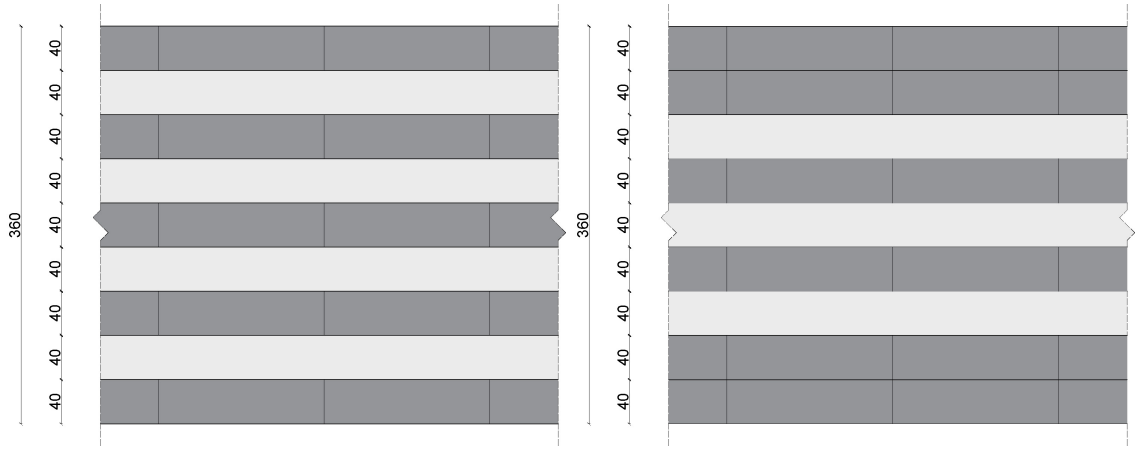

(a) CLT 360mm (360a)

(b) CLT 360mm (360b)

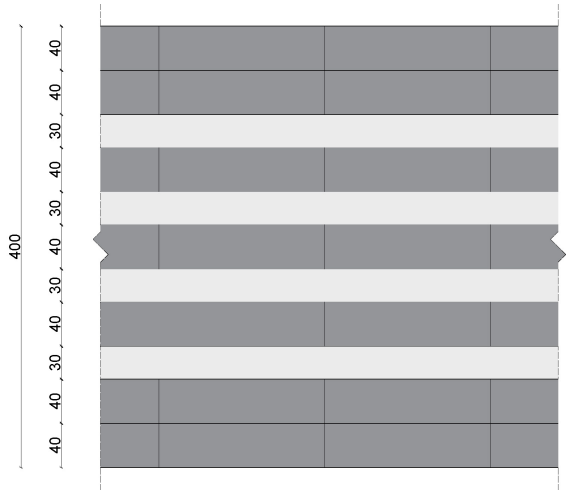

(a) CLT 400mm

Appendix B

Example calculation of a floor element

In this appendix, the structural capacity demand of the floor elements for each of the design criteria will be elaborated step-by-step to provide an example of the calculation approach used to obtain the results presented in Chapter 6. While the principles on which the calculations and structural analysis are based on are presented in Chapter 5, these principles will be presented with actual numbers and calculation steps in this appendix.
For the example calculation, a six-meter span is chosen. CLT elements placed in a continuous layout will be designed for the fundamental (ULS and SLS) and accidental design combinations.

B.1 Moment resistance elements

W_{net} for CLT ULS stress checks

The *net section modulus* W_{net} is used to assess the CLT floor elements in the ULS situations, as described in section 5.1.4. For the 220 mm CLT plate, visualized in Figure B.1, the calculation is as follows:

$$W_{\text{net}} = \left(\sum_{i=1}^{n} (I_i) + \sum_{i=1}^{n} \left(A_i e_i^2 \right) \right) / z_s$$

Where:

$$\begin{array}{lcll} I_{\text{i}} & = & \frac{1}{12} \cdot b_i \cdot h_i^3 & [mm^4] \\ A_{\text{i}} & = & b_i \cdot h_i & [mm^2] \\ e_{\text{i}} & = & e_i & [mm] \\ z_{\text{s}} & = & h/2 & [mm] \end{array}$$

Resulting in:

$$W_{\text{net}} = (4 \cdot \frac{1}{12} \cdot 1000 \cdot 40^3) + (1000 \cdot 40) \cdot 2 \cdot (30^2 + 90^2)/110$$

$$W_{\text{net}} = 6.74 \cdot 10^6 \quad [mm^3] \tag{100}$$

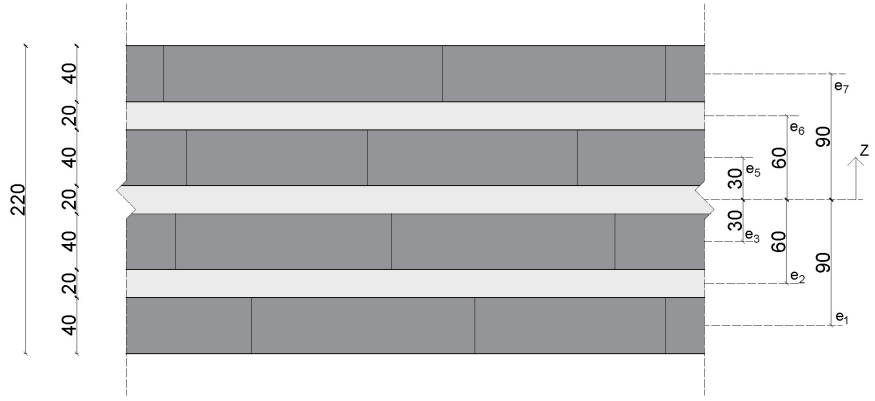

Figure B.1: 220mm CLT with the relevant dimensions for the section modulus calculation indicated

To find the maximum bending moment each floor element can take, the value for W_{net} is multiplied by the *design bending strength* $f_{y,d}$, resulting for the 220 [mm] CLT floor in:

$$M_{max} = W_{net} \cdot f_{y,d}$$

$$M_{max} = 6.74 \cdot 10^6 \cdot 0.8 \cdot \frac{24}{1.25}$$

$$M_{max} = 103.5 \quad [kNm] \tag{101}$$

I_{ef} for CLT SLS deflection checks

For the *effective Moment of Inertia* I_{ef} used for the deflection calculations, the gamma-method is used for CLT plates, as described in Section 5.1.4. The I_{ef} calculation for the five-layer 180 [mm] CLT element that is required to meet the deflection demand for the six-meter span is as follows:

$$I_{ef} = \sum_{i=1}^{3} \frac{b \cdot d_i^3}{12} + \sum_{i=1}^{3} y_i \cdot b \cdot d_i \cdot a_i^2$$

With the reduction factor γ_i for each of the three longitudinal CLT layers i:

$$\gamma_1 = \frac{1}{\left(1 + \frac{\pi^2 \cdot E \cdot A_1}{\ell_{ref}{}^2} \cdot \frac{d_{1,2}}{b \cdot G_{R,12}}\right)} = 0.93 \quad \left[\frac{1}{m}\right]$$

$$\gamma_2 = 1,0 \quad \left[\frac{1}{m}\right]$$

$$\gamma_3 = \frac{1}{\left(1 + \frac{\pi^2 \cdot E \cdot A_3}{\ell_{ref}{}^2} \cdot \frac{d_{2,3}}{b \cdot G_{R,23}}\right)} = 0.93 \quad \left[\frac{1}{m}\right]$$

Where (for a 180 mm CLT plate):

E	=	11000	$[N/mm^2]$
A_i	=	$1000 \cdot 40$	$[mm]$
l_{ref}	=	6000	$[mm]$
$G_{\text{R,ij}}$	=	50	$[N/mm^2]$
b	=	1000	$[mm]$
$d_{\text{i,j}}$	=	30	$[mm]$

Resulting in an *effective Moment of Inertia* I_{ef} of:

$$I_{ef} = 3 \cdot \frac{1000 \cdot 40^3}{12} + 2 \cdot 0.93 \cdot 1000 \cdot 40 \cdot 70^2$$

$$I_{ef} = 3.81 \cdot 10^8 \quad [mm^4]$$

B.2 Loads and load combinations

Loads

Height *independent* self-weight of the floor $G_{h,i}$ (mostly service layers):

$$G_{h,i} = 1.1\ [kN/m^2]$$

Height *dependent* self-weight of the floor $G_{h,d}$ (CLT plate thickness):

$$G_{h,d} = 4 \cdot h_{CLT}\ [kN/m^2/m]$$

For the 220 mm CLT plate, the total self-weight G_k of the lay-up is:

$$G_k = 1.1 + 4 \cdot 0.22\ [kN/m^2/m]$$

$$G_k = 1.98\ [kN/m^2]$$

Fundamental load combination

Following from Section 5.2.1, the governing load combination in the fundamental situation is the least favorable of:

$$E_d = \begin{cases} \gamma_{\text{G},j} G_{\text{k},j} + \gamma_{\text{Q},1} \psi_{0,1} \text{Q}_{\text{k},1} \\ \xi_j \gamma_{\text{G},j} G_{\text{k},j} + \gamma_{\text{Q},1} \text{Q}_{\text{k},1} \end{cases}$$

Where (for a 220 mm CLT plate):

$\gamma_{\text{G},j}$	=	1.35	[-]
$G_{\text{k},j}$	=	1.98	$[kN/m^2]$
$\gamma_{\text{Q},1}$	=	1.5	[-]
$\psi_{0,1}$	=	0.5	[-]
$\text{Q}_{\text{k},1}$	=	3.0	$[kN/m^2]$
$\gamma_{\text{Q},i}$	=	1.5	[—]
ξ_j	=	0.85	[-]

Resulting in (the least favorable of):

$$E_d = \begin{cases} 1.35 \cdot 1.98 + 1.5 \cdot 0.5 \cdot 3.0 \\ 0.85 \cdot 1.35 \cdot 1.98 + 1.5 \cdot 3.0 \end{cases}$$

$$E_d = \begin{cases} 4.92\ [kN/m^2] \\ 6.77\ [kN/m^2] \end{cases}$$

$$\Rightarrow E_d = 6.77\ [kN/m^2] \tag{102}$$

Accidental load combination

The governing load combination in the accidental situation follows from Section 5.3.1 as well and is described by Equation 53:

$$E_{d,acc} = G_\mathrm{k} + 0.3 \cdot Q_\mathrm{k}$$

Resulting in (for a 220 [mm] CLT plate):

$$E_{d,acc} = 1.98 + 0.3 \cdot 3.0$$

$$E_{d,acc} = 2.88\ [kN/m^2]$$

B.3 Fundamental moments

For a continuous floor element on three supports loaded by a distributed load, the largest bending moment is situated above the middle support (see figure F.1). The middle span bending moment has a value of:

$$M_{mid} = -\frac{1}{8} \cdot q \cdot l^2$$

For the 120 [mm] CLT floor required for the span of 6 meters (see the results table in Section 6.1), the normative bending moment is:

$$M_d = -\frac{1}{8} \cdot 6.31 \cdot 6^2$$

$$M_d = 28.4 \quad [kNm]$$

For a span of six meters, the bending moment resistance of the 120 [mm] CLT floor elements is (see Table A.2):

$$M_{R,d} = 35.5 \quad [kNm]$$

$$M_d \leq M_{R,d}$$

$$28.4 \leq 35.5 \quad \text{[OK]}$$

B.4 Deflections

From Section 5.2.2 (*Deflection*) follows that the deflection combination with only one floor-field loaded by the live load for the continuous elements is normative. Taking into account the creep effect of timber structures and the relevant combination factors results in the following design equation:

$$u_{\text{fin},2} \leq \frac{l}{500}$$

$$\frac{1}{185}\frac{g_{\text{d}} l^4}{EI}(1+k_{\text{def}}) + 0.00911\frac{q_{\text{d}} l^4}{(EI)_{ef}}\left(1+\varphi_{2,1}k_{\text{def}}\right) \leq \frac{l}{500}$$

Where:

g_{d}	=	$\xi \cdot \gamma_g \cdot g_{\text{k,180mm}} = 0.85 \cdot 1.35 \cdot 1.82 = 2.09$	$[kN/m^2]$
l	=	6000	$[mm]$
E_0	=	11000	$[MPa]$
I_{ef}	=	$1.43 \cdot 10^9$	$[mm^4]$
k_{def}	=	0.6	[-]
q_{d}	=	$\gamma_Q \cdot q_k = 1.5 \cdot 3.0 = 4.5$	$[kN/m^2]$
$\psi_{2,1}$	=	0.3	[-]

Resulting in the equation for the deflection, using a 180mm CLT plate (which follows as demanded cross-sectional height from Chapter 6: *results*):

$$\frac{1}{185}\frac{2.9 \cdot 10^{-3} \cdot 6000^4}{11000 \cdot 1.43 \cdot 10^9}(1+0.6) + 0.00911\frac{4.5 \cdot 10^{-3} 6000^4}{11000 \cdot 1.43 \cdot 10^9}(1+0.3 \cdot 0.6) \leq \frac{6000}{500} \tag{103}$$

$$8.51\ mm \leq 12\ mm \tag{104}$$

B.5 Vibrations

From section 5.2.3 (*vibrations*) follows that the first frequency of the continuously spanned floors should be equal to or greater than 8 $[Hz]$. The first frequency of the continuous floors follows from Equation (48):

$$f_1 = \frac{(\beta_1 L)^2}{2\pi L^2}\sqrt{\frac{(EI)_L}{m}}$$

The required CLT element height for the vibrations given in chapter 6: *results* yield the following equation:

f_1	=	first modal frequency of the two-span floor	$[Hz]$
$\beta_1 L$	=	3.142 [45]	[-]
L	=	6	$[m]$
$(EI)_L$	=	$7.88 \cdot 10^6$	$[Nm^2/m]$
m	=	198	$[kg/m^2]$

$$f_1 = \frac{(3.142)^2}{2\pi 6^2}\sqrt{\frac{7.88 \cdot 10^6}{198}}$$

$$f_1 = 8.7\ [Hz]$$

Now that the $f_1 \geq 8\ [Hz]$ requirement has been met, the following two requirements given by Equations (50) (*instantaneous deflection*) and (51) (vertical velocity by a unit impulse) have to be satisfied:

$$\frac{w}{F} \leq a\ [mm/kN]$$

Where:

w	=	maximum instantaneous deflection by the vertical point load F	$[mm]$
F	=	1 [12]	$[kN]$
a	=	1 [32]	$[mm/kN]$

For a two-span structure with a point load on one floor span, the equation for the deflection is [51]:

$$w = 0.015 \cdot \frac{F \cdot l^3}{EI_{ef}}$$

$$w = 0.015 \cdot \frac{1 \cdot 6000^3}{7.55 \cdot 10^9}$$

$$w = 0.43\ [mm]$$

Resulting in:

$$\frac{0.43}{1} \leq 1\ [mm/kN]$$

$$0.43 \leq 1\ [mm/kN]$$

Satisfying the instantaneous deflection requirement of equation 50.

For the second vibration requirement, the vertical velocity by a unit impulse, governed by Equation (51), the following calculations are performed:

$$v \leq b^{(f_1\zeta - 1)}\ [m/Ns^2]$$

Where:

v	=	vertical velocity response	$[m/Ns^2]$
b	=	120 [32])	[-]
f_1	=	8.7	$[Hz]$
ζ	=	0.01 [34]	[-]

The equation for the vertical velocity response v is given by Eurocode 5 [34]:

$$v = \frac{4\left(0,4 + 0,6n_{40}\right)}{mbl + 200} \tag{105}$$

Where:

n_{40}	=	amount of first-order vibrations below 40 Hz	[-]
m	=	mass of the floor	$[kg/m^2]$
b	=	width of the floor	$[m]$
l	=	floor span	$[m]$

The value for n_{40} can be obtained using [34]:

$$n_{40} = \left\{\left(\left(\frac{40}{f_1}\right)^2 - 1\right)\left(\frac{b}{\ell}\right)^4 \frac{(EI)_\ell}{(EI)_b}\right\}^{0,25} \tag{106}$$

Where:

$(EI)_b$ = bending stiffness of the element perpendicular to the span $[Nm^2/m]$

For 220mm CLT, $(EI)_b$ is:

$$(EI)_b = \sum_{i=1}^{3} E_i \cdot \frac{b \cdot d_i^3}{12} + \sum_{i=1}^{2} \cdot E_i \cdot b \cdot d_i \cdot a_i^2$$

$$(EI)_b = \sum_{i=1}^{3} 11000 \cdot \frac{1000 \cdot 20^3}{12} + \sum_{i=1}^{2} \cdot 11000 \cdot 1000 \cdot 20 \cdot 60$$

$$(EI)_b = 1.61 \cdot 10^6\ [Nm^2/m]$$

Resulting in:

$$n_{40} = \left\{\left(\left(\frac{40}{8.7}\right)^2 - 1\right)\left(\frac{1}{6}\right)^4 \frac{7.88 \cdot 10^6}{1.61 \cdot 10^6}\right\}^{0,25}$$

$$n_{40} = 0.53\ [-]$$

From which the value for v can be obtained:

$$v = \frac{4(0,4 + 0,60.53)}{198 \cdot 1 \cdot 6 + 200}$$

$$v = 2.03 \cdot 10^{-3}\ [m/Ns^2]$$

Applying the value found for v in the governing requirement of Equation (51) yields:

$$v \leq b^{(f_1\zeta - 1)}\ [m/Ns^2]$$

$$2.03 \cdot 10^{-3} \leq 120^{(8.7 \cdot 0.01 - 1)}$$

$$2.03 \cdot 10^{-3} \leq 1.3 \cdot 10^{-2}$$

Satisfying the vertical velocity response requirement of Equation (51).

B.6 Shear and rolling shear

The rolling shear design stress $\tau_{v,R,d}$ is calculated using Equation (32), explained in Section 5.1.5. For a 280mm CLT element (280a, the cross-section which is normative in the column loss scenario for spans of six meters), the check of the rolling shear is as follows:

$$\tau_{v,R,d} = \frac{V_{0,d} \cdot S_{0,R,net}}{I_{0,net} \cdot b}$$

The shear load $V_{0,d}$ follows from the structural scheme of the two-span floors, as illustrated in Appendix F by means of Figure F.1.

$$V_{0,d} = \frac{5}{8} qL$$

$$V_{0,d} = \frac{5}{8} \cdot 7.05 \cdot 6$$

$$V_{0,d} = 26.4\,[kN]$$

The net static moment $S_{0,R,net}$ is calculated using Equation 33 [12]:

$$S_{0,R,net} = \sum_{i=1}^{m_L} b \cdot t_i \cdot a_i$$

$$S_{0,R,net} = \sum_{i=1}^{m_L} 1000 \cdot 40 \cdot (40 + 120)$$

$$S_{0,R,net} = 6.4 \cdot 10^6\,[mm3]$$

Resulting in the value for $\tau_{v,R,d}$:

$$\tau_{v,R,d} = \frac{26.4 \cdot 10^3 \cdot 6.4 \cdot 10^6}{1.21 \cdot 10^9 \cdot 1000}$$

$$\tau_{v,R,d} = 0.14\,[MPa]$$

The rolling shear stress $\tau_{v,R,d}$ should remain below the rolling shear strength $f_{v,R,d}$, which is given by Equation (34):

$$f_{v,R,d} = k_{mod} \cdot \frac{f_{v,R,k}}{\gamma_M}$$

$$f_{v,R,d} = 0.80 \cdot \frac{1.1}{1.25}$$

$$f_{v,R,d} = 0.70 \quad [MPa]$$

Resulting in the Unity Check for the rolling shear:

$$\tau_{v,R,d} \leq f_{v,R,d}$$

$$0.14 \leq 0.70 \quad \text{OK}$$

B.7 Accidental moments

The normative bending moment in the floor elements in the accidental situation is found in the corner column loss scenario. It is obtained using the approach described in Section 5.3.2. For the continuous CLT elements and a 6 $[m]$ span, the normative bending moment is:

$$M_{d,acc} = -212.0 \quad [kNm]$$

The moment resistance of the CLT plate elements is higher in the accidental scenario due to momentarily increased material strength properties.

$$f_{y,d,acc} = 1.1 \cdot \frac{24}{1.0} = 26.4 \quad [MPa]$$

A 280 $[mm]$ CLT plate has the required capacity to sustain the loads in the accidental situation, CLT plate element *280a* in Table A.2 visualized in Figure A.4b.

$$W_{net,280a} = 8.68 \cdot 10^6 \quad [mm^3] \tag{107}$$

Resulting in a moment capacity of:

$$M_{Rd,acc} = W_{net,280a} \cdot f_{y,d,acc}$$

$$M_{Rd,acc} = 229.1 \quad [kNm] \tag{108}$$

$$|M_{d,acc}| < M_{Rd,acc} \tag{109}$$

Appendix C

Example calculation of adjacent elements

C.1 Columns

The example calculation of the dimensioning of a column in the standard situation and the corner column loss scenario is elaborated in this appendix as an example. The elaborated structure is 6 stories of 3 $[m]$ tall and has a floor span of 6 $[m]$ in both directions. The location of the elaborated column is indicated in Figure C.1.

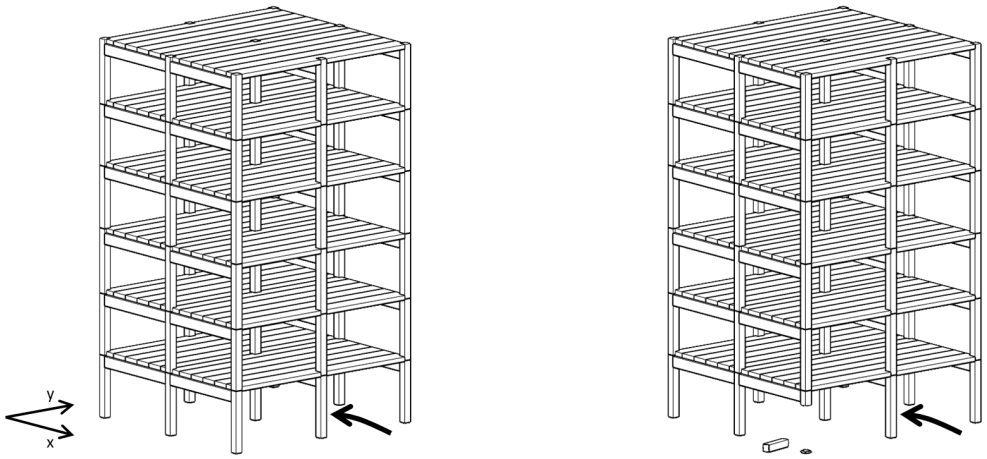

(a) Standard situation (b) Corner column loss scenario

Figure C.1: Location of the column for which the analysis is elaborated as an example.

Standard design situation

First, the dimensioning of the column in the standard design situation is elaborated. The required dimensions of the column are $360\ x\ 360\ [mm^2]$. The calculation approach is described in Section 5.4.3.

Loads on the column in the standard design situation:

Standard floor load for two stories	=	253.7	$[kN]$
Reduced floor load for four stories	=	350.8	$[kN]$
Dead load columns	=	32.5	$[kN]$
Dead load beams	=	45.1	$[kN]$
Dead load facade	=	145.8	$[kN]$
Total load	=	812.9	$[kN]$

Calculation of $\lambda_{rel,y}$:

$$\lambda_y = \frac{h}{i_y} = \frac{360}{103.9} = 28.9\,[mm]$$

Where:

$$i_y = \sqrt{\frac{I_y}{A}} = \sqrt{\frac{1.4 \cdot 10^9}{1.3 \cdot 10^5}} = 103.9\,[mm^2]$$

$$\lambda_{rel,y} = \frac{\lambda_y}{\pi}\sqrt{\frac{f_{c,0,k}}{E_{0.05}}} = \frac{28.9}{\pi}\sqrt{\frac{21}{9100}} = 0.44$$

Since the column has a square cross-section, $\lambda_{rel,z} = \lambda_{rel,y}$. And since $\lambda_{rel,z}$ and $\lambda_{rel,y}$ are both larger than 0.3, and Equations (110) and (111) should be used (see Section 5.4.3).

$$\frac{\sigma_{c,0,d}}{k_{c,y} \cdot f_{c,0,d}} + \frac{\sigma_{m,y,d}}{f_{m,y,d}} + k_m \frac{\sigma_{m,z,d}}{f_{m,z,d}} \leq 1 \tag{110}$$

$$\frac{\sigma_{c,0,d}}{k_{c,z} \cdot f_{c,0,d}} + k_m \frac{\sigma_{m,y,d}}{f_{m,y,d}} + \frac{\sigma_{m,z,d}}{f_{m,z,d}} \leq 1 \tag{111}$$

Calculation of 2nd order moment increase factor:

$$\frac{n}{n-1} = 1.06\,[\text{-}]$$

Where:

$$n = \frac{F_{cr}}{F} = \frac{13968}{812.9} = 17.2\,[\text{-}]$$

$$F_{cr} = \frac{\pi^2 EI}{L_{eff}^2} = \frac{\pi^2 \cdot 11000 \cdot 1.4 \cdot 10^9}{3000^2} = 13968\,[kN]$$

Eccentricities of the connection e_y and e_z:

$$e_y = 150 + \frac{b_y}{2} = 150 + \frac{360}{2} = 330\,[mm]$$

$$e_z = 150 + \frac{b_z}{2} = 150 + \frac{360}{2} = 330\,[mm]$$

Eccentricity by element imperfections e_0:

$$e_0 = \frac{L}{500} = \frac{3000}{500} = 6\,[mm]$$

Eccentricity by imperfectly centered vertical load application e_i:

$$e_i = \frac{1}{400} \cdot L_{eff} = \frac{1}{400} \cdot 3000 = 7.5\,[mm]$$

Calculation of $k_{c,y}$ and $k_{c,z}$ ($k_{c,y}$ and $k_{c,z}$ are equal due to the square cross-section of the columns):

$$k_{c,y} = k_{c,z} = \frac{1}{k_y + \sqrt{k_y^2 - \lambda_{rel,y}^2}} = \frac{1}{0.604 + \sqrt{0.604^2 - 0.44^2}} = 0.983$$

Where:

$$k_y = k_z = 0.5 \cdot \left(1 + \beta_c \left(\lambda_{rel,y} - 0.3\right) + \lambda_{rel,y}^2\right)$$

$$\beta_c = 0.1 \qquad [34]$$

$$k_y = k_z = 0.5 \cdot \left(1 + 0.1\,(0.44 - 0.3) + 0.44^2\right) = 0.604$$

Implementing all contributions into Equations (110) and (111) results in the following equilibrium requirements.

$$\frac{\frac{F}{A}}{k_{c,y} \cdot f_{c,0,d}} + \frac{n}{n-1} \cdot \frac{\frac{e_y \cdot V_y + (e_i + e_0) \cdot F}{W_y}}{f_{m,y,d}} + \frac{n}{n-1} \cdot k_m \cdot \frac{\frac{e_z \cdot V_z + (e_i + e_0) \cdot F}{W_z}}{f_{m,z,d}} \leq 1$$

$$\frac{\frac{F}{A}}{k_{c,z} \cdot f_{c,0,d}} + \frac{n}{n-1} \cdot k_m \cdot \frac{\frac{e_y \cdot V_y + (e_i + e_0) \cdot F}{W_y}}{f_{m,y,d}} + \frac{n}{n-1} \cdot \frac{\frac{e_z \cdot V_z + (e_i + e_0) \cdot F}{W_z}}{f_{m,z,d}} \leq 1$$

With:

$$V_y = 129.4\,[kN]$$

$$W_y = W_z = \frac{1}{6} \cdot b \cdot h^2 = 7.76 \cdot 10^6\,[mm^3]$$

Resulting in the following unity checks:

$$0.95 \leq 1.0$$

$$0.83 \leq 1.0$$

Accidental corner column loss scenario column design

Secondly, the dimensioning of the column in the accidental design situation is elaborated for the normative corner column loss scenario. The required dimensions of the column are $360\ x\ 360\ [mm^2]$. The calculation approach is described in Section 5.4.3.

Loads on the column in the standard design situation:

Accidental accidental floor loads (with DLF)	=	1234.1	$[kN]$
Facade (front) (with DLF)	=	224.3	$[kN]$
Facade (side) (with DLF)	=	224.3	$[kN]$
Facade (side) (without DLF)	=	108.0	$[kN]$
Dead load columns	=	9.6	$[kN]$
Dead load beams	=	44.5	$[kN]$
Total load	=	1844.9	$[kN]$

Calculation of $\lambda_{rel,y}$:

$$\lambda_y = \frac{h}{i_y} = \frac{390}{112.6} = 26.6\,[mm]$$

Where:

$$i_y = \sqrt{\frac{I_y}{A}} = \sqrt{\frac{1.93 \cdot 10^9}{1.52 \cdot 10^5}} = 112.6\,[mm^2]$$

$$\lambda_{rel,y} = \frac{\lambda_y}{\pi}\sqrt{\frac{f_{c,0,k}}{E_{0.05}}} = \frac{26.6}{\pi}\sqrt{\frac{21}{9100}} = 0.407$$

Since the column has a square cross-section, $\lambda_{rel,z} = \lambda_{rel,y}$. And since $\lambda_{rel,z}$ and $\lambda_{rel,y}$ are both larger than 0.3, Equations (110) and (111) should be used (see Section 5.4.3).

Calculation of 2nd order moment increase factor:

$$\frac{n}{n-1} = 1.11\,[\text{-}]$$

Where:

$$n = \frac{F_{cr}}{F} = \frac{19239}{1844.9} = 10.4\,[\text{-}]$$

$$F_{cr} = \frac{\pi^2 EI}{L_{eff}^2} = \frac{\pi^2 \cdot 11000 \cdot 1.93 \cdot 10^9}{3000^2} = 19239\,[kN]$$

Eccentricities of the connection e_y and e_z:

$$e_y = 150 + \frac{b_y}{2} = 150 + \frac{390}{2} = 345\,[mm]$$

$$e_z = 150 + \frac{b_z}{2} = 150 + \frac{390}{2} = 345\,[mm]$$

Eccentricity by element imperfections e_0:

$$e_0 = \frac{L}{500} = \frac{3000}{500} = 6\,[mm]$$

Eccentricity by imperfectly centered vertical load application e_i:

$$e_i = \frac{1}{400} \cdot L_{eff} = \frac{1}{400} \cdot 3000 = 7.5\,[mm]$$

Calculation of $k_{c,y}$ and $k_{c,z}$ ($k_{c,y}$ and $k_{c,z}$ are equal due to the square cross-section of the columns):

$$k_{c,y} = k_{c,z} = \frac{1}{k_y + \sqrt{k_y^2 - \lambda_{rel,y}^2}} = \frac{1}{0.588 + \sqrt{0.588^2 - 0.407^2}} = 0.987$$

Where:

$$k_y = k_z = 0.5 \cdot \left(1 + \beta_c \left(\lambda_{rel,y} - 0.3\right) + \lambda_{rel,y}^2\right)$$

$$\beta_c = 0.1 \qquad [34]$$

$$k_y = k_z = 0.5 \cdot \left(1 + 0.1\,(0.407 - 0.3) + 0.407^2\right) = 0.588$$

The values for V_y, V_z, W_y, and W_z are:

$$V_y = 208.2\,[kN]$$

$$V_z = 39.9\,[kN]$$

$$W_y = W_z = 9.89 \cdot 10^6\,[mm^3]$$

Resulting in the following unity checks:

$$0.98 \leq 1.0$$

$$0.90 \leq 1.0$$

Appendix D

Floor element analysis result tables

D.1 Corner column loss scenario

Table D.1: Required structural element height [mm] per design criterion for **continuous Lignatur** box floor elements in a **corner** column loss scenario.

Floor span	3.0	3.5	4.0	4.5	5.0	5.5	6.0	6.5	7.0	7.5	8.0	8.5	9.0
Deflection	120	120	120	120	140	160	180	180	200	220	240	280	280
Vibrations	120	120	120	140	160	180	220	240	280	320	360	400	440
Fund. moment	120	120	120	120	120	120	140	160	160	180	200	220	240
Acc. moment	**200**	**240**	**280**	**320**	**360**	**400**	**440**	**480**	-	-	-	-	-

Table D.2: Required structural element height [mm] per design criterion for **continuous CLT** elements in a **corner** column loss scenario.

Floor span	3.0	3.5	4.0	4.5	5.0	5.5	6.0	6.5	7.0	7.5	8.0	8.5	9.0
Deflection	80	120	120	120	150	150	180	180	220	220	220	250	280a
Vibrations	80	120	120	150	180	180	220	250	**280b**	**280b**	**360b**	**400**	-
Fund. moment	60	80	80	120	120	120	120	150	150	180	180	180	220
Acc. moment	**150**	**180**	**180**	**220**	**220**	**250**	**280a**	**280**	**280**	**280**	360a	360b	360b

Table D.3: Required structural element height [mm] per design criterion for **staggered Lignatur** box floor elements in a **corner** column loss scenario.

Floor span	3.0	3.5	4.0	4.5	5.0	5.5	6.0	6.5	7.0	7.5	8.0	8.5	9.0
Deflection	120	120	120	120	140	160	180	180	200	220	240	280	280
Vibrations	120	120	120	140	160	180	220	240	280	320	360	400	440
Fund. stress	120	120	120	120	120	120	140	160	160	180	200	220	240
Acc. moment	**280**	**360**	**400**	**440**	-	-	-	-	-	-	-	-	-

Table D.4: Required structural element height [mm] per design criterion for **staggered CLT** elements in a **corner** column loss scenario.

Floor span	3.0	3.5	4.0	4.5	5.0	5.5	6.0	6.5	7.0	7.5	8.0	8.5	9.0
Deflection	80	120	120	120	150	150	180	180	220	220	220	250	280a
Vibrations	80	120	120	150	180	180	220	250	280b	280b	360b	400	-
Fund. moment	60	80	80	120	120	120	120	150	150	180	180	180	220
Acc. moment	**180**	**220**	**250**	**280b**	**280b**	**360a**	**360b**	**360b**	**400**	-	-	-	-

D.2 Edge column loss scenario

Table D.5: Required structural element height [mm] per design criterion for **continuous Lignatur** box floor elements in a **edge** column loss scenario.

Floor span	3.0	3.5	4.0	4.5	5.0	5.5	6.0	6.5	7.0	7.5	8.0	8.5	9.0
Deflection	120	120	120	120	140	160	180	180	200	220	240	280	280
Vibrations	120	120	120	140	160	180	220	240	280	320	360	400	440
Fund. moment	120	120	120	120	120	120	140	160	160	180	200	220	240
Acc. moment	**160**	**180**	**220**	**240**	**280**	**320**	**360**	**400**	**440**	**440**	**480**	-	-

Table D.6: Required structural element height [mm] per design criterion for **continuous CLT** elements in a **edge** column loss scenario.

Floor span	3.0	3.5	4.0	4.5	5.0	5.5	6.0	6.5	7.0	7.5	8.0	8.5	9.0
Deflection	80	**120**	120	120	150	150	180	180	220	220	220	250	280a
Vibrations	80	**120**	120	150	**180**	180	**220**	**250**	**280b**	**280b**	**360b**	**400**	-
Fund. moment	60	80	80	120	120	120	120	150	150	180	180	180	220
Acc. moment	**120**	**120**	**150**	**180**	**180**	**220**	**220**	**250**	280a	**280b**	280b	320	360a

Table D.7: Required structural element height [mm] per design criterion for **staggered Lignatur** box floor elements in a **edge** column loss scenario

Floor span	3.0	3.5	4.0	4.5	5.0	5.5	6.0	6.5	7.0	7.5	8.0	8.5	9.0
Deflection	120	120	120	120	140	160	180	180	200	220	240	280	280
Vibrations	120	120	120	140	160	180	220	240	280	320	360	400	440
Fund. stress	120	120	120	120	120	120	140	160	160	180	200	220	240
Acc. moment	**200**	**240**	**280**	**360**	**400**	**440**	**480**	-	-	-	-	-	-

Table D.8: Required structural element height [mm] per design criterion for **staggered CLT** elements in a **edge** column loss scenario.

Floor span	3.0	3.5	4.0	4.5	5.0	5.5	6.0	6.5	7.0	7.5	8.0	8.5	9.0
Deflection	80	120	120	120	150	150	180	180	220	220	220	250	280a
Vibrations	80	120	120	150	180	180	220	250	280b	280b	360b	400	-
Fund. moment	60	80	80	120	120	120	120	150	150	180	180	180	220
Acc. moment	**150**	**180**	**220**	**220**	**250**	**280b**	**280b**	**360a**	**360b**	**360b**	**400**	**400**	-

D.3 Middle column loss scenario

Table D.9: Required structural element height [mm] per design criterion for **continuous Lignatur** box floor elements in a **middle** column loss scenario.

Floor span	3.0	3.5	4.0	4.5	5.0	5.5	6.0	6.5	7.0	7.5	8.0	8.5	9.0
Deflection	**120**	**120**	120	120	140	160	180	180	200	220	240	280	280
Vibrations	**120**	**120**	120	140	160	180	220	240	280	320	360	400	**440**
Fund. moment	**120**	**120**	120	120	120	120	140	160	160	180	200	220	240
Acc. moment	**120**	**120**	**140**	**160**	**200**	**220**	**240**	**280**	**320**	**360**	**400**	**440**	**440**

Table D.10: Required structural element height [mm] per design criterion for **continuous CLT** elements in a **middle** column loss scenario

Floor span	3.0	3.5	4.0	4.5	5.0	5.5	6.0	6.5	7.0	7.5	8.0	8.5	9.0
Deflection	**80**	**120**	**120**	120	150	150	180	180	220	220	220	250	280*a*
Vibrations	**80**	**120**	**120**	**150**	**180**	**180**	**220**	**250**	**280b**	**280b**	**360b**	**400**	-
Fund. moment	60	80	80	120	120	120	120	150	150	180	180	180	220
Acc. moment	**80**	**120**	**120**	120	150	**180**	180	220	220	250	280*a*	280*b*	280*b*

Table D.11: Required structural element height [mm] per design criterion for **staggered Lignatur** box floor elements in a **middle** column loss scenario.

Floor span	3.0	3.5	4.0	4.5	5.0	5.5	6.0	6.5	7.0	7.5	8.0	8.5	9.0
Deflection	120	120	120	120	140	160	180	180	200	220	240	280	280
Vibrations	120	120	120	140	160	180	220	240	280	320	360	400	440
Fund. stress	120	120	120	120	120	120	140	160	160	180	200	220	240
Acc. moment	**160**	**200**	**220**	**280**	**320**	**360**	**440**	**480**	-	-	-	-	-

Table D.12: Required structural element height [mm] per design criterion for **staggered CLT** elements in a **middle** column loss scenario

Floor span	3.0	3.5	4.0	4.5	5.0	5.5	6.0	6.5	7.0	7.5	8.0	8.5	9.0
Deflection	80	120	120	120	150	150	180	180	220	220	220	250	280*a*
Vibrations	80	120	120	150	180	180	220	250	280*b*	280*b*	**360b**	**400**	-
Fund. moment	60	80	80	120	120	120	120	150	150	180	180	180	220
Acc. moment	**120**	**150**	**180**	**180**	**220**	**250**	**280a**	**280b**	**360a**	**360b**	**360b**	**400**	400

D.4 Lignatur performance with doubled bottom and end plate thicknesses

Table D.13: Required structural element height [mm] per design criterion for **continuous Lignatur** box floor elements in a **corner** column loss scenario with *62* [mm] top and bottom plates.

Floor span	3.0	3.5	4.0	4.5	5.0	5.5	6.0	6.5	7.0	7.5	8.0	8.5	9.0
Deflection	120	120	120	120	140	140	160	180	180	200	220	240	240
Vibrations	120	120	120	140	160	180	200	220	280	280	320	360	400
Fund. moment	120	120	120	120	120	120	120	120	140	140	160	160	180
Acc. moment	**180**	**200**	**220**	**280**	**280**	**320**	**320**	**360**	**400**	**440**	**440**	**480**	-

Table D.14: Required structural element height [mm] per design criterion for **continuous Lignatur** box floor elements in an **edge** column loss scenario with *62* [mm] top and bottom plates.

Floor span	3.0	3.5	4.0	4.5	5.0	5.5	6.0	6.5	7.0	7.5	8.0	8.5	9.0
Deflection	120	120	120	120	140	140	160	180	180	200	220	240	240
Vibrations	120	120	120	140	160	180	200	220	280	280	320	360	400
Fund. moment	120	120	120	120	120	120	120	120	140	140	160	160	180
Acc. moment	**140**	**160**	**180**	**200**	**220**	**280**	**280**	**320**	**320**	**360**	**400**	**400**	**440**

Table D.15: Required structural element height [mm] per design criterion for **continuous Lignatur** box floor elements in a **middle** column loss scenario with *62* [mm] top and bottom plates.

Floor span	3.0	3.5	4.0	4.5	5.0	5.5	6.0	6.5	7.0	7.5	8.0	8.5	9.0
Deflection	**120**	**120**	120	120	140	140	160	180	180	200	220	240	240
Vibrations	**120**	**120**	120	140	160	180	200	220	**280**	**280**	**320**	**360**	**400**
Fund. moment	**120**	**120**	120	120	120	120	120	120	140	140	160	160	180
Acc. moment	**120**	**120**	**140**	**160**	**180**	**200**	**220**	**240**	**280**	**280**	**320**	**360**	360

Table D.16: Required structural element height [mm] per design criterion for **staggered Lignatur** box floor elements in a **corner** column loss scenario with *62* [mm] top and bottom plates.

Floor span	3.0	3.5	4.0	4.5	5.0	5.5	6.0	6.5	7.0	7.5	8.0	8.5	9.0
Deflection	120	120	120	120	140	140	160	180	180	200	220	240	240
Vibrations	120	120	120	140	160	180	200	220	280	280	320	360	400
Fund. moment	120	120	120	120	120	120	120	120	140	140	160	160	180
Acc. moment	**240**	**280**	**320**	**360**	**400**	**440**	-	-	-	-	-	-	-

Table D.17: Required structural element height [mm] per design criterion for **staggered Lignatur** box floor elements in an **edge** column loss scenario with *62* [mm] top and bottom plates.

Floor span	3.0	3.5	4.0	4.5	5.0	5.5	6.0	6.5	7.0	7.5	8.0	8.5	9.0
Deflection	120	120	120	120	140	140	160	180	180	200	220	240	240
Vibrations	120	120	120	140	160	180	200	220	280	280	320	360	400
Fund. moment	120	120	120	120	120	120	120	120	140	140	160	160	180
Acc. moment	**180**	**220**	**240**	**280**	**320**	**360**	**400**	**440**	**480**	-	-	-	-

Table D.18: Required structural element height [mm] per design criterion for **staggered Lignatur** box floor elements in a **middle** column loss scenario with *62* [mm] top and bottom plates.

Floor span	3.0	3.5	4.0	4.5	5.0	5.5	6.0	6.5	7.0	7.5	8.0	8.5	9.0
Deflection	120	120	120	120	140	140	160	180	180	200	220	240	240
Vibrations	120	120	120	140	160	180	200	220	280	280	320	360	400
Fund. moment	120	120	120	120	120	120	120	120	140	140	160	160	180
Acc. moment	**140**	**180**	**200**	**240**	**280**	**320**	**360**	**400**	**440**	**480**	-	-	-

Appendix E

Comparison calculation results to SCIA models

Accidental scenarios

Corner column loss

Table E.1: Comparison between manual calculations and SCIA model results for the corner column loss scenario, span $L = 6\,[m]$.

	Calculations	SCIA	Difference
$M_{floor,max}$ $[kNm]$	-212.0	-215.8	+1.78%
Adjacent elements:			
Columns/connections [kN] :			
Front 1	-	-	-
Front 2	28.08	28.86	+2.8%
Mid 1	280.46	266.11	-5.1%
Mid 2	161.35	175.30	+8.7%
Back 1	-46.10	-61.63	+33.7%
Back 2	-14.28	-18.68	+30.9%
Beams $[kNm]$:			
Front	-	-	-
Mid	304.95	303.96	−0.3%
Back	-47.80	-49.57	+3.7%

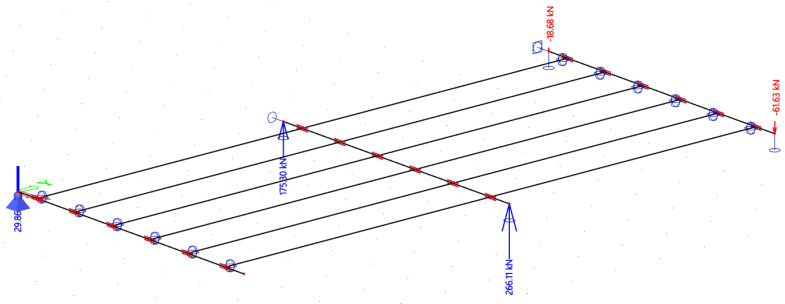

Figure E.1: SCIA model: Corner column loss load combination, $L = 6\,[m]$, reaction forces representing connection and column loads shown.

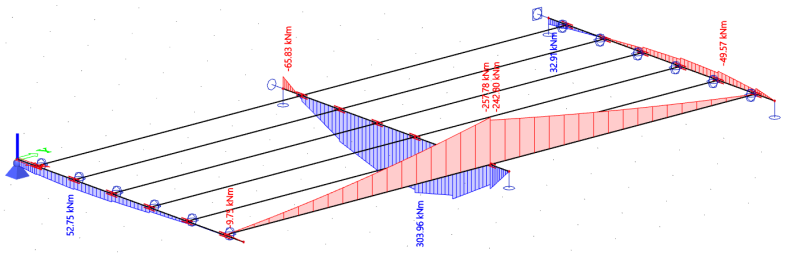

Figure E.2: SCIA model: Corner column loss load combination, $L = 6\,[m]$, bending moments beams and outer floor element shown.

Note: The *Back* column/connection forces are taken conservatively in the manual calculations since this negative (thus upward) force is a beneficial load, reducing the remaining *"standard"* loads (such as dead loads from the structure higher up, and live loads from floors field that are not connected to the lost column. This explains the large difference ($> 30\%$) between the manual calculations and the SCIA results in Tables E.1 and E.2. $M_{floor,max}$ indicates the maximum bending moment in the outermost floor element.

Table E.2: Comparison between manual calculations and SCIA model results for the corner column loss scenario, span $L = 9\,[m]$.

	Calculations	SCIA	Difference
$M_{floor,max}$ $[kNm]$	-389.2	-445.1	-12.6%
Adjacent elements:			
Columns/connections $[\mathrm{kN}]$:			
Front 1	-	-	-
Front 2	63.2	65.9	$+4.2\%$
Mid 1	589.4	546.72	-7.3%
Mid 2	339.4	368.1	$+8.4\%$
Back 1	-80.7	-113.6	$+41.9\%$
Back 2	-20.3	27.9	$+37.2\%$
Beams $[kNm]$:			
Front	-	-	-
Mid	947.4	943.0	-0.5%
Back	-120.4	-133.1	$+10.5\%$

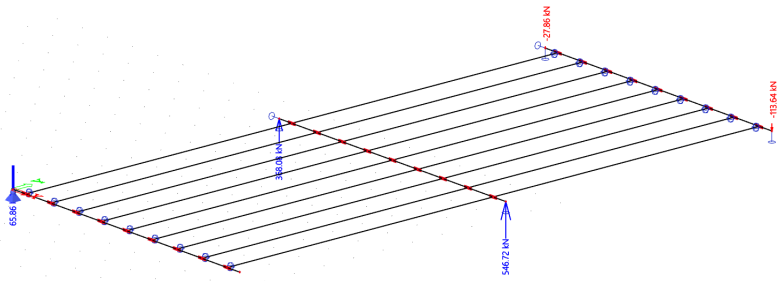

Figure E.3: SCIA model: Corner column loss load combination, $L = 9\,[m]$, reaction forces representing connection and column loads shown.

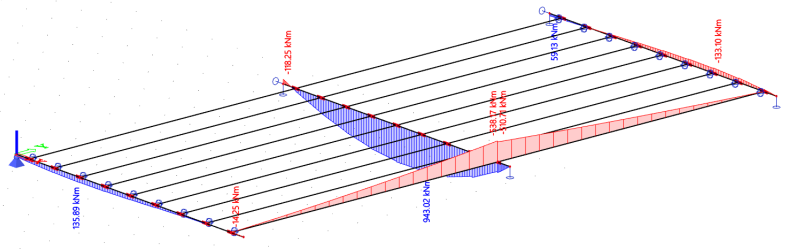

Figure E.4: SCIA model: Corner column loss load combination, $L = 9\,[m]$, bending moments beams and outer floor element shown.

Edge column loss

Table E.3: Comparison between manual calculations and SCIA model results for the edge column loss scenario, span $L = 6\,[m]$.

	Calculations	SCIA	Difference
$M_{floor,max}$ $[kNm]$	153.5	171.8	+11.9%
Adjacent elements:			
Columns/connections [kN] :			
Front 1	136.5	130.32	−5.0%
Front 2	73.8	61.41	−16.8%
Mid 1	-	-	-
Mid 2	113.4	101.81	−10.2%
Back 1	136.5	130.32	−5.0%
Back 2	73.8	61.41	−16.8%
Beams $[kNm]$:			
Front	136.4	143.73	+5.4%
Mid	-	-	-
Back	136.4	143.73	+5.4%

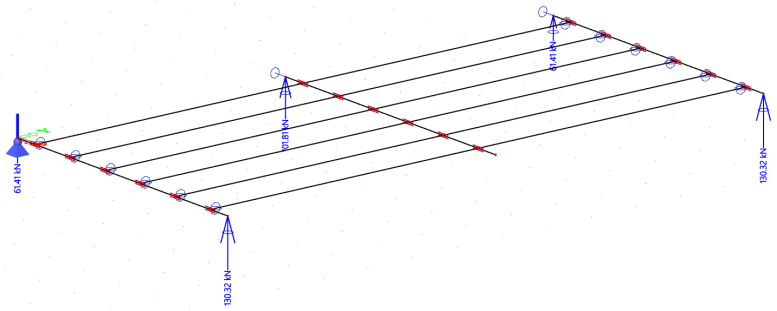

Figure E.5: SCIA model: Edge column loss load combination, $L = 6\,[m]$, reaction forces representing connection and column loads shown.

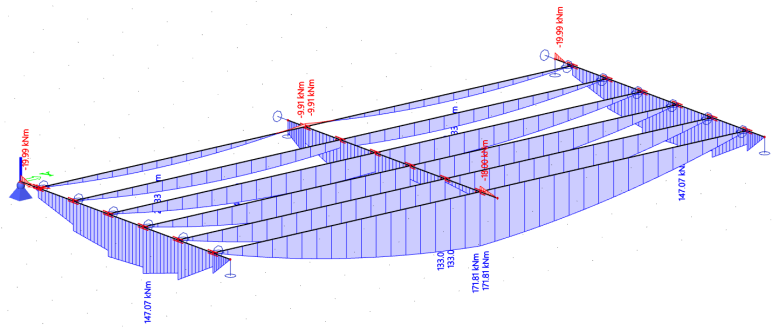

Figure E.6: SCIA model: Edge column loss load combination, $L = 6\,[m]$, bending moments beams and outer floor element shown.

Table E.4: Comparison between manual calculations and SCIA model results for the edge column loss scenario, span $L = 9\,[m]$.

	Calculations	SCIA	Difference
$M_{floor,max}$ $[kNm]$	355.3	379.4	+6.8%
Adjacent elements:			
Columns/connections [kN] :			
Front 1	293.3	279.7	−4.64%
Front 2	160.2	182.7	14.1%
Mid 1	-	-	-
Mid 2	146.9	140.0	−4.7%
Back 1	293.3	279.7	−4.64%
Back 2	160.2	182.7	14.1%
Beams $[kNm]$:			
Front	439.9	459.9	+4.5%
Mid	-	-	-
Back	439.9	459.9	+4.5%

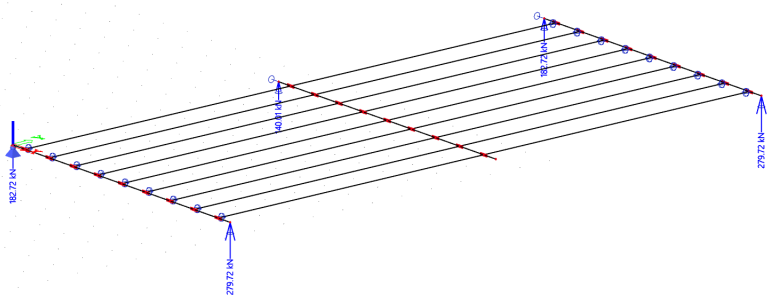

Figure E.7: SCIA model: Edge column loss load combination, $L = 9\,[m]$, reaction forces representing connection and column loads shown.

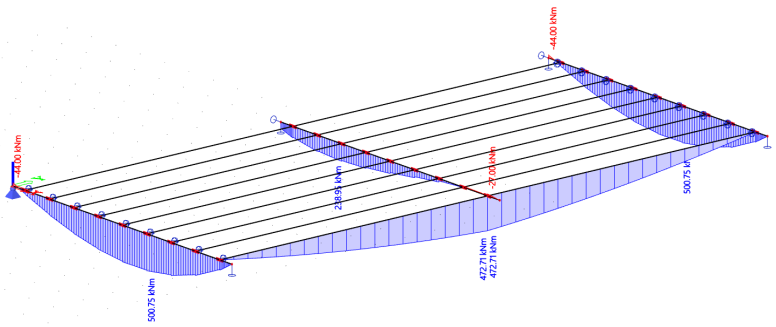

Figure E.8: SCIA model: Edge column loss load combination, $L = 9\,[m]$, bending moments beams and outer floor element shown.

Middle column loss

Table E.5: Comparison between manual calculations and SCIA model results for the middle column loss scenario, span $L = 6\,[m]$.

	Calculations	SCIA	Difference
$M_{floor,max}$ $[kNm]$	103.7	101.6	-2.0%
Adjacent elements:			
Columns/connections $[\mathrm{kN}]$:			
Front 1	45.5	39.31	-13.6%
Front 2	88.9	112.32	$+26.3\%$
Mid 1	127.4	145.5	$+14.6\%$
Mid 2	-	-	-
Back 1	45.5	39.31	-13.6%
Back 2	88.9	112.32	$+26.3\%$
Beams $[kNm]$:			
Front	117.2	129.4	$+10.4\%$
Mid	-	-	-
Back	117.2	129.4	$+10.4\%$

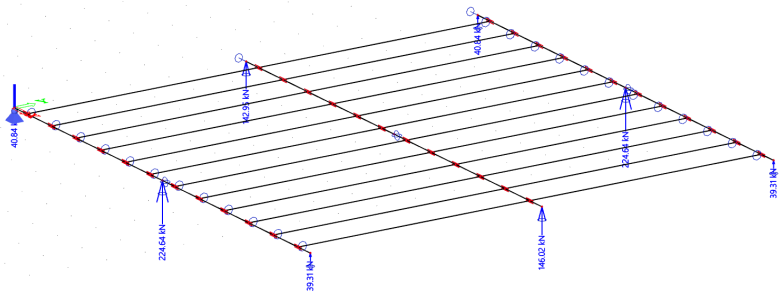

Figure E.9: SCIA model: Middle column loss load combination, $L = 6\,[m]$, reaction forces representing connection and column loads shown.

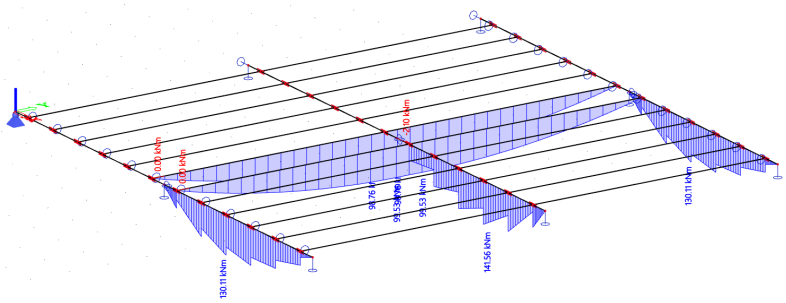

Figure E.10: SCIA model: Middle column loss load combination, $L = 6\,[m]$, bending moments beams and outer floor element shown.

Table E.6: Comparison between manual calculations and SCIA model results for the middle column loss scenario, span $L = 9\,[m]$.

	Calculations	SCIA	Difference
$M_{floor,max}$ $[kNm]$	252.7	269.2	+6.5%
Adjacent elements:			
Columns/connections [kN] :			
Front 1	140.6	147.4	−4.6%
Front 2	200.1	252.7	+26.3%
Mid 1	210.6	224.2	+6.5%
Mid 2	-	-	-
Back 1	140.6	147.4	−4.6%
Back 2	200.1	252.7	+26.3%
Beams $[kNm]$:			
Front	395.6	424.1	+7.2%
Mid	-	-	-
Back	395.6	424.1	+7.2%

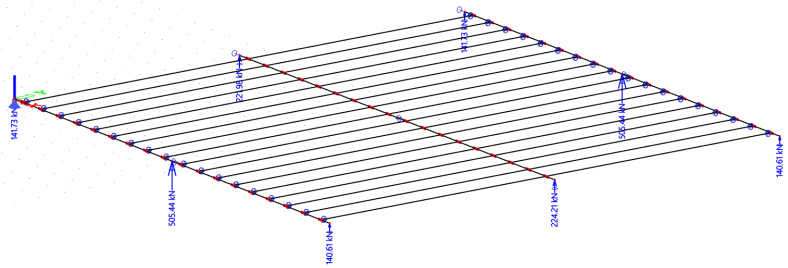

Figure E.11: SCIA model: Middle column loss load combination, $L = 9\,[m]$, reaction forces representing connection and column loads shown.

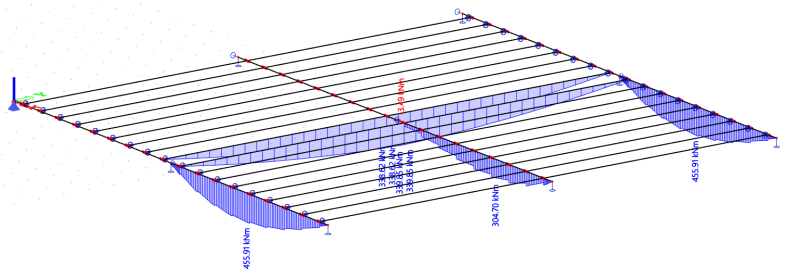

Figure E.12: SCIA model: Middle column loss load combination, $L = 9\,[m]$, bending moments beams and outer floor element shown.

Appendix F

Structural schematizations used

The schematizations of the floor elements in different loading configurations and the resulting shear force and bending moment diagrams are listed below.

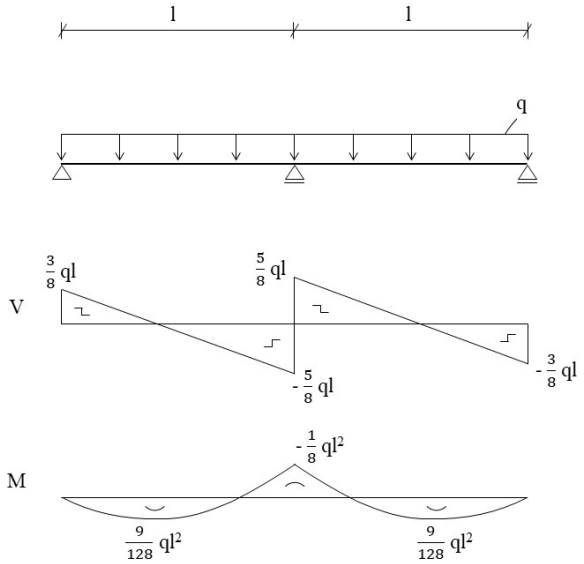

Figure F.1: Two-span floor element with a distributed load

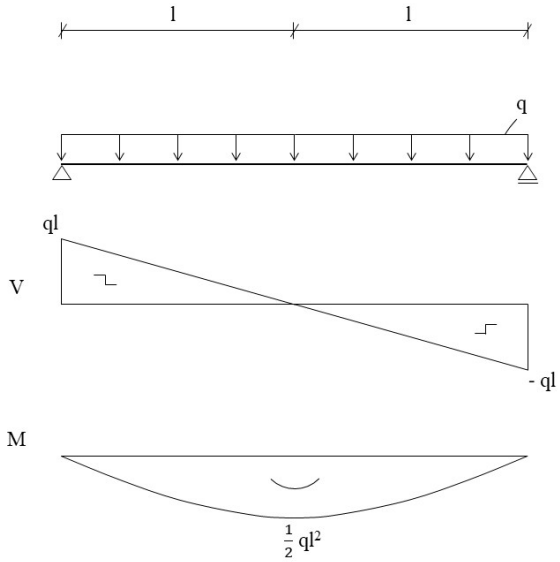

Figure F.2: Two-span floor element with a distributed load after the middle column is lost

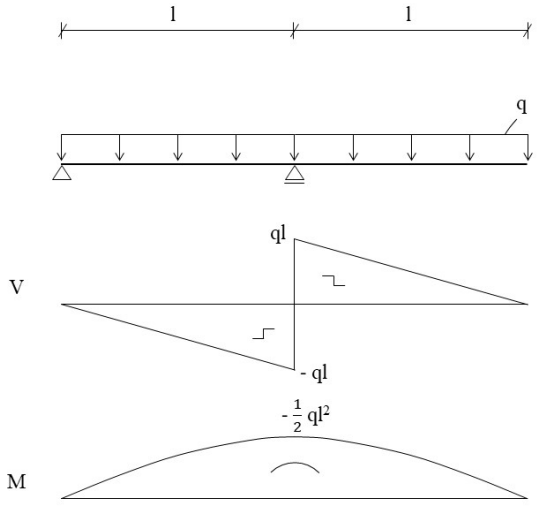

Figure F.3: Two-span floor element with a distributed load after the end column is lost

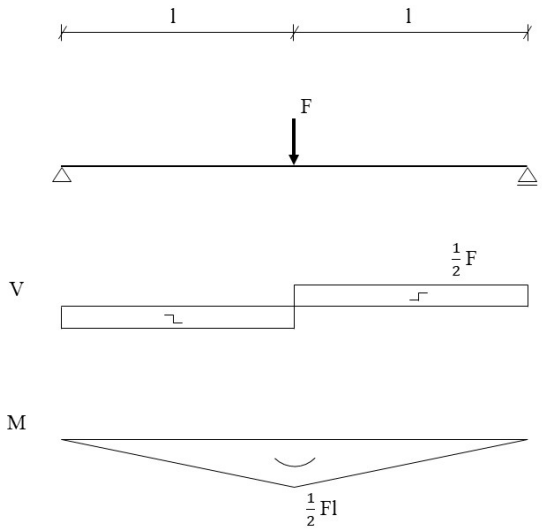

Figure F.4: Two-span floor element with a point load after the middle column is lost

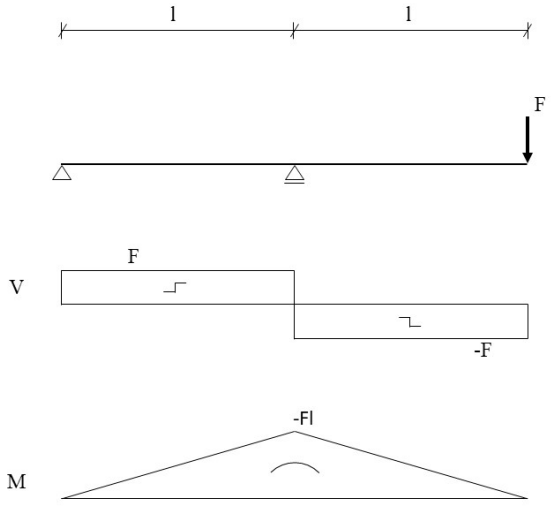

Figure F.5: Two-span floor element with a point load after the end column is lost

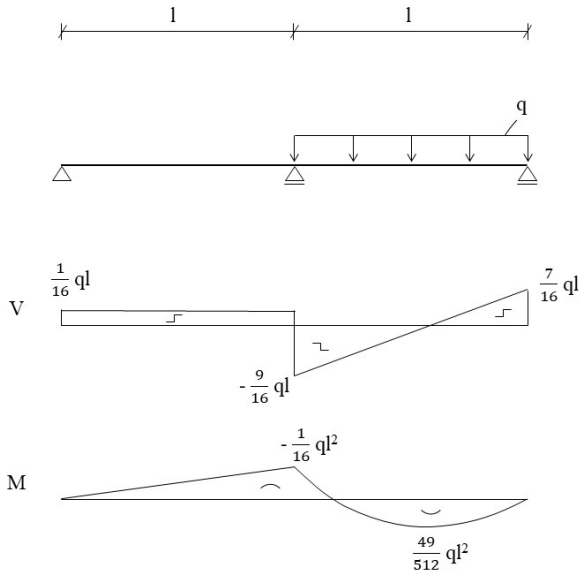

Figure F.6: Two-span floor element with a distributed load on one floor span

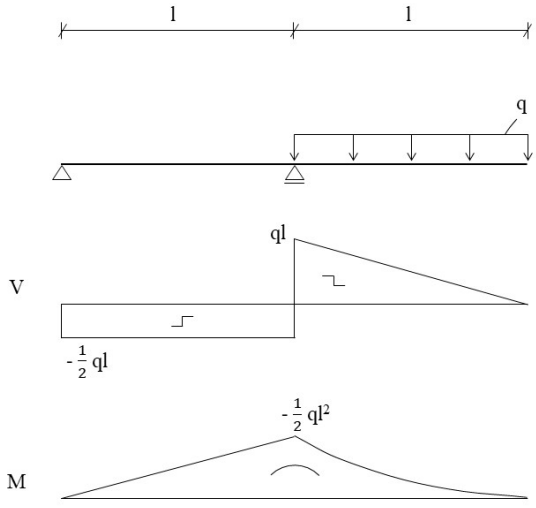

Figure F.7: Two-span floor element with a distributed load on one floor span after the end column is lost